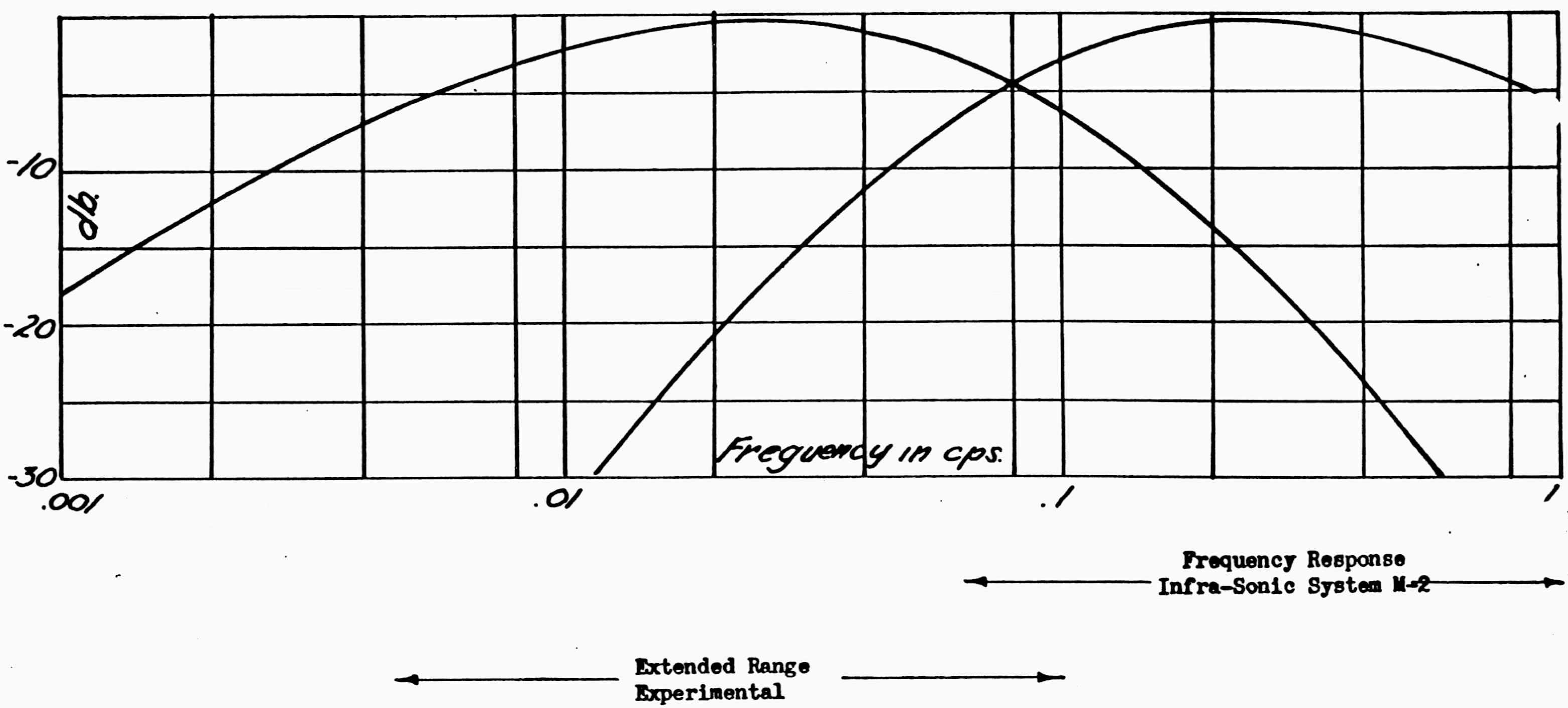

FIG. 4

FREQUENCY RESPONSE OF EQUIPMENT

APPENDIX A

SCHRÖDINGER'S TREATMENT OF DISPERSION AND ATTENUATION IN THE ATMOSPHERE

Schrödinger (Physikalische Zeitschrift, Vol. 19, pp 445-453, 1917) has shown that sound traveling to a considerable altitude is modified in two ways:

a. It undergoes dispersion at frequencies for which the density of the atmosphere changes appreciably in a space of one wavelength and,

b. It is attenuated when the atmosphere becomes so rarefied that the mean free path of the gas molecules approaches the order of magnitude of the wavelength.

Schrödinger computed the amount of dispersion assuming a wave traveling vertically, and arrived at the conclusion that the effect is negligible for audible sound. He also calculated the attenuation due to <u>b</u> above, and arrived at the conclusion that the upper limit of travel of audible sound is about 80 KM.

The longest wavelength for which Schrödinger has published results is 100 meters, corresponding to about 3.4 cps. Experience indicates that most of the energy of large explosions recorded at distances of over a hundred miles lies in a frequency band corresponding to wavelengths of 350 m to 3500 m. In the following discussion, Schrödinger's results have therefore been extended to longer wavelengths to be applicable to recent experimental work.

A. Distortion of a Transient Sound Pulse due to Dispersion

The velocity of sound for vertical travel in an isothermal atmosphere is shown by Schrödinger to be

$$v = c\left(1 + \frac{\lambda^2}{32\pi^2 H^2}\right) \qquad (1)$$

where c is the limiting velocity of sound at high frequencies, λ is the wavelength, and H is the height of the "homogeneous atmosphere" (H = 8 KM).

Schrödinger's analysis does not explicitly give the corresponding result for a sound path having a horizontal component. However, if his analysis is modified by taking components along a path which is inclined at angle θ to the horizontal, the solution of the resulting modified differential equation gives a velocity value of

$$v = c\left(1 + \frac{\lambda^2 \sin^2 \theta}{32\pi^2 H^2}\right) \qquad (2)$$

If we assume a path shaped like an isoceles triangle with a base length of 1000 KM and an altitude of 100 KM, θ will be 11.3°. For a wavelength of 10 KM

$$\frac{v}{c} = 1 + \frac{10^2 \sin^2 11.3^\circ}{32\pi^2 \times 8^2} = 1.00019$$

If we postulate that the maximum allowable dispersion of a transient occurs when the lowest frequency component experiences a 45° phase shift with respect to the highest frequency component, it is possible to use the above expression to calculate the maximum range of undistorted transmission.

The variation in travel time due to a change in velocity dv is given by

$$\left|\frac{dt}{t}\right| = \frac{dv}{v}$$

As we have assumed a 45° phase shift, we shall substitute T/8 for dt in this expression, T being the period, and set $t = s/v$ where s is total distance traveled by the wave, giving

$$\frac{T}{8} \cdot \frac{v}{s} = \frac{dv}{v}$$

For $\lambda = 10$ KM, we have seen that $dv/v = .00019$

$$\therefore \frac{Tv}{8s} = .00019$$

or $s = \dfrac{Tv}{.00152} = \dfrac{\lambda}{.00152} = \dfrac{10}{.00152} = 6580$ KM

The projection of this path on a horizontal plane would be $6580 \cdot \cos 11.3^\circ = 6450$ KM. Thus an explosion pulse, the lowest frequency component of which has a wavelength of 10 KM, would have to travel 6450 KM horizontally before that frequency component is shifted 45° in phase with respect to high frequencies. It is therefore obvious that the effect of dispersion is negligible at the wavelength assumed for sound refracted at the 100 KM level, and for ranges less than 6000 KM. The effect would be still smaller for sound refracted at lower levels.

B. <u>Effect of Dispersion on the Sound Path</u>

In a recent paper (Journal of the Acoustical Society, Vol. 21, pp 6 - 16, 1949) Cox has used Schrödinger's results in an attempt to prove that, because of dispersion, the paths traversed by sound of different frequencies vary in such a manner that low frequency sounds are refracted at higher altitudes and hence are attenuated more than high frequency sounds. In his discussion Cox uses equation (1), which only holds for vertical sound travel, to describe the performance of the sound ray throughout its entire path, no part of which is vertical. His analysis, in addition to being based upon the wrong expression for v, does not explicitly give the difference between the altitudes of the high frequency and low frequency paths.

For a sound ray traveling at an angle θ with respect to the horizontal, the correct expression for the phase velocity is given by equation (2) which indicates zero dispersion for horizontal travel. This is just what would be expected, as the dispersion is due solely to change in density of the medium in the direction of travel.

The investigation of the effect of dispersion on the sound path is facilitated by using Snell's Law in the form

$$\frac{v}{\cos\theta} = \text{const.} \tag{3}$$

In the absence of wind, this quantity is invariant along the sound path, irrespective of the cause of the change in velocity.

If we use subscript γ to refer to low frequencies, and ∞ to refer to high frequencies for which no dispersion occurs, we can write equation (3) for low frequencies,

$$\frac{(v_0)_\gamma}{(\cos\theta_0)_\gamma} = \text{const.} = V_\gamma \tag{4}$$

where subscript $_0$ refers to conditions at the earth's surface and V is the velocity at the apex of the path, where $\cos\theta = 1$.

For high frequencies,

$$\frac{(v_0)_\infty}{(\cos\theta_0)_\infty} = \text{const.} = V_\infty \tag{5}$$

If we assume a high frequency and low frequency wave starting off at the same elevation angle, $(\cos\theta_0)_\gamma = (\cos\theta_0)_\infty$ and equations (4) and (5) can be combined to give

$$\frac{V_\gamma}{V_\infty} = \frac{(\nu_0)_\gamma}{(\nu_0)_\infty}$$

Substituting values of V_o from equation (2) we get

$$\frac{V_\gamma}{V_\infty} = 1 + \frac{\lambda^2 \sin^2 \theta_o}{32 \pi^2 H^2}$$

If λ is given in meters,

$$\frac{V_\gamma}{V_\infty} = 1 + 4.95 \times 10^{-11} \lambda^2 \sin^2 \theta_o$$

If both rays leave the source horizontally, $\theta_o = 0$, and $V_\gamma = V_\infty$ which means that both rays are refracted at the same altitude.

If $\theta_o = 30^o$ and $\lambda = 3300$ m (corresponding to a period of 10 sec.),

$$\frac{V_\gamma}{V_\infty} = 1 + 1.35 \times 10^{-4}$$

$$\text{or} \qquad \frac{dv}{V} = 1.35 \times 10^{-4}$$

Total refraction can take place at either the first or second inversion, the respective levels of refraction being approximately 50 and 120 KM. From the results of paragraph C below, it is obvious that no attenuation of sound having periods near 10 sec. could occur at the lower of these two levels. In the neighborhood of 120 KM the phenomenon discussed by Cox might conceivably occur, if the altitudes of the respective paths differed sufficiently.

From the NACA data on the standard atmosphere, we find that the sound velocity gradient at the 120 KM level varies from 2.24 meters sec^{-1} km^{-1} in the daytime to 5.17 meters sec^{-1} km^{-1} at night; the value of V at 120 KM being 436.3 m/sec. Taking the smaller of these values we get

$$\frac{dv}{V} = \frac{2.24}{436.3} \text{ per KM}$$

$$= 5.14 \times 10^{-3} \text{ per KM}$$

From this we see that the dv/V value of 1.35×10^{-4} corresponds to an altitude difference of only 26.3 meters. It is therefore obvious that the maximum altitude of the sound path does not vary with frequency for periods up to 10 seconds.

C. Attenuation of Sound in a Rarefied Gas

Schrödinger has shown that the damping coefficient for the sound intensity (square of the amplitude) can be expressed as

$$k = -30.10 \frac{\ell Z}{\lambda^2} \qquad (6)$$

where ℓ is the mean free path of the gas molecules, Z the distance traveled, and λ the wavelength. At a distance x above the earth's surface,

$$\ell = 10^{-5} e^{\alpha x} \text{ cm.} \qquad (7)$$

where $\alpha = 1.2516 \times 10^{-6}$ cm^{-1} for a temperature of 0°C.

If we set $Z = 10^5$ cm = 1 KM, the above relation can be used to evaluate the altitude x at which the intensity of the wave is reduced to the fraction e^k of its initial value after traveling a distance of 1 KM.

Replacing k by its equivalent $\log_e e^k$ and solving for x, we get

$$x = \frac{1}{\alpha}\left(2 \log_e \lambda + \log_e \frac{-\log_e e^k}{30.10}\right) \qquad (8)$$

By assuming fixed values of x, e^k, the fractional transmission can be calculated as a function of frequency. As e^k represents fractional energy transmission, fractional amplitude transmission can be obtained by taking the square root of the e^k values. Such a computation has been carried out for levels of 80, 100 and 120 KM., for a horizontal path of 100 KM, the results being plotted in the accompanying figure. If we assume that the sound ray travels near the maximum level for approximately 10% of the total path, the results will be applicable to a total path length of the order of 1000 KM. The curves are applicable to a temperature of 0°C; at higher temperatures the attenuation is decreased.

As an increase in temperature causes the attenuation at a given altitude to decrease and at the same time alters the gradient in such a way as to lower the path apex, absorption of a sound ray refracted at a given level would be a rapidly changing function of temperature, for frequencies on the steepest slope of the curve. For the particular path assumed above, near the 120 KM level, sound transmission in the band from 0.1 to 1 cps would be very sensitive to changes in the temperature gradient, if the mean temperature were in the neighborhood of 0°C.

D. Conclusions

1. The discussion of paragraph A indicates that no appreciable distortion of a transient sound pulse as a result of dispersion is to be expected for component periods up to 30 seconds.

2. It has been demonstrated that the altitude of the path apex is independent of frequency for periods up to 10 seconds.

3. For periods of the order of 1 to 10 sec., attenuation due to the effect discussed in paragraph C becomes appreciable at levels of 120 KM. Whether attenuation will occur or not will depend upon the exact altitude of the apex of the path, which in turn may vary diurnally or seasonally.

RELATIVE AMPLITUDE OF PLANE WAVE AFTER 100KM HORIZONTAL TRAVEL AT VARIOUS LEVELS AT 0° C.

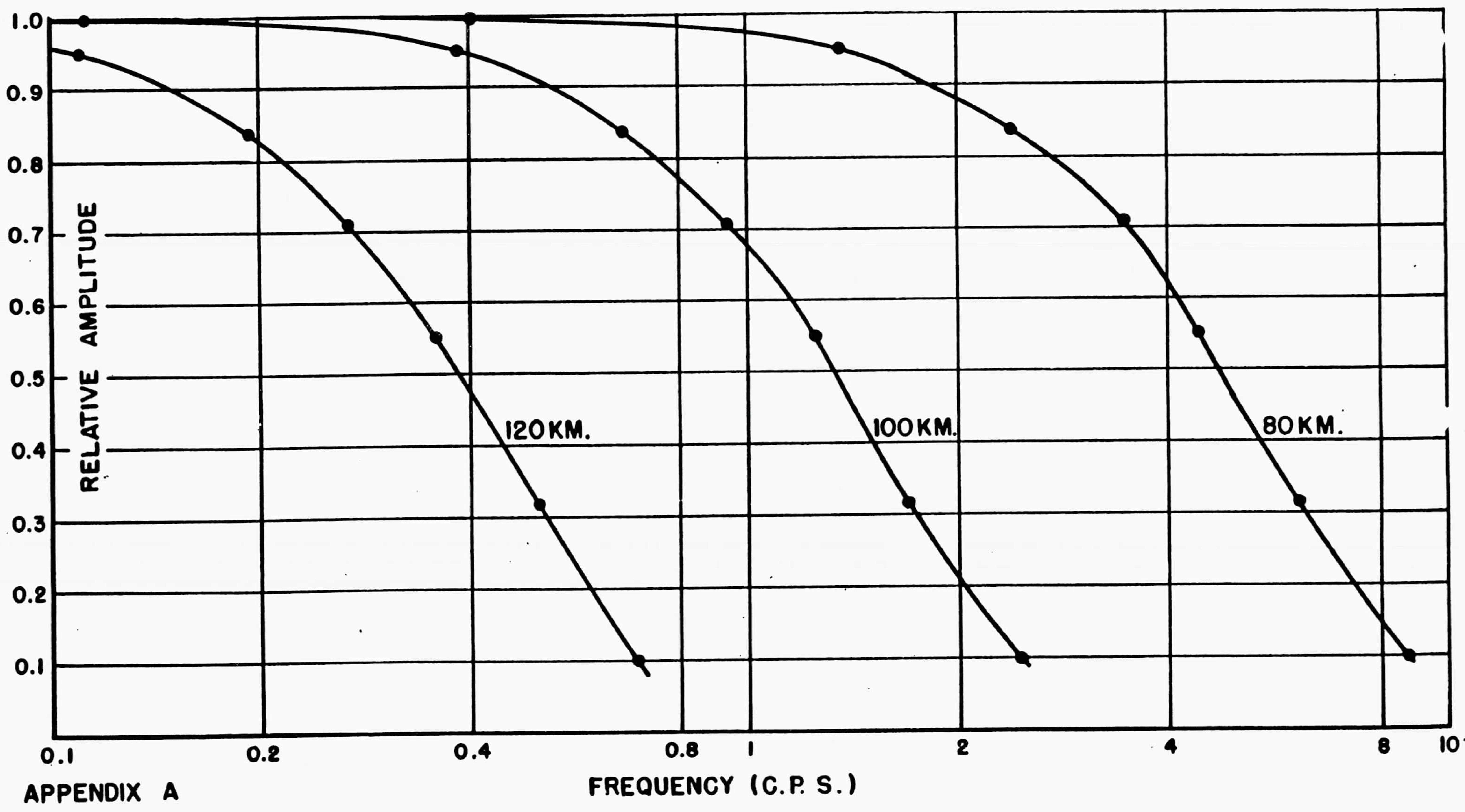

APPENDIX A

APPENDIX B

DESCRIPTION OF EQUIPMENT

I. INTRODUCTION:

A. General

1. Infra-sonic System M-2 is an equipment installation consisting of four (4) microphone stations and a central recording station. The four microphone stations are located on the corners of a ten (10) mile square. The ten mile square is the design center configuration and is not a rigid requirement. These stations are each connected by a wire line to the central recording station which is located within or adjacent to the ten mile square.

2. Each of the microphone stations is essentially a microbarograph, measuring pressure variations as small as 0.1 sound bar in the frequency range of 1 cycle in 15 seconds to 1 cycle per second. The signals from each microphone station are recorded independently on continuously moving record charts at the central recording station.

B. Microphone Station Equipment

A condenser microphone is the pressure sensitive element and is employed in the infra-sonic system as one arm of a bridge net-work. The bridge is normally balanced and variations in the condenser microphone capacity cause the bridge to become unbalanced in either a positive or negative sense. A 1000 cycle signal is applied to the bridge network and the amplitude of the signal from the bridge is modulated as pressure variations cause the capacitance of the microphone to vary. The modulated 1000 cycle signal is amplified and applied to a detector to which the unmodulated 1000 cps signal is also applied (the detector requires the mixing of these two signals in order to indicate whether the capacitance change which caused the modulation of the carrier is positive or negative); the detected signal is then applied to the wire line terminals.

C. Central Station Equipment

1. The Central Station equipment consists of four amplifier channels, powered either from a 110V AC, or a 6V DC source, and four recording meters. One spare amplifier and one spare recorder are provided.

2. Each channel functions as follows:

The signal from a microphone station is received over a wire line, is mixed with an agitation signal, and both signals are passed through an amplifier and are then applied to the recording meter. Two chronograph pens, located one on either side of the record chart, are used to indicate time; one receives a pulse approximately every 5 seconds from the automatic timing device, every 12th pulse being omitted; the other pen receives a pulse when the manual push button is operated.

D. Circuit Diagrams

Schematics of the capacitance bridge, a Central Station amplifier section and power supply are shown in Figures 1, 2 and 3, respectively.

II. DETAILED DESCRIPTION OF COMPONENTS:

A. Condenser Microphone

The condenser microphone assembly consists of the condenser head and a two-section acoustical low pass filter. The condenser head is mounted at the top of the inner chamber and consists of a thin (.001") stretched aluminum diaphragm mounted symmetrically .004 inches from an insulated metal plate. The low frequency cut-off is controlled by the time constant of the acoustical leak connected to the inner chamber (chamber behind the diaphragm); the high frequency cut-off is controlled by a two section acoustical filter. The band of sound pressure frequencies to which this microphone is responsive is 1 cycle per 15 seconds to 2.5 cycles per second. The upper end of this range is subsequently reduced to 1 cps by the limitations of the recording meter. When a noise reducing array is used, the array itself performs the function of the two-section filter.

B. Capacitance Bridge

The Capacitance Bridge consists of an oscillator, a capacitance bridge modulator, a two-stage amplifier, and a demodulator.

1. Oscillator: The oscillator is of the Hartley type and the frequency of oscillation is determined chiefly by the constants of the tank circuit connected between the grid and the plate circuits of the tube. The plate blocking capacitor (.02 mf) is used to provide a low impedance path for the 1000 cps current while preventing the DC plate voltage from being short circuited to ground. The grid condenser (.005 mc) insulates the grid from ground to permit the bias voltage to develop across the grid resistor and yet allow the 1000 cps voltage to be applied to the grid. This oscillator operates near the Class "A" region.

2. Modulator: A 1000 cps signal of constant amplitude is applied to two terminals of the bridge through an audio transformer and the output of the bridge is connected to the first stage of an audio amplifier as indicated in Figure 1.

3. Amplifier:

a. The audio amplifier is entirely conventional, the first stage being resistance coupled to the second, and the second stage being transformer coupled to the detector. The step attenuator in the input to the second stage consists of ten 3 db steps.

b. A switch allows the first stage of this amplifier to be cut out when the extra amplification is not necessary.

4. Demodulator: The demodulator circuit is a phase sensitive rectifier bridge in which the signal from the oscillator is combined with the amplified unbalance voltage from the bridge to give a rectified output voltage which changes phase when the direction of unbalance of the bridge is reversed. This type of rectifier has been described by Tamm and Bath (Veröffentlichungen aus dem Gebiete der Nachrichtentechnik, vol. 6, pp.51-68, 1936).

5. Meter: A 25-0-25 microampere meter is connected in series with a 250,000 ohm resistor across the detector output for indicating bridge balance and for checking performance.

6. Lightning Protection: A neon bulb is connected across the output terminals of the capacitance bridge to protect the latter against damage by line transients due to lightning.

7. Bridge Power Supply: The bridge is powered from dry batteries which furnish 45 volts plate and 1.5 volts filament. Normally, for the plate supply, one Battery BA-26 is used, or two BA-36's in parallel. For the filament supply, three Batteries BA-35 or 65 in parallel are used. A Battery BA-34 is used for the bias supply.

C. Central Station Equipment

1. Amplifier Assembly

a. The amplifier assembly consists of five identical amplifiers and a power supply. Four amplifiers are in use; the fifth amplifier, a spare, is mounted in the assembly, but has no input or output connections.

b. Amplifier Channel (see Figure 2): The amplifier is essentially an impedance matching device to tran form the voltage input to a current output. The in put circuit is balanced and provides a push-pull input for the two amplifier tubes through an attenuator which has five steps each of 6 db. The tubes are operated approximately Class "B" and the necessary bias is obtained from the resistor in the common cathode circuit. A balance control is provided to equalize the two plate voltages under zero signal conditions. The recording meter is connected directly from plate to plate of the two tubes. Biased (3V) rectifier units are placed across this output circuit to limit the maximum voltage output to ± 3V in order to protect the meter. An agitation circuit which produces a signal of approximately 10 cps is incorporated in each amplifier channel and agitates the pen movement of the corresponding recording meter. This increases linearity of response, particularly for low amplitude signals. A neon lamp relaxation oscillator forms the agitation circuit, the output of which is applied as a push-pull voltage to the grids of the amplifier tubes.

c. Power Supply (see Figure 3): The power supply is actually a dual unit, operating normally from 110V AC and, in case of interruption of service, from a 6V storage battery. The switch over from 110V AC to 6V DC is accomplished automatically by a relay in the 110V AC line when a failure occurs in AC power. When operating on 110V AC power, the line voltage is stepped up by means of a transformer, rectified and filtered. When a power failure occurs, the relay connects the input of a vibrator power supply to a 6V storage battery, and the output of the vibrator is connected to the filter. When operating on 6V, the filter operates with condenser input, whereas when operating on 110V AC, a choke input filter is used. A 0.1 mfd condenser is connected across the relay contacts to prevent excessive arcing when switchover from DC to AC occurs.

2. Recording Meters: Four Esterline-Angus 1 ma recording meters are used to record the signals from the four amplifier channels. The meters are coupled mechanically to insure synchronization. Two chronograph pens have been added to each of these meters to enable time marks to be recorded. These pens are located one on either side of the record chart.

3. Timing Device: The timing device consists of a 6 volt DC battery-driven electric motor geared to a cam which closes a switch approximately every 5 seconds, omitting every 12th pulse to indicate the one minute intervals. A separate battery is provided for this motor. The circuits controlled by this switch apply voltage pulses to the left hand chronograph pens on the recording meters.

4. __Manual Timing Marks:__ An electric pulse can be applied to the second chronograph pen on each recorder by pressing a manual timing push button switch. Time signals from WWV or a similar source are used for the manual timing marks.

CONFIDENTIAL

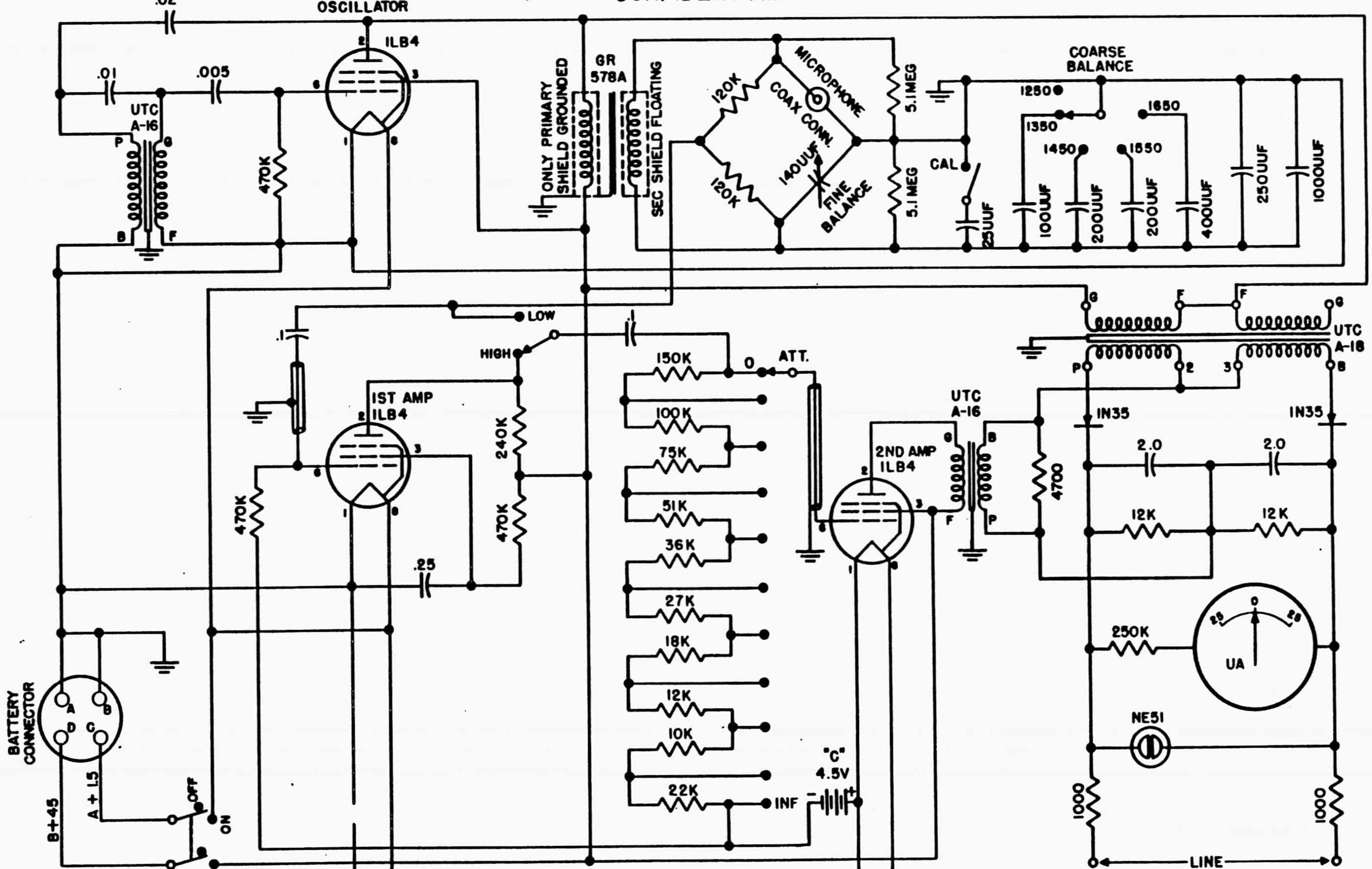

BATTERIES:
"A"-3 BA35 IN PARELLEL
"B"-2 BA36 IN PARELLEL OR 1-BA26
"C"-1 BA34

MICROPHONE STATION EQUIPMENT
CONFIDENTIAL

APPENDIX B

FIG I

This document is part of an unclassified series

CONFIDENTIAL

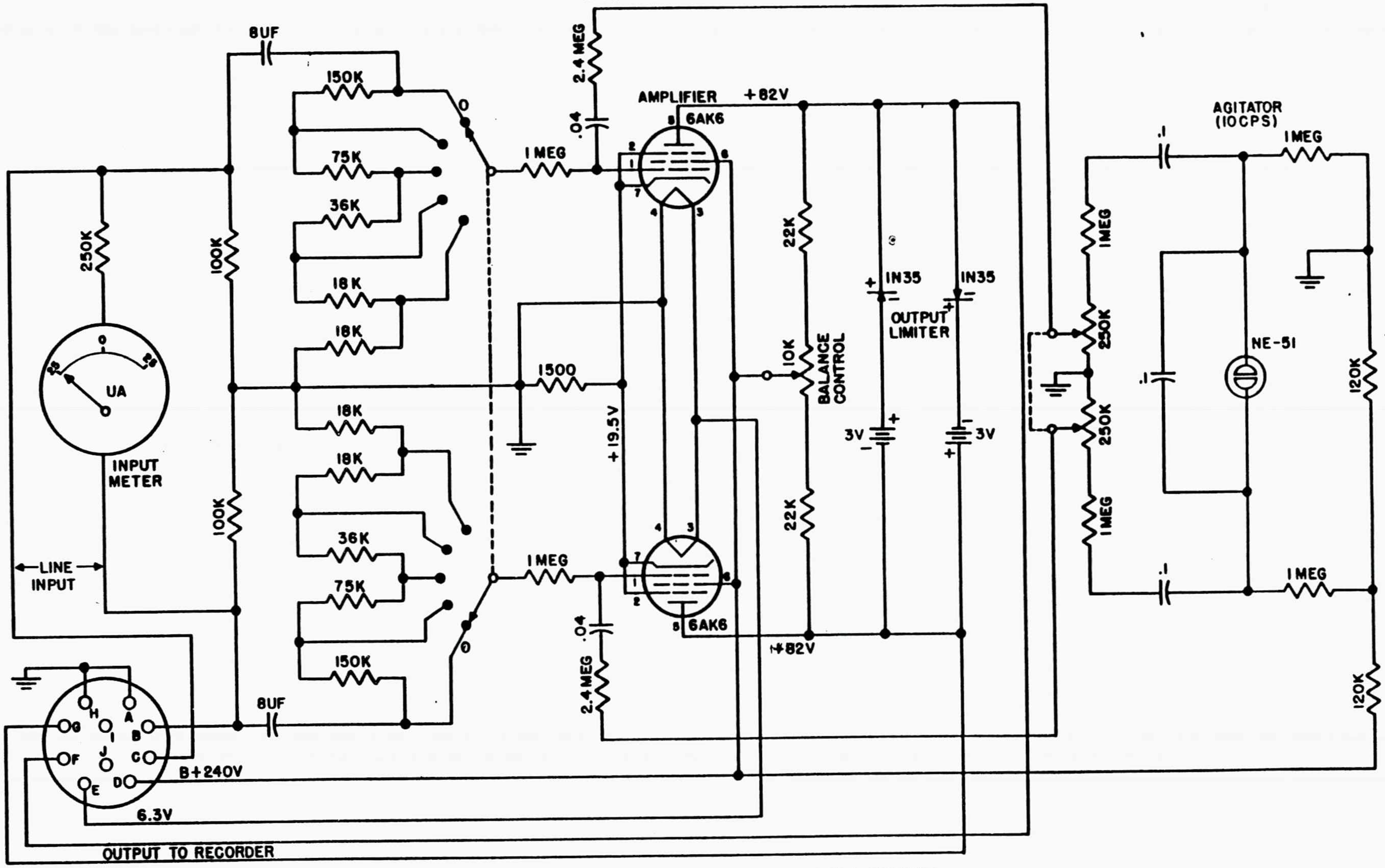

ALL RESISTORS 1/2 WATT

APPENDIX B

FIG 2

CENTRAL STATION CHANNEL AMPLIFIER
CONFIDENTIAL

CONFIDENTIAL

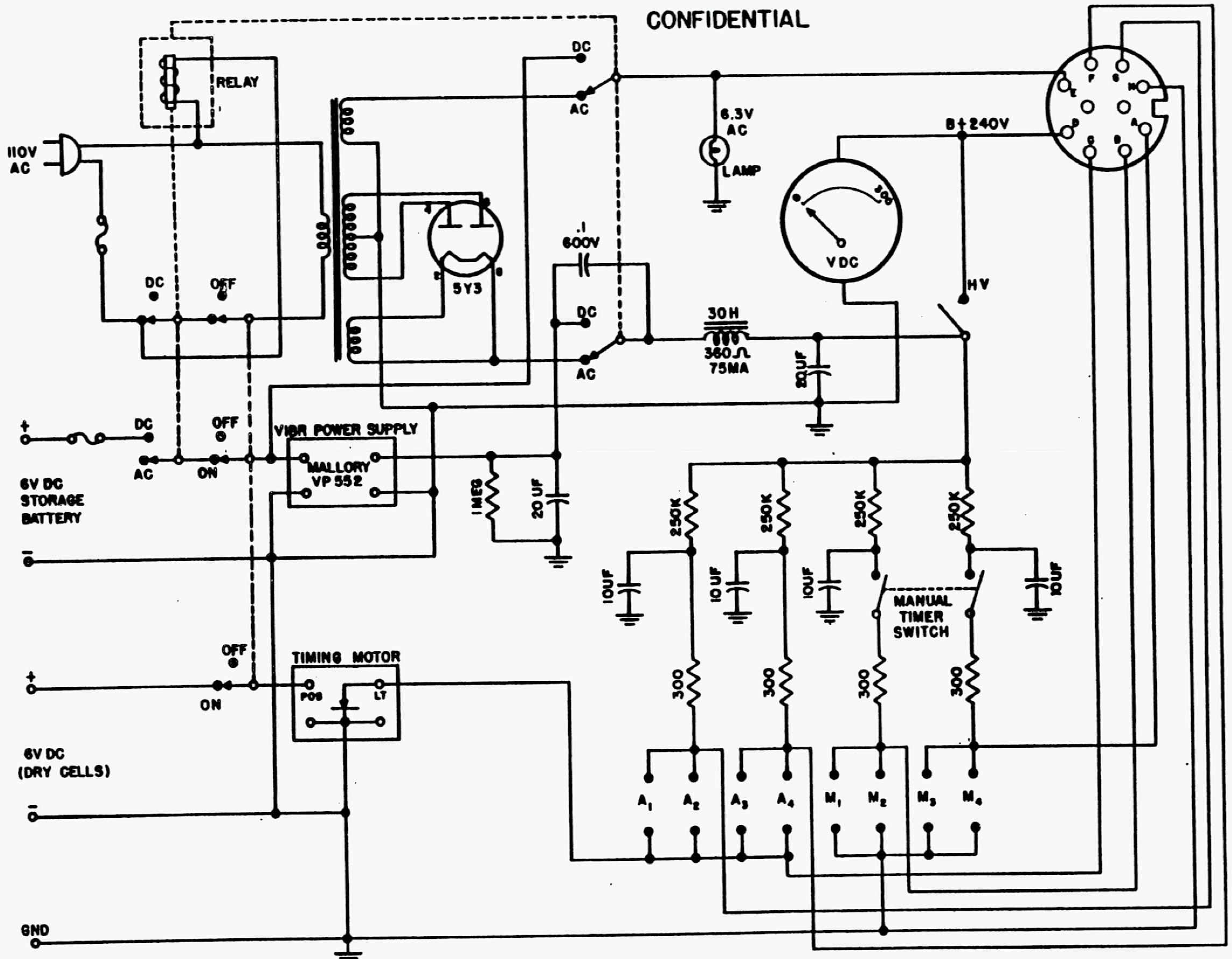

CENTRAL STATION POWER SUPPLY AND TIMER
CONFIDENTIAL

APPENDIX B

FIG 3

APPENDIX C

NOISE REDUCING ACOUSTICAL ARRAY

1. INTRODUCTION

a. The Noise Reducing Acoustial Array is essentially a network of pipes coupling an infra-sonic microphone to the atmosphere through a large number of openings which are distributed over an area. The microphone will then register average pressure fluctuations over the area, instead of fluctuations at a point. In this way "noise" due to atmospheric turbulence is reduced. The noise reduction should not be accompanied by signal attenuation, if maximum sensitivity is to be maintained. If signal attenuation does occur, the loss can be compensated for by increase in amplifier gain but the system must be so designed that attenuation does not vary with frequency. The array described below was so designed that no attenuation occurs throughout the desired frequency range.

b. For practical reasons, it was decided to use as small an array as possible, and the arrangement shown in Figure 1 was chosen. This array consists of four sub-arrays, each of which is coupled to the atmosphere through 16 openings (acoustical resistances) and to a center section containing the microphone through a series resistance. The maximum dimension of each sub-array is taken to be approximately one tenth wavelength at the upper end of the desired frequency range. This permits use of an equivalent electrical circuit in which all quantities are lumped constants. The equivalent circuit is shown in Figure 2 in which the parallel resistance of all openings in each sub-array is designated by the single resistance R_1. This equivalent circuit is seen to be a two section RC filter, and by suitable choice of the quantities R_1, R_2, C_1, and C_2 is given a "cut-off" frequency of 2.5 cps, (i.e., output is down 2 db at 1.25 cps, 6 db at 2.5 cps, 15 db at 5 cps, and drops at a rate of 12 db per octave at higher frequencies.)

2. THEORY

a. Evaluation of the Network Parameters

In order to obtain numerical values for the constants of Figure 2, it is necessary to develop a general theory of the electrical analogy for sound transmission in a conduit. In this development, the following notation is used:

ρ density
f frequency
ω $2\pi f$
C_p specific heat at constant pressure
K thermal conductivity
μ viscosity
η $(\omega \rho C_p/2K)^{1/2} = 4.06f^{1/2}$ for air at 20°C
σ $(\omega \rho/2\mu)^{1/2} = 4.57f^{1/2}$ for air at 20°C

k	$(-j\rho\omega/\mu)^{1/2} = \sigma(-2j)^{1/2}$
a	radius of conduit
V	velocity of sound in conduit
c	velocity of sound in air
γ	propagation constant

The transmission characteristics of conduit for sound waves may be investigated by using the equivalent T section of Fig. 3. The series elements in this T section represent the effective mass of the gas in the tube and the frictional losses due to viscosity. The shunt elements represent the acoustical capacitance of the enclosed volume of gas and the energy loss due to heat conduction to the walls.

In this representation, L, R, C' and G are, in general, not constants, but are functions of $af^{1/2}$. R and L are obtained from the real and imaginary parts of the expression for the impedance of a conduit derived by Crandall, (Theory of Vibrating Systems and Sound, D. Van Nostrand Co., Appendix A). C' and G are obtained from the real and imaginary parts of the expression for the impedance of a cylindrical enclosure derived by Daniels (Acoustical Impedance of Enclosures, Journal of the Acoustical Society of America, Vol. 19, No. 4, 569-571 July, 1947).

From equation (G) of the first reference, after solving for Z and dividing by the cross sectional area in order to express the result in terms of acoustical ohms, we get

$$Z = R + j\omega L = \frac{1}{\pi a^2} \; \frac{-\mu k^2}{1 - \dfrac{2}{ka}\dfrac{J_1(ka)}{J_o(ka)}} \tag{1}$$

From the second reference, taking the reciprocal of impedance and dividing by the length in order to express the result as admittance per unit length, we get

$$Y = G + j\omega C' = \frac{\pi a^2 \omega}{\rho c^2} (C^2 + D^2)^{1/2} e^{-j\phi} \tag{2}$$

(The quantities $(C^2 + D^2)^{1/2}$ and ϕ are defined in the reference.)

Substituting the value of k into (1), we get

$$Z = \frac{j\rho\omega}{\pi a^2}\left\{1 - \frac{2}{\sigma a(-2j)^{1/2}} \; \frac{J_1\left[\sigma a(-2j)^{1/2}\right]}{J_o\left[\sigma a(-2j)^{1/2}\right]}\right\}^{-1}$$

$$= \frac{j\rho\omega}{\pi a^2}(A + jB)^{-1} = \frac{\rho\omega}{\pi a^2}(A^2 + B^2)^{-1/2} e^{j\Psi} \tag{3}$$

where $\sigma = (\rho\omega/2\mu)^{1/2}$
$\Psi = \tan^{-1} A/B$
$A = 1 + (1/\sigma a)\ (F + G)$
$B = (1/\sigma a)\ (G - F)$
$F = (VX - UY)/(U^2 + V^2)$
$G = (UX + VY)/(U^2 + V^2)$
$V =$ Imaginary part of $J_0[\sigma a(-2j)^{1/2}]$
$U =$ Real part of $J_0[\sigma a(-2j)^{1/2}]$
$X =$ Real part of $J_1[\sigma a(-2j)^{1/2}]$
$Y =$ Imaginary part of $J_1[\sigma a(-2j)^{1/2}]$

From electrical network theory, the characteristic impedance Z_0 and propagation constant γ are given by

$$Z_0 = (Z/Y)^{1/2}$$
$$\gamma = \alpha + j\beta = (ZY)^{1/2}$$

Substituting the values of Z and Y from (1) and (2),

$$Z_0 = \frac{\rho c}{\pi a^2} (C^2 + D^2)^{-1/4} (A^2 + B^2)^{-1/4} e^{j\frac{(\Psi + \phi)}{2}} \tag{4}$$

$$\gamma = \frac{\omega}{c} (C^2 + D^2)^{1/4} (A^2 + B^2)^{-1/4} e^{j\frac{(\Psi - \phi)}{2}} \tag{5}$$

whence $$\alpha = |\gamma| \cos \frac{(\Psi - \phi)}{2} \tag{6}$$

$$\beta = |\gamma| \sin \frac{(\Psi - \phi)}{2} \tag{7}$$

and $$V = \omega/\beta \tag{8}$$

From the above results, numerical values have been computed, assuming the conduit to be filled with air at 20°C. The following procedure was used in carrying out the computation. For a series of assumed values of $a\eta$, the corresponding values of $a\sigma$ and $af^{1/2}$ were tabulated, using the relation

$$\frac{a\sigma}{a\eta} = \frac{4.57\ af^{1/2}}{4.06\ af^{1/2}} = 1.126$$

The quantities $A^2 + B^2$, $C^2 + D^2$, Ψ, and ϕ were computed for each set of values of $a\eta$, $a\sigma$, and $af^{1/2}$, using the relations derived above and in the reference by Daniels. Then, using equations (2) to (8) inclusive, the following quantities were calculated and plotted as functions of $af^{1/2}$:

$$\frac{\rho c^2}{\pi a^2 \omega}|Y|,\ \phi,\ \frac{\pi a^2}{\rho\omega}|Z|,\ \psi,\ \frac{\pi a^2}{\rho c}|Z_o|,\ \theta_{Z_o}\ (= \arg Z_o),$$

$$\frac{c}{\omega}|\gamma|,\ \theta_\gamma\ (= \arg \gamma),\ V/c, \text{ and } \tan\psi.$$

(Figures 4 to 13 inclusive). This last quantity ($\tan\psi$) is equal to the Q of a short length of narrow tubing open at the end. The attenuation constant α has been plotted as a function of f for conduit of a wide range of radii. (Figure 14).

b. <u>Equivalent T Section of a Finite Length of Conduit</u>

It is shown in texts on network theory that a section of transmission line of length ℓ can be represented by the equivalent T section of Figure 15. For $\gamma\ell$ sufficiently small, the series and shunt elements become, respectively

$$Z_o \tanh\frac{\gamma\ell}{2} = \frac{Z_o\gamma\ell}{2} = \frac{\sqrt{\frac{Z}{Y}}\sqrt{ZY}\,\ell}{2} = \frac{Z\ell}{2}$$

$$\frac{Z_o}{\sinh\gamma\ell} = \frac{Z_o}{\gamma\ell} = \sqrt{\frac{Z}{Y}} \times \frac{1}{\sqrt{ZY}\,\ell} = \frac{1}{Y\ell}$$

(These values are the ones which would be obtained by lumping the distributed values of impedance and admittance).

The ratio of the absolute value of the total series impedance to that of the total shunt impedance is

$$\left|\frac{Z\ell}{\frac{1}{Y\ell}}\right| = \frac{\ell^2\,\omega^2}{c^2}\frac{(C^2 + D^2)^{1/2}}{(A^2 + B^2)^{1/2}}$$

This ratio may be used to study the following two special cases, which are of particular importance:

(1) Output short circuited, corresponding to an open ended tube.

If $\quad |Z\ell| \ll \left|\frac{1}{Y\ell}\right|,$

the input impedance will be $Z\ell$. Setting $c = f\lambda$, this inequality can be expressed as

$$4\pi^2\frac{\ell^2}{\lambda}\frac{(C^2 + D^2)^{1/2}}{(A^2 + B^2)^{1/2}} \ll 1$$

or $$\frac{\ell}{\lambda} \ll \frac{1}{2\pi} \frac{(A^2 + B^2)^{1/4}}{(C^2 + D^2)^{1/4}}$$

(Note that λ is the wavelength of sound in air, and not in the tube). Whenever the output load is of such value that the open ended condition is approximated, a tube of length ℓ/λ which satisfies this inequality may be used as a series circuit element of value $Z\ell$.

(2) Output open-circuited, corresponding to a closed tube. In this case, because of open-circuited output, if ℓ/λ satisfies the above inequality, the input impedance will be equal to $1/Y\ell$. If the tube diameter is large enough so viscous resistance can be neglected, the condition is approximately $\ell \ll \lambda/10$. A particular application of the above special cases occurs when one considers a large diameter tube of length $\ell (\ll \lambda/10)$ plugged at both ends, with a very short small hole of length ℓ' drilled through one of the plugs. The equivalent circuit of this combination is an impedance $Z\ell'$ in series with an impedance $1/Y\ell$. Values of Z and Y may be obtained from the curves. For sufficiently large $af^{1/2}$ the large tube becomes a pure capacitance $C = \pi a^2 \ell / \rho c^2$, and for small values of $af^{1/2}$ the small hole becomes a pure resistance, the value of which may be calculated by Poseulle's formula... $R = 8\mu\ell/\pi a^4$. By appropriate choice of $af^{1/2}$ for the small hole, the LCR system can be given any desired Q value, and consequently any desired degree of damping.

3. DESIGN OF ARRAY

a. Application of the Theory

In applying the general theory outlined above to the actual design of the pipe network, approximate values for R and C were first calculated, using Poiseulle's formula for R, and taking $C = \pi a^2 \ell / \rho c^2$. In this approximate solution, the resistance of all 16 openings of each sub-array were considered as being in parallel, and the total length of pipe was taken for ℓ in the expression for C. (This procedure assumes adiabatic pressure changes and neglects equivalent inductance). The design was then checked by setting up the complete equivalent electrical circuit of the array, using exact values of Y and Z from the plotted curves to calculate the attenuation of a signal traveling from one of the most remote openings to the center, where the microphone was located.

b. Design Constants

(1) Choice of Pipe Diameter

If the pipe is to function as a pure acoustical capacitance, its dimensions must be so chosen that pressure changes in the pipe are either adiabatic or isothermal throughout the entire frequency range. The plotted values of Y indicate that the impedance of a two inch diameter pipe is close enough to a pure reactance and constant enough over the desired frequency range of 0.06 cps to 1 cps for practical purposes. (Pressure changes in pipe of this diameter are approximately adiabatic.) Eight foot lengths of pipe were used for the initial design, but this was changed to ten feet for later installations, in order to utilize standard lengths.

(2) Acoustical Plugs

At each point indicated by a circle in Figure (1) there is either a tee or a cap which is drilled and tapped for a brass pipe plug. A hole in each plug serves as an acoustical impedance which couples the air enclosed in the pipe to the atmosphere. Using the Q values plotted in Figure 13 the dimensions of this hole are so chosen that it is a pure resistance of the desired value. (A value is chosen for the radius which makes the reactive component negligible.)

c. Installation of Array

For the first array constructed, the entire system was buried in the ground, the center of the pipe being about 9 inches below the surface. At those points where the acoustical plugs are located, holes 10 inches in diameter and 18 inches deep were excavated. These holes were walled with stainless steel cylinders to prevent caving in of earth and were covered by stainless steel caps into which a one-inch diameter tube, 5 inches long was set for communication with the atmosphere. (see Figure 16). This arrangement eliminates pressure variations due to the turbulence which would be created if any part of the system were to project above the surface of the earth. It also prevents obstruction of the acoustical plugs by moisture in case of rain. Subsequent arrays were installed on the surface of the earth, with provision for frequent drainage of any water which may collect.

d. Microphone

The microphone is connected directly to the center section of the array and is identical with the microphone used in standard equipment for Project SPECTACLES, with the exception that both acoustical plugs are removed because their function is performed by the acoustical plugs in the array.

4. TEST RESULTS

a. Comparison with Standard Microphone

A direct comparison was made between the output of a microphone connected to the array and a standard microphone having identical sensitivity and frequency characteristics placed on the ground near the center of the array. Figure 17 is a record of the output of the standard microphone, and Figure 18 that of the array. Figure 19 is a record of the output of the standard microphone, located in a wooded area, a few hundred yards distant from the open field in which the array was installed. It is seen that use of the array results in a decided improvement, but that location of the microphone in woods is about as effective.

b. Results on an Infra-Sonic Signal

Figure 20 is a record of an infra-sonic signal of unknown origin made with the array and Figure 21 is a record of the same signal made with a standard microphone located in a wooded area a few hundred yards distant. It is obvious that the array doesnot attenuate a true sound wave, but only attenuates noise due to turbulence.

5. CONCLUSIONS

The Noise Reducing Acoustical Array when installed in an open field greatly attenuates noise due to atmospheric turbulence without attenuating the desired signal. Approximately the same degree of noise attenuation can be obtained however, by locating a standard microphone in woods with dense underbrush. Use of the array would be indicated in locations where no wooded areas of the desired type exist.

NOISE REDUCING ACOUSTICAL ARRAY

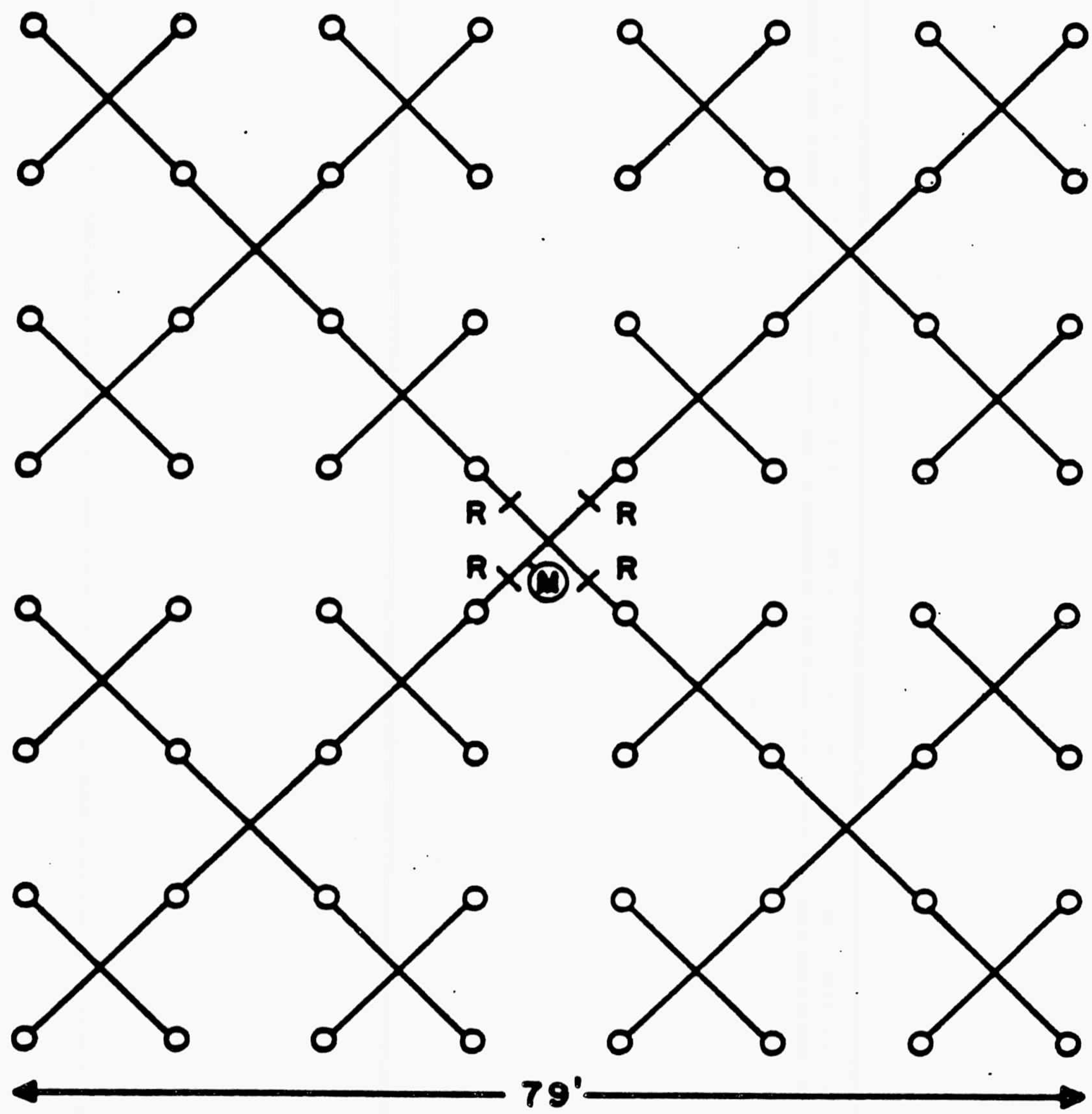

M - MICROPHONE
R - COUPLING RESISTANCES
O - ACOUSTICAL PLUGS

FIGURE 1
APPENDIX C

EQUIVALENT ELECTRICAL CIRCUIT OF ARRAY

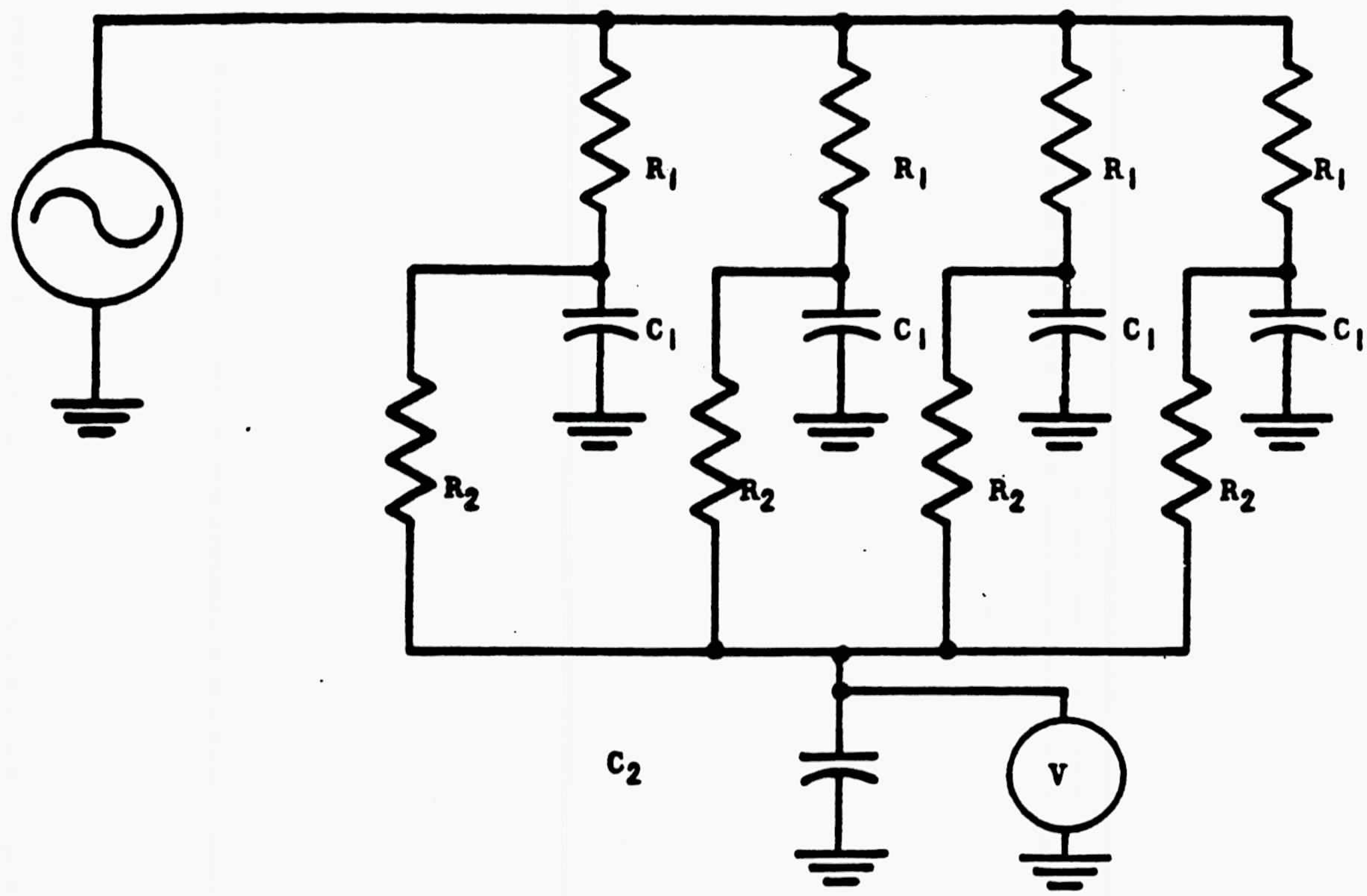

R_1 - parallel resistance of openings in one sub-array.

C_1 - Acoustical capacitance of volume of air in one sub-array.

R_2 - coupling resistance

C_2 - Acoustical capacitance of volume of center section containing microphone.

V - Voltmeter representing microphone (pressure is analogous to voltage)

FIGURE 2
APPENDIX C

EQUIVALENT T SECTION OF A CONDUIT

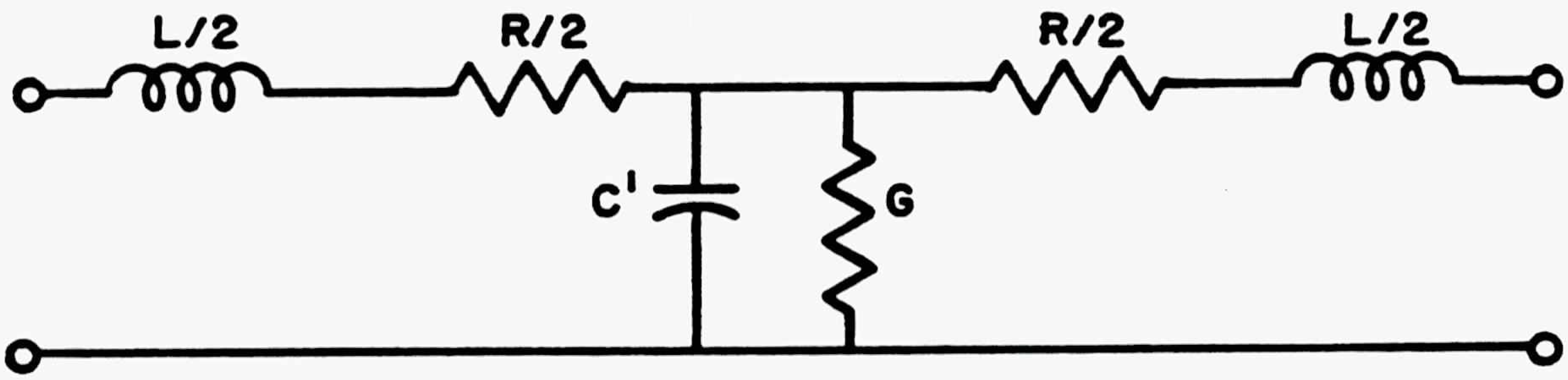

FIGURE 3
APPENDIX C

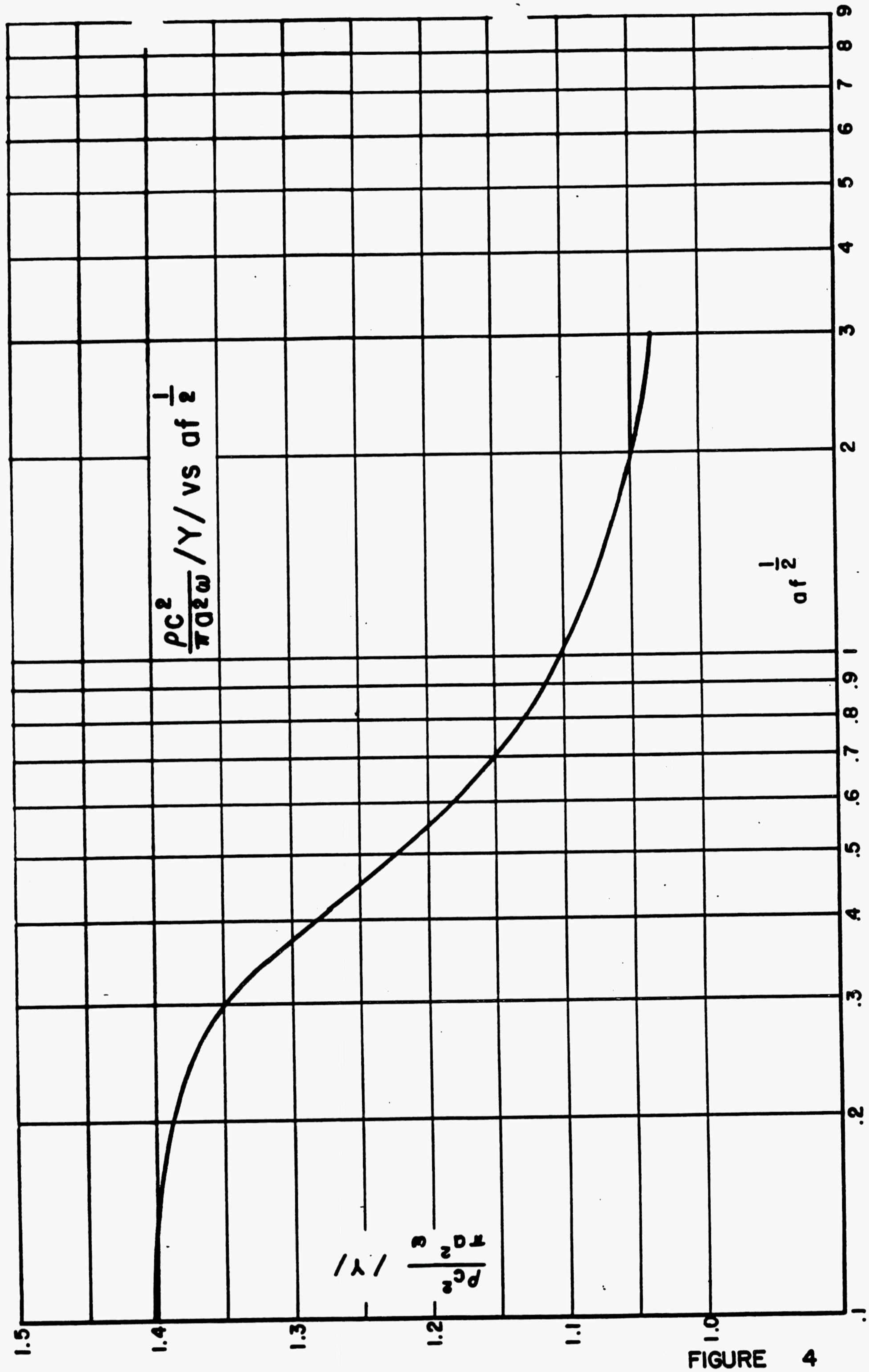

FIGURE 4
APPENDIX C

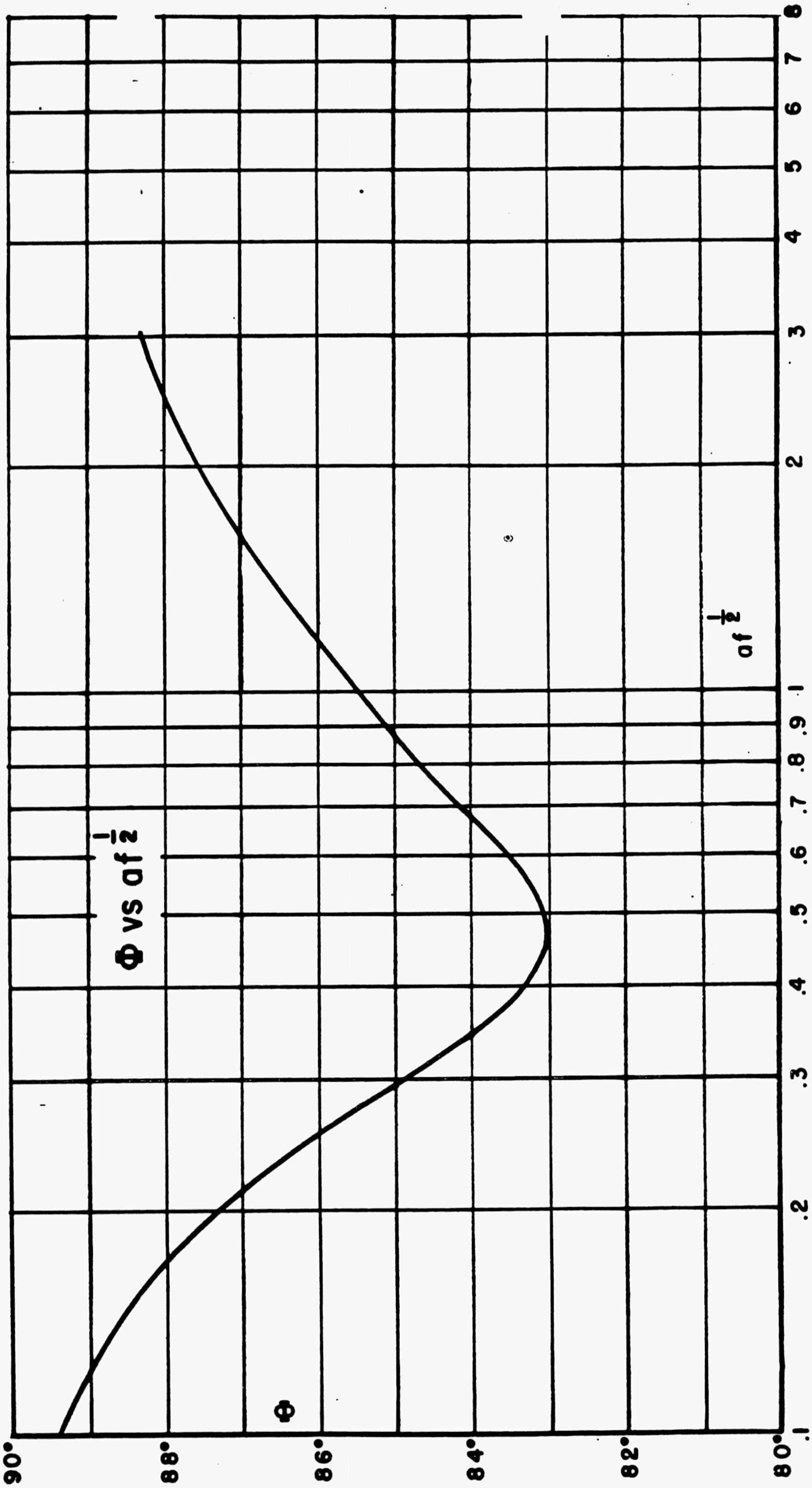

FIGURE 5
APPENDIX C

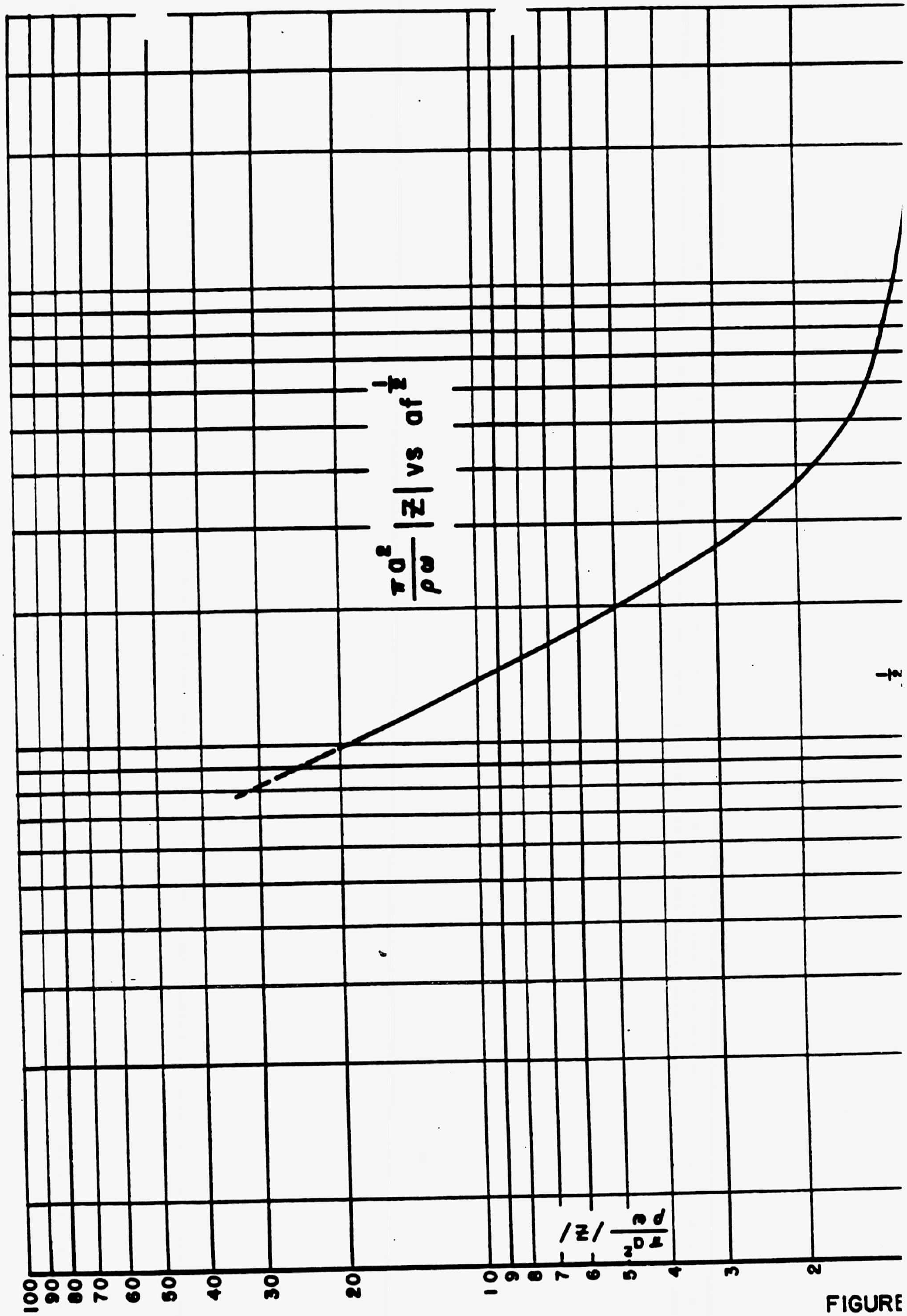

FIGURE

APPENDI

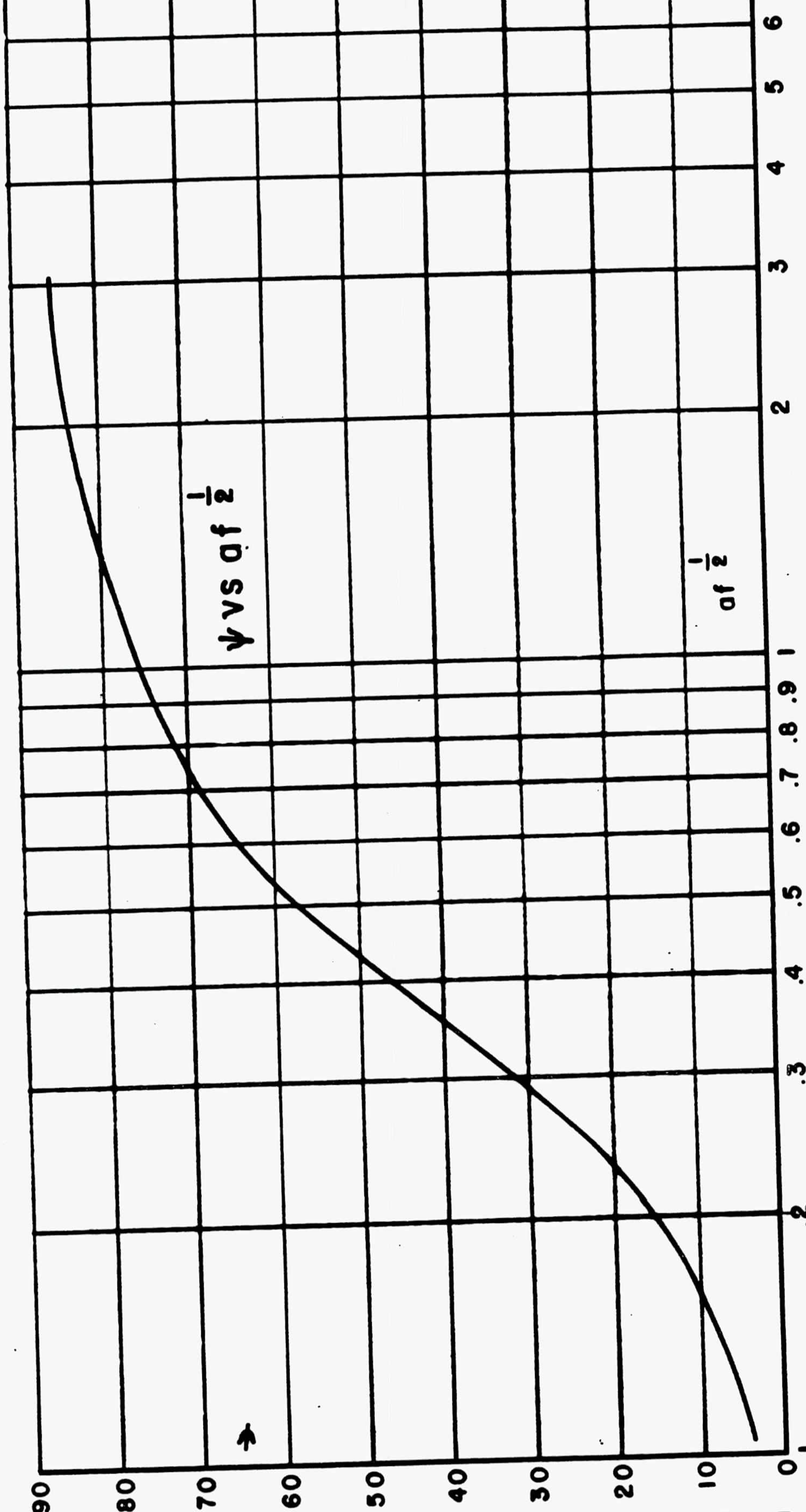

FIGURE 7
APPENDIX C

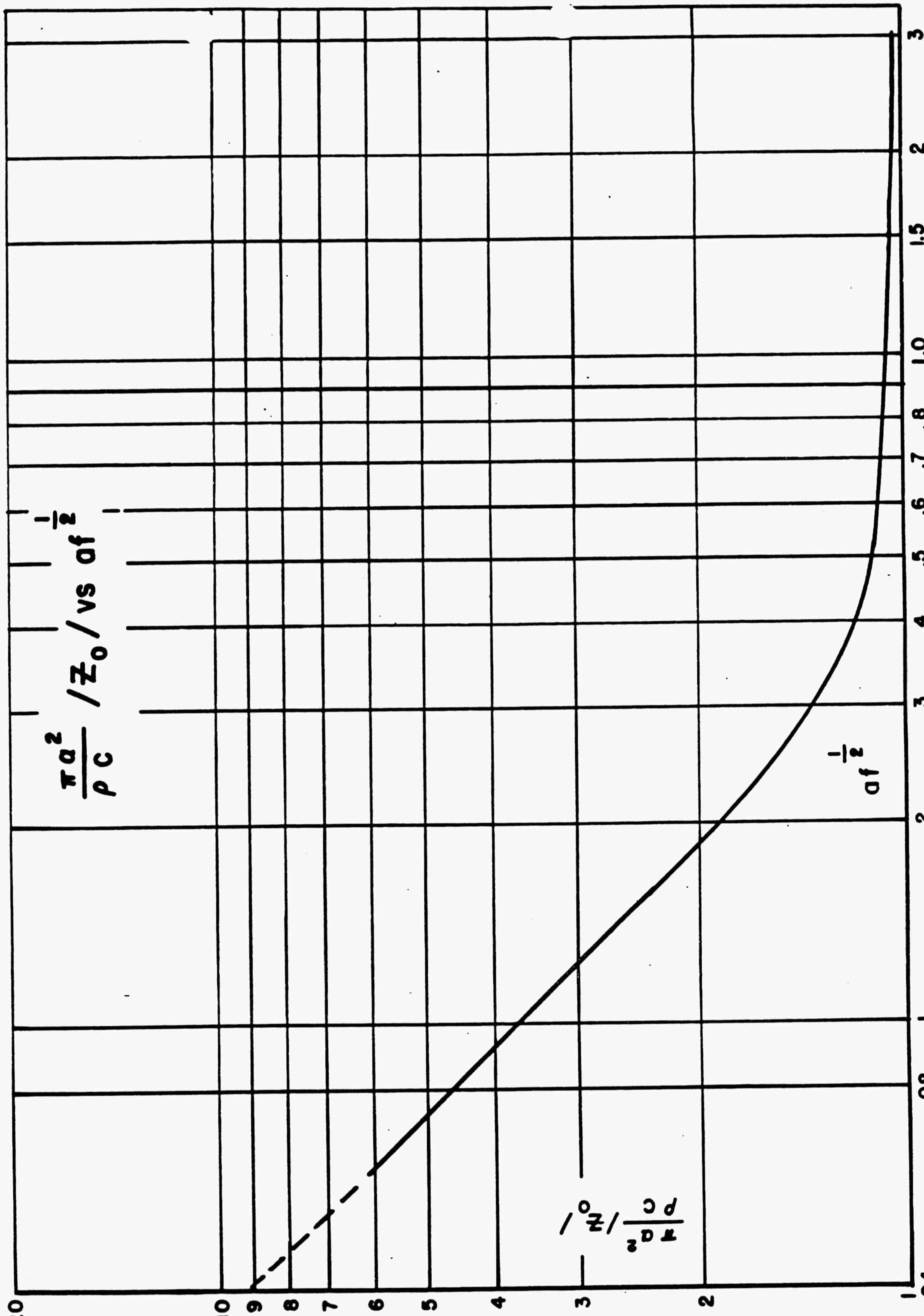

FIGURE 8
APPENDIX C

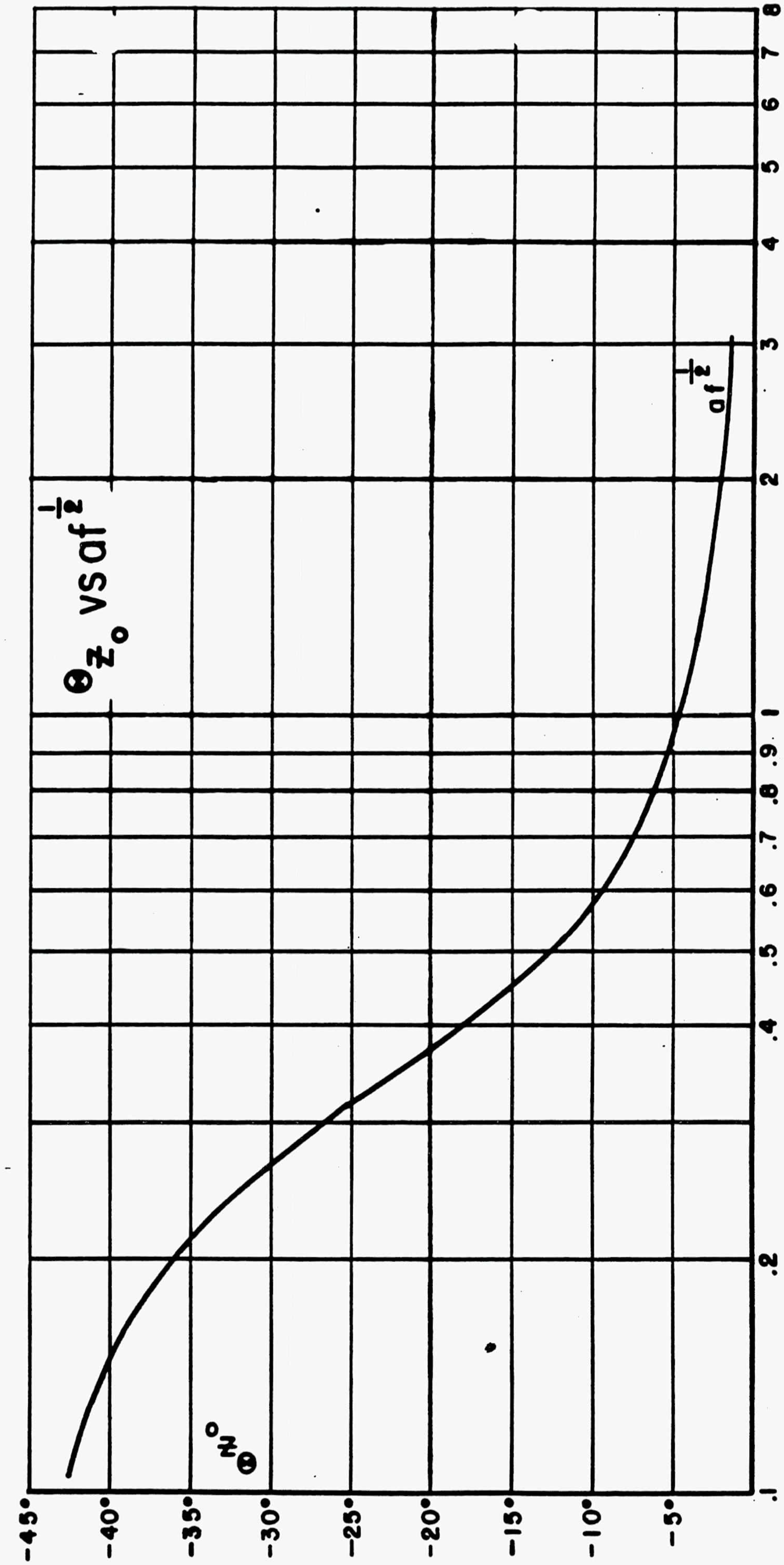

FIGURE 9
APPENDIX C

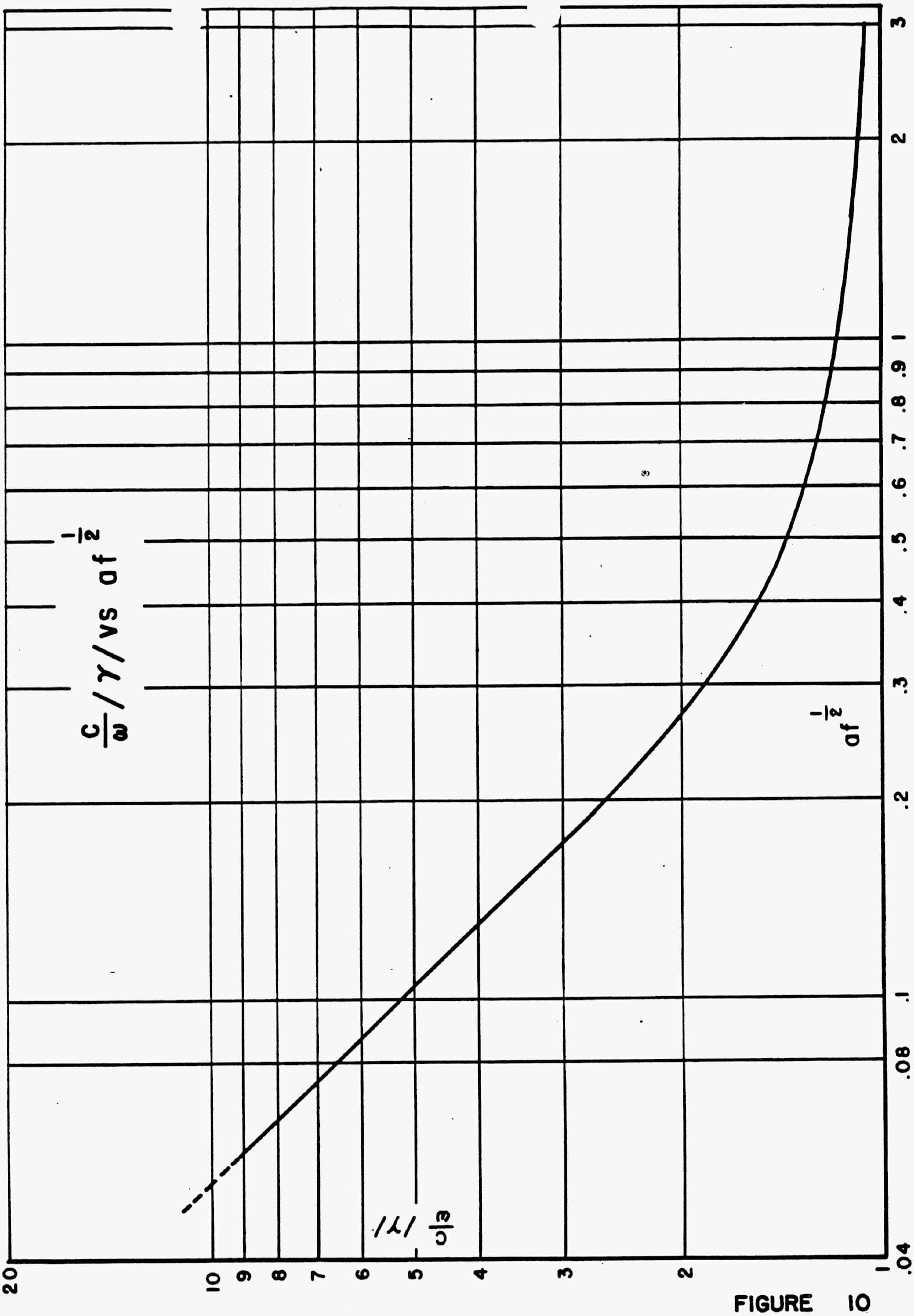

FIGURE 10
APPENDIX C

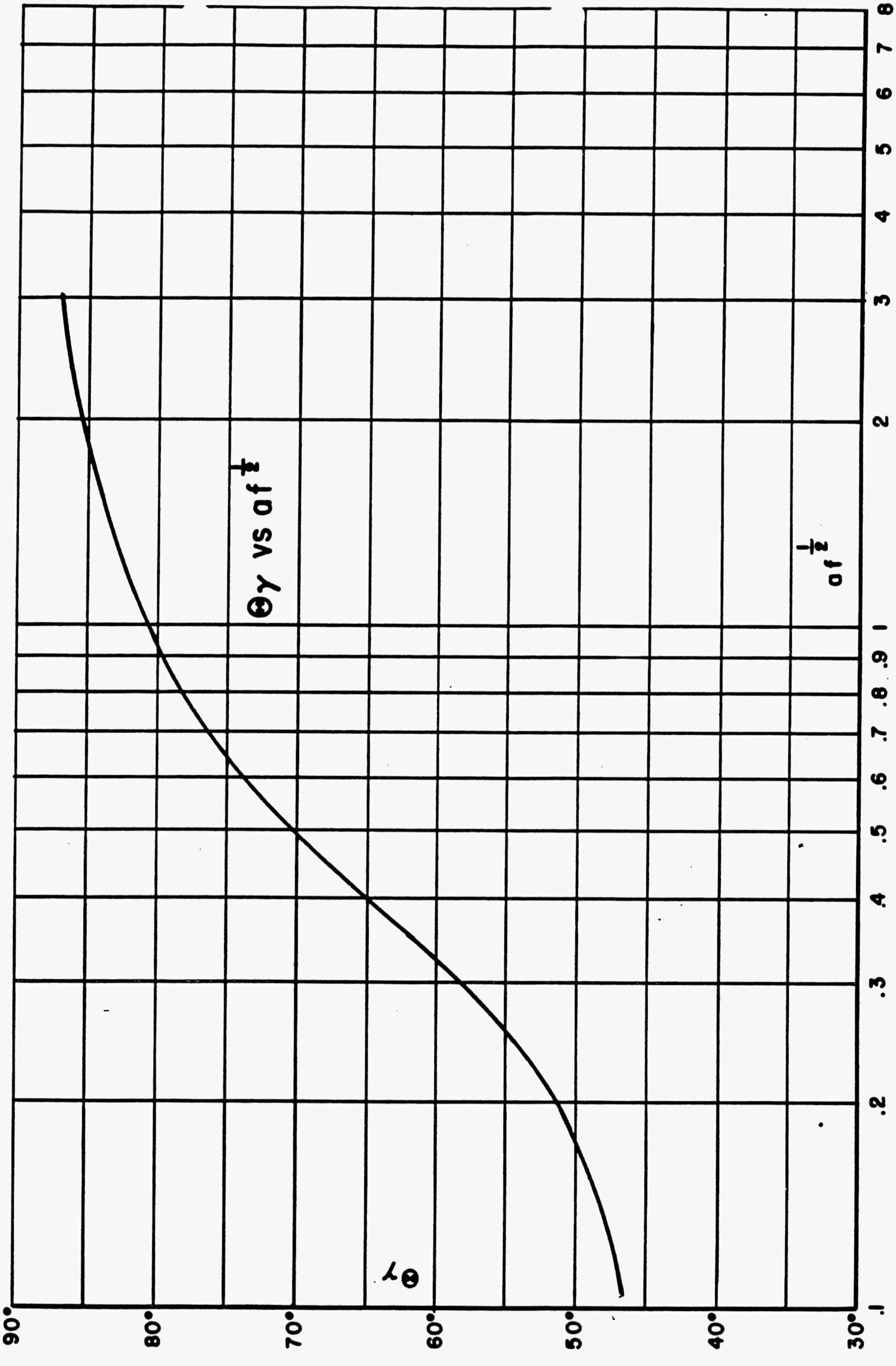

FIGURE 11
APPENDIX C

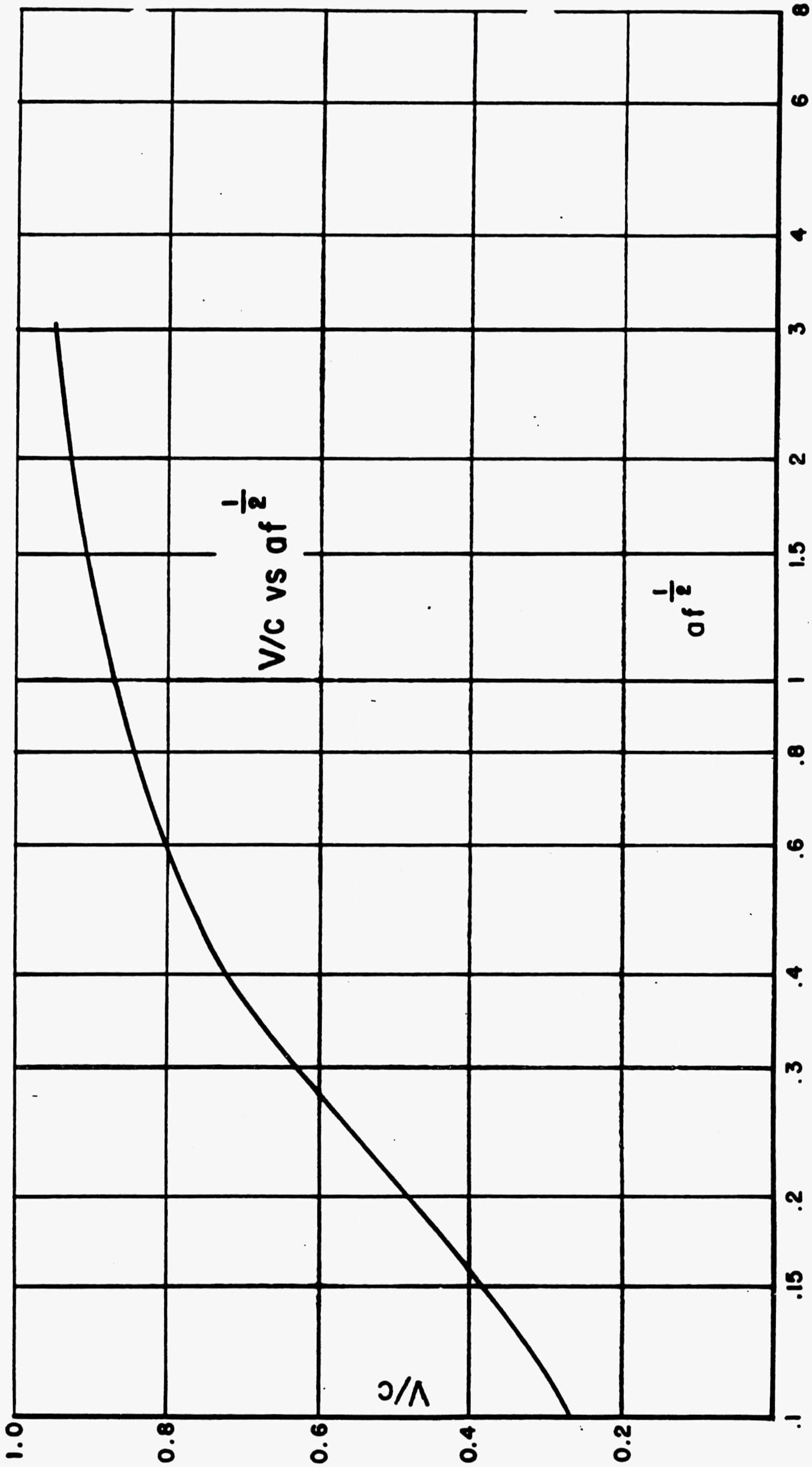

FIGURE 12
APPENDIX C

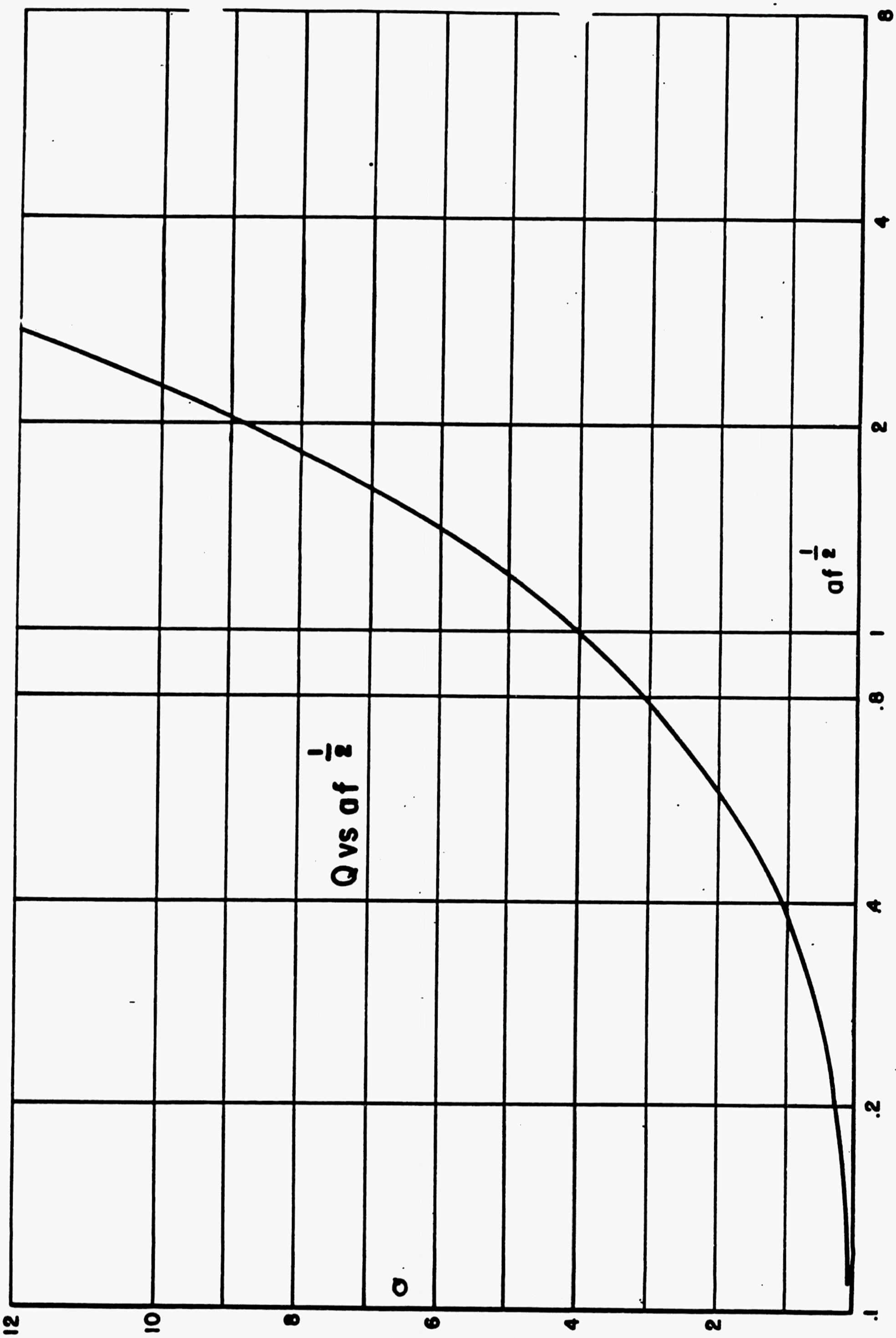

FIGURE 13
APPENDIX C

ATTENUATION CONSTANT α vs FREQUENCY
FOR PIPES OF RADIUS a

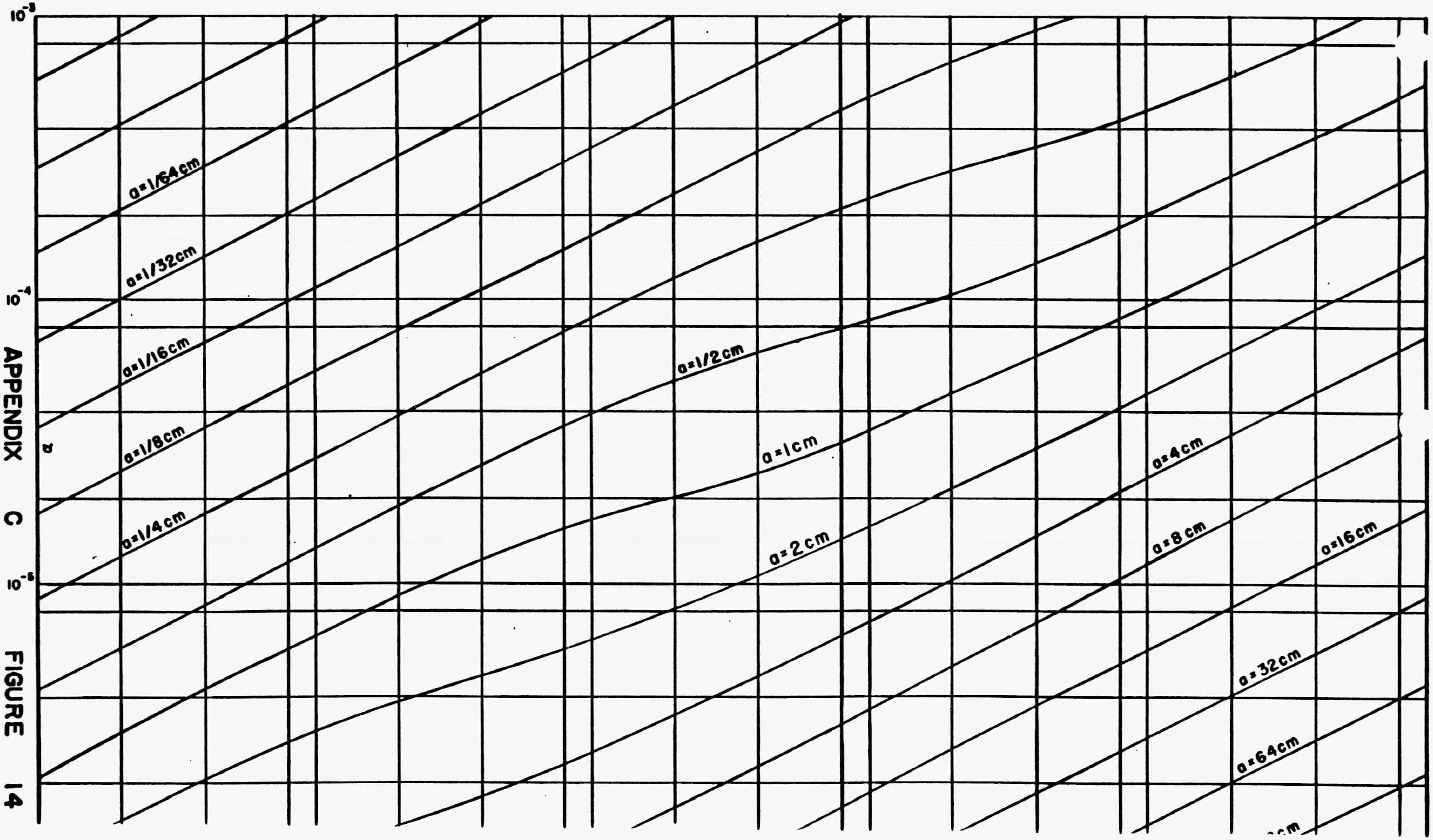

APPENDIX C FIGURE 14

EQUIVALENT T SECTION OF TRANSMISSION LINE

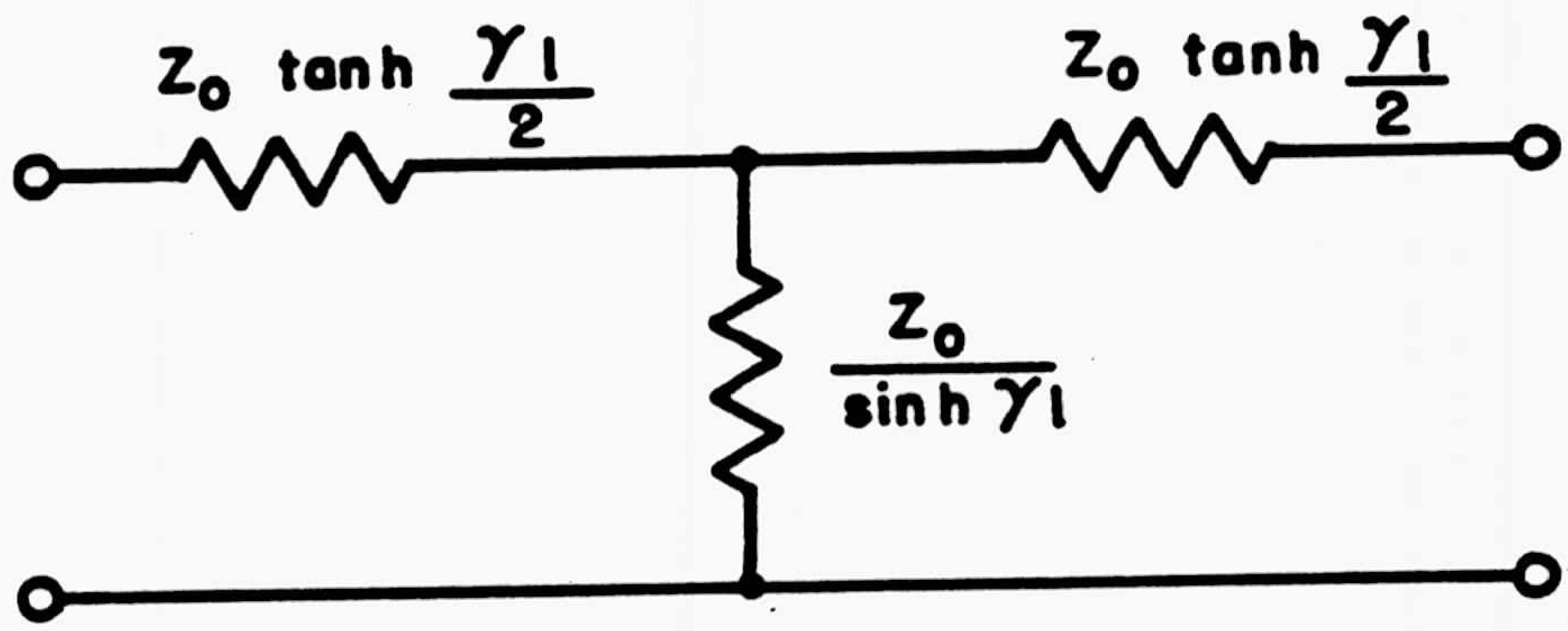

FIGURE 15
APPENDIX C

NOISE REDUCING ACOUSTICAL ARRAY (DETAIL)

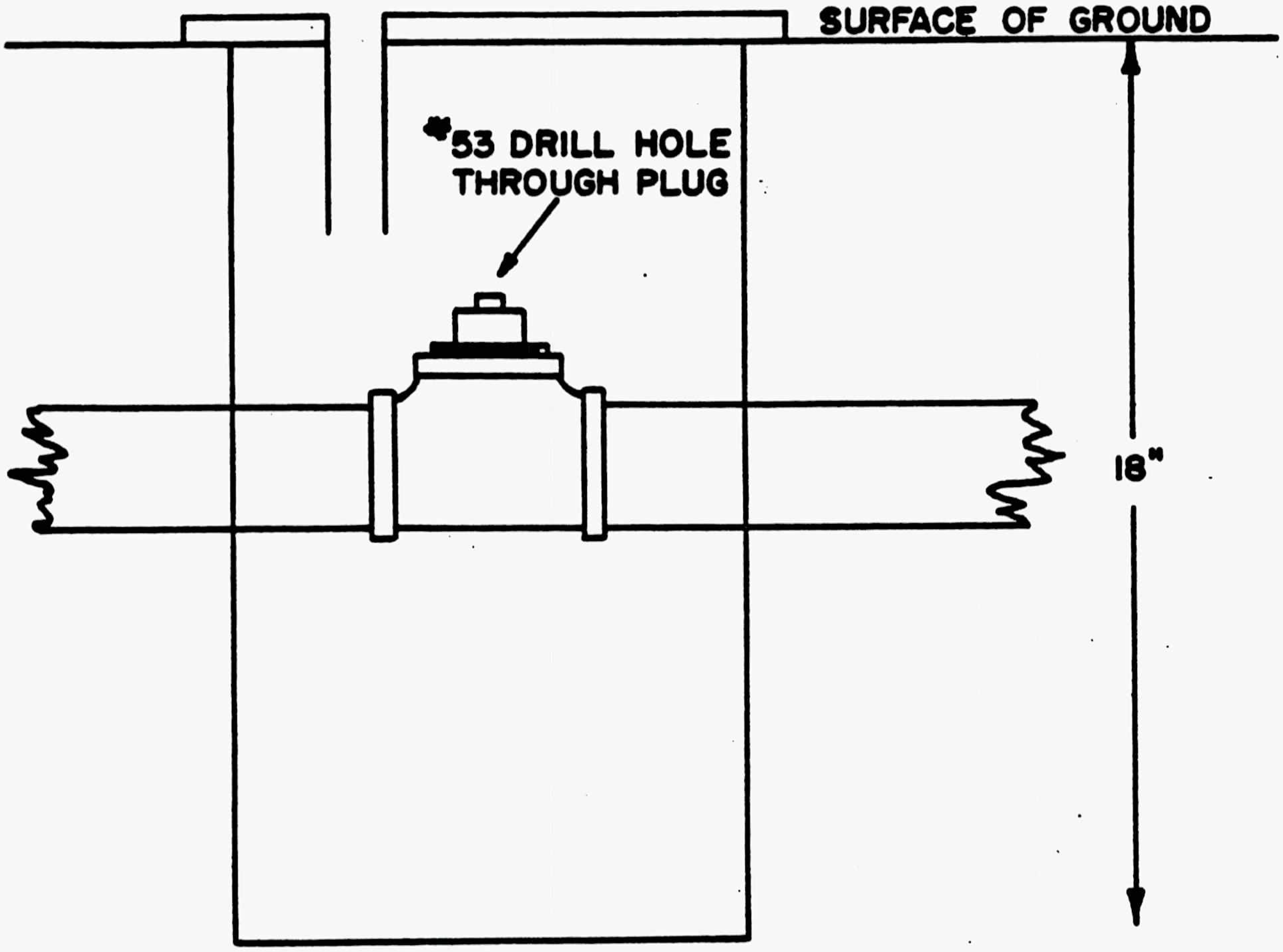

FIGURE 16
APPENDIX C

Fig. 17

Standard Microphone
in open Field

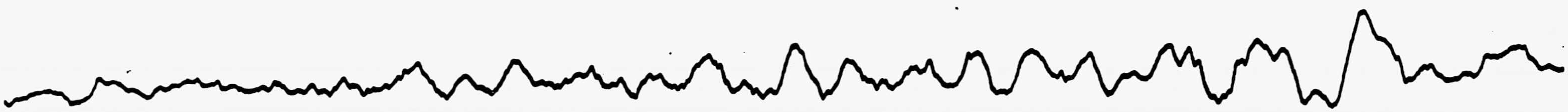

APPENDIX C

Fig. 18

Noise Reducing Array

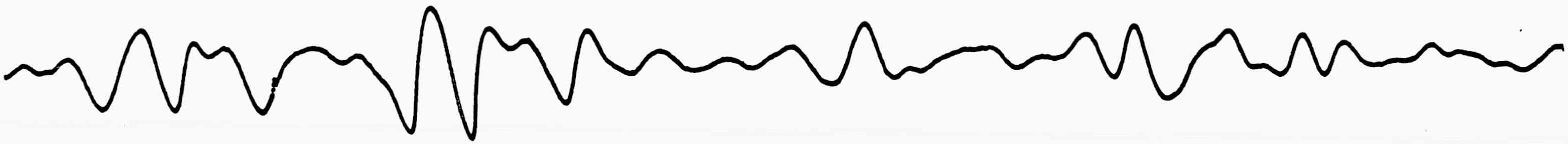

Fig. 19

Standard Microphone in Woods

APPENDIX C

Fig. 20

Infra Sonic Signal
(Noise Reducing Array)

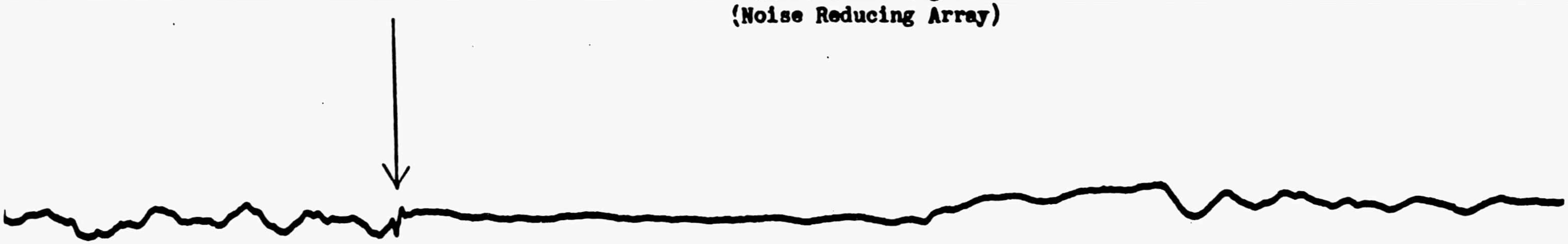

Fig. 21
Infra Sonic Signal
(Microphone in Woods)

APPENDIX C

APPENDIX D

PROCEDURE FOR ANALYSIS OF DATA FROM INFRASONIC SYSTEM M-2

1. General Principles

a. It is the purpose of this report to provide procedures for the interpretation of recordings, for the identification of significant signals and for the evaluation of direction and velocity of a sound arrival.

b. The physical principles involved in the evaluation of direction and velocity of sound by the array of microphones employed in this system are the following:

(1) The significant signal to be detected is a pressure change in a relatively short interval of time, i.e., a pulse or transient. As an example, the sound wave due to the firing of an artillery piece is a transient pressure change.

(2) The signal, if significant, will display certain identifying characteristics on all microphones in the array. That is to say, the recorded time changes of pressure on all four microphones in the array will show a marked degree of resemblance, except in certain details which are discussed in subparagraph (3) of paragraph 4d below.

(3) These significant signals, provided their origin is beyond the area encompassed by the array, will propagate over the array at a definite velocity. Accordingly, depending on the direction from which the sound is approaching the array, there will be a certain time difference in arrival of the significant signals as recorded by individual microphones on their corresponding recorders.

(4) From the time differences in arrivals of the significant signals, and from a knowledge of the dimensions (distance between microphones) and orientation of the array, it is mathematically possible to evaluate the direction from which the particular significant pulse or transient arrived, and the apparent velocity with which it swept the array. These two quantities - the azimuth and velocity of sound arrival - in addition to the arrival time of the sound wave at any one microphone in the array, are the desired data to be evaluated and computed.

2. Interpretation of Recordings

a. The interpretation of recordings requires the exercise of keen judgment and a thorough review of all recorded signals for possible significance. Obviously it would be ideal if under all atmospheric conditions the recorded trace would be a straight line and all significant sound arrivals would stand out conspicuously, as illustrated in Class A recording, Figure I. However, there always exists a certain amount of atmospheric "noise", varying from little to great intensity depending on the meteorological conditions of the atmosphere in the vicinity of the array. This "noise" results from the turbulent motion of the atmosphere, either from its instability or turbulence due to obstacles to wind movement, or both. Turbulence is an eddy motion of the atmosphere and is therefore associated with local fluctuations of atmospheric pressure. If these fluctuations in pressure occur at a range of frequencies to which the infrasonic microphones have a response characteristic, these turbulent pressure variations will be recorded by the infrasonic system and will appear on the record as "noise" (See Class B and Class C recordings, Figure I). In the present equipment design, the system has no way to discriminate between noise and significant signals. Accordingly, analysis of the recordings requires that this discrimination be provided through interpretation by the analyst.

b. Insofar as practicable, selection of microphone sites has been made with the objective of minimizing the occurrence of atmospheric noise. Wooded areas, preferably with growth of underbrush, have been selected as sites for microphone positions to provide further screening from wind. Lastly, microphones have been installed in excavations in the ground to provide for their operation at the lowest practicable level at which wind speed will be a minimum. In spite of these installation procedures, it is still to be expected that local atmospheric pressure fluctuations will be recorded, to extents varying with meteorological conditions.

c. In order to gain maximum advantage in recording sound signals of exceptionally small amplitude, such as those propagating over exceedingly long distances, it is technically desirable to adjust the gain controls on the station amplifier to bring the recorded trace just barely into this noise level. This operational procedure will require that the significant signals be spotted out of the background noise; however, no particular difficulty should be encountered if proper procedure in setting of gain controls has been followed at the time of recording. It should be further noted that significant signals will be distinguishable from noise by consideration of the following factors:

(1) noise will be random and in general dissimilar among the microphones in the array, whereas significant signals will display characteristic points of identity.

(2) The difference of arrival time of significant signals at microphones in the array will be unique in that these signals will be propagated at the velocity of sound, i.e., the order of 360 yards per second. Noise, being random and local, will display no such unique time sequence of arrival at the microphones of the array. Figure II illustrates these differences in appearance of noise and significant signals.

d. Interpretation of recordings can be facilitated materially by use of a light table for superimposing suspected signal from several microphones, by use of devices for scaling time differences of arrival of apparent significant signals, and by use of nomograms designed specifically for the geometry of the particular microphone array for evaluation of azimuth and velocity of sound arrival. These devices are discussed in detail in paragraph 4 below. To better understand their use, it is desirable to consider first the mathematical principles involved in the evaluation of azimuth and sound velocity from significant signals.

3. Mathematical Principles for Evaluation of Data.

a. Geometry of microphone array.

The infrasonic microphone array consists of four microphones, one each at the vertices of a quadrilateral, preferably a square of dimensions 8 to 12 miles on a side. An array of this size is required in order to evaluate the azimuth of sound arrival to an accuracy of 2 degrees and the velocity of sound to an accuracy of four yards per second. The computation of azimuth of sound arrival and velocity of propagation from such an array is based on the following assumptions being satisfied:

(1) That the source of sound be at a distance large compared to the separation of microphones in the array. Satisfaction of this condition means in essence that the sound wave can be represented as a plane wave front, the azimuth of arrival being the same at each of the four microphones in the array and the velocity of propagation uniform over the area encompassed by the array.

(2) That the wave front be identifiable through significant characteristics of the recorded transients or pulses. In the event that multiple arrivals occur (as a result of several different paths of propagation to the array) care must be taken to read arrival times at microphones that correspond to the same wave front.

Satisfaction of condition (2) will depend on the meteorological conditions prevalent at the time of recording, and accordingly, to a very large extent on the ability of the analyst to interpret the recorded traces. The minimum number of microphones required for an evaluation of azimuth and velocity are three; however, the use of four microphones provides additional independent data of greater dependability. Accordingly, the solutions provided below for four microphones should always be used, except only in those instances when one microphone is inoperative or the recorded trace questionable, in which case the solution for a triangular array should be followed.

b. Derivation of trigonometrical relationships.

Refer to Figure III. The following definitions apply in the subsequent derivations:

M_1, etc.	microphones numbered clockwise from true north
S	source of sound at azimuth A from true north
T_1	time of sound arrival at microphone (1) (the lines labeled T_1, T_2, etc., in Figure III represent the sound wave at successive times as it reaches each microphone)
V	apparent velocity of sound
B_{13}	bearing of microphone M_3 from microphone M_1 using true north as a reference.
A	azimuth of sound arrival from source S (at an infinite distance)
M_1P_1	path of the portion of the sound wave detected at M_1. Point P_1 is its location at time T_3.
M_2P_2	path of the portion of the sound wave detected at M_2. Point P_2 is its location at time T_4.

(1) Solution for quadrilateral array of microphones.

(a) Consider sub-base M_1M_3 first.

M_1P_1 is parallel to azimuth of sound arrival by construction.

length $M_1P_1 = V(T_3 - T_1)$ (1)

angle $c_1 = A + 180^\circ - B_{13}$ (2)

length $M_1P_1 = M_1M_3 \cos c_1$
since $\triangle M_1P_1M_3$ is a right $\triangle$. (3)

Then $V(T_3 - T_1) = \overline{M_1P_1} = \overline{M_1M_3} \cos c_1$, from (1) and (3)

or $V(T_3 - T_1) = \overline{M_1M_3} \cos(180^\circ + A - B_{13}) = -\overline{M_1M_3} \cos(A-B_{13})$

or $V(T_1 - T_3) = \overline{M_1M_3} \cos(A - B_{13})$ (4)

(b) <u>Consider sub-base M_2M_4 next</u>

M_2P_2 is parallel to azimuth of sound arrival and to M_1P_1 by construction.

length $\overline{M_2P_2} = V(T_4 - T_2)$ (5)

angle $c_2 = A + 180^\circ - B_{24}$ (6)

angle $M_2P_2M_4$ is a right angle by construction.

length $\overline{M_2P_2} = \overline{M_2M_4} \cos c_2$ (7)

Then $V(T_4 - T_2) = \overline{M_2P_2} = \overline{M_2M_4} \cos c_2$ from (5) and (7)

or $V(T_4 - T_2) = \overline{M_2M_4} \cos(180^\circ + A - B_{24})$

$V(T_4 - T_2) = -\overline{M_2M_4} \cos(A - B_{24})$

or $V(T_2 - T_4) = \overline{M_2M_4} \cos(A - B_{24})$ (8)

(c) <u>Next solve equations (4) and (8) for angle A and velocity V.</u>

$V(T_1 - T_3) = \overline{M_1M_3} \cos(A - B_{13})$ (4)

$V(T_2 - T_4) = \overline{M_2M_4} \cos(A - B_{24})$ (8)

Divide equation (8) by equation (4):

$$\frac{V(T_2 - T_4)}{V(T_1 - T_3)} = \frac{\overline{M_2M_4} \cos(A - B_{24})}{\overline{M_1M_3} \cos(A - B_{13})} \qquad (9)$$

or $$\frac{(T_2 - T_4)}{(T_1 - T_3)} = \frac{\overline{M_2M_4}}{\overline{M_1M_3}} \frac{\cos\left[(A - B_{13}) + (B_{13} - B_{24})\right]}{\cos(A - B_{13})} \tag{10}$$

$$\frac{(T_2 - T_4)}{(T_1 - T_3)} = \frac{\overline{M_2M_4}}{\overline{M_1M_3}} \frac{\cos(A - B_{13}) \cos(B_{13} - B_{24}) - \sin(A - B_{13}) \sin(B_{13} - B_{24})}{\cos(A - B_{13})}$$

$$\frac{(T_2 - T_4)}{(T_1 - T_3)} = \frac{\overline{M_2M_4}}{\overline{M_1M_3}} \left[\cos(B_{13} - B_{24}) - \frac{\sin(A - B_{13}) \sin(B_{13} - B_{24})}{\cos(A - B_{13})}\right]$$

$$\frac{T_2 - T_4}{T_1 - T_3} = \frac{\overline{M_2M_4}}{\overline{M_1M_3}} \cos(B_{13} - B_{24}) - \frac{\overline{M_2M_4}}{\overline{M_1M_3}} \tan(A - B_{13}) \sin(B_{13} - B_{24})$$

or

$$\frac{\overline{M_2M_4}}{\overline{M_1M_3}} \sin(B_{13} - B_{24}) \cdot \tan(A - B_{13}) = \frac{\overline{M_2M_4}}{\overline{M_1M_3}} \cos(B_{13} - B_{24}) - \left[\frac{T_2 - T_4}{T_1 - T_3}\right]$$

or

$$\tan(A - B_{13}) = \frac{\cos(B_{13} - B_{24})}{\sin(B_{13} - B_{24})} - \left[\frac{T_2 - T_4}{T_1 - T_3}\right] \frac{\overline{M_1M_3}}{\overline{M_2M_4}} \cdot \frac{1}{\sin(B_{13} - B_{24})}$$

or

$$\tan(A - B_{13}) = \operatorname{ctn}(B_{13} - B_{24}) - \left[\frac{T_2 - T_4}{T_1 - T_3}\right] \frac{\overline{M_1M_3}}{\overline{M_2M_4}} \frac{1}{\sin(B_{13} - B_{24})} \tag{11}$$

Thus the equation for azimuth A of sound arrival can be written:

$$\tan(A - B_{13}) = \frac{(T_2 - T_4)}{(T_1 - T_3)} \cdot \frac{\overline{M_1M_3}}{\overline{M_2M_4}} \cdot \frac{1}{\sin(B_{24} - B_{13})} - \operatorname{ctn}(B_{24} - B_{13}) \tag{11a}$$

Equation (11a) can be written:

$$\tan(A - B_{13}) = \frac{(T_2 - T_4)}{(T_1 - T_3)} C + D \tag{12}$$

where $C = \frac{\overline{M_1M_3}}{\overline{M_2M_4}} \cdot \frac{1}{\sin(B_{24} - B_{13})}$

and $D = -\operatorname{ctn}(B_{24} - B_{13})$

All the terms in the expressions for C and D are known in advance from the survey of microphone positions in the array.

(d) <u>To find V, the velocity of propagation of the sound wave over the array, substitute the value of A from (12) in (4) and (8).</u>

$$V = \frac{\overline{M_1M_3}}{(T_1 - T_3)} \cos(A - B_{13}) \qquad \text{from (4)} \qquad (13a)$$

$$V = \frac{\overline{M_2M_4}}{(T_2 - T_4)} \cos(A - B_{24}) \qquad \text{from (8)} \qquad (13b)$$

Use both equations (13a) and (13b) to find V as a check on arithmetic. Use the value from that equation for which the time difference is largest in order to obtain the best accuracy in computing the velocity of propagation.

(e) <u>The following derivation presents another method for determining V.</u>

$$V(T_1 - T_3) = \overline{M_1M_3}\cos(A - B_{13}) \qquad (4)$$

$$V(T_2 - T_4) = \overline{M_2M_4}\cos(A - B_{24}) \qquad (8)$$

From (4), $$\cos(A - B_{13}) = \frac{V(T_1 - T_3)}{\overline{M_1M_3}} \qquad (14)$$

Also, $$\sin(A - B_{13}) = \sqrt{1 - \cos^2(A - B_{13})} = \sqrt{1 - \frac{V^2(T_1 - T_3)^2}{\overline{M_1M_3}^2}}. \qquad (15)$$

$$V(T_2 - T_4) = \overline{M_2M_4}\cos\left[(A - B_{13}) + (B_{13} - B_{24})\right]$$

or, $V(T_2-T_4) = \overline{M_2M_4}\left[\cos(A-B_{13})\cos(B_{13}-B_{24}) - \sin(A-B_{13})\sin(B_{13}-B_{24})\right]$, or

$$\frac{V(T_2-T_4)}{\overline{M_2M_4}} = \frac{V(T_1-T_3)}{\overline{M_1M_3}}\cos(B_{13}-B_{24}) - \sqrt{1-\frac{V^2(T_1-T_3)^2}{\overline{M_1M_3}^2}}\sin(B_{13}-B_{24}) \qquad \text{from (4), (14) \& (15)}$$

$$\sqrt{1-\frac{V^2(T_1-T_3)^2}{\overline{M_1M_3}^2}}\sin(B_{13}-B_{24}) = \frac{V(T_1-T_3)}{\overline{M_1M_3}}\cos(B_{13}-B_{24}) - \frac{V(T_2-T_4)}{\overline{M_2M_4}} \qquad (16)$$

Now square the equation (16)

$$\left\{1-\frac{V^2(T_1-T_3)^2}{\overline{M_1M_3}^2}\right\}\sin^2(B_{13}-B_{24}) = \frac{V^2(T_1-T_3)^2}{\overline{M_1M_3}^2}\cos^2(B_{13}-B_{24}) - 2\frac{V(T_1-T_3)}{\overline{M_1M_3}} \cdot \frac{V(T_2-T_4)}{\overline{M_2M_4}} \cdot \cos(B_{13}-B_{24}) + \frac{V^2(T_2-T_4)^2}{\overline{M_2M_4}^2}$$

$$\text{or } \sin^2(B_{13} - B_{24}) = V^2 \left[\frac{(T_1 - T_3)^2}{\overline{M_1M_3}^2} \sin^2(B_{13} - B_{24}) + \frac{(T_1 - T_3)^2}{\overline{M_1M_3}^2} \right.$$

$$\left. \cos^2(B_{13} - B_{24}) - 2\frac{(T_1 - T_3)}{\overline{M_1M_3}} \frac{(T_2 - T_4)}{\overline{M_2M_4}} \cos(B_{13} - B_{24}) + \frac{(T_2 - T_4)^2}{\overline{M_2M_4}^2} \right]$$

$$\text{or } \sin^2(B_{13} - B_{24}) = V^2 \left[\frac{(T_1 - T_3)^2}{\overline{M_1M_3}^2} - 2\frac{(T_1 - T_3)}{\overline{M_1M_3}} \frac{(T_2 - T_4)}{\overline{M_2M_4}} \right.$$

$$\left. \cos(B_{13} - B_{24}) + \frac{(T_2 - T_4)^2}{\overline{M_2M_4}^2} \right]$$

$$\text{or finally } V = \frac{\sin(B_{13} - B_{24})}{\sqrt{\frac{(T_1 - T_3)^2}{\overline{M_1M_3}^2} - 2\frac{(T_1 - T_3)}{\overline{M_1M_3}} \frac{(T_2 - T_4)}{\overline{M_2M_4}} \cos(B_{13} - B_{24}) + \frac{(T_2 - T_4)^2}{\overline{M_2M_4}^2}}} \qquad (17)$$

Expression (17) does not lend itself to computation easily; however, it is the basis for the construction of the station nomogram discussed in subparagraph c below.

(2) Solution for triangular array of microphones.

(a) The solution is identical to that derived for the quadrilateral array in subparagraph (1) above, except that some subscripts are different. There was nothing in the previous derivation that required microphones No. 2 and No. 3 to be different points. Let microphone No. 2 coincide with microphone No. 3 and change all subscripts 3 into 2. Then equation (11a) becomes:

$$\tan(A - B_{12}) = \frac{T_2 - T_4}{T_1 - T_2} \cdot \frac{\overline{M_1M_2}}{\overline{M_2M_4}} \cdot \frac{1}{\sin(B_{24} - B_{12})} - \operatorname{ctn}(B_{24} - B_{12})$$

Now change microphone No. 4 into No. 3 (for sake of simplicity, since the triangular array consists of 3 microphones) and we get finally for the azimuth A of sound arrival

$$\tan(A - B_{12}) = \frac{T_2 - T_3}{T_1 - T_2} \frac{\overline{M_1M_2}}{\overline{M_2M_3}} \frac{1}{\sin(B_{23} - B_{12})} - \operatorname{ctn}(B_{23} - B_{12}) \qquad (18)$$

instead of (11a). This is the same form as equation (12)

(b) Using equations (13a) and (13b) and as in (a) above, since we have changed microphone No. 3 to microphone 2 and microphone 4 to microphone 3, we have for the velocity V of sound propagation

$$V = \frac{\overline{M_1M_2}}{(T_1 - T_2)} \cos(A - B_{12}) \qquad \text{from (13a)} \tag{19a}$$

$$V = \frac{\overline{M_2M_3}}{(T_2 - T_3)} \cos(A - B_{23}) \qquad \text{from (13b)} \tag{19b}$$

(c) For the triangular array equation (17) becomes the following:

$$V = \frac{\sin(B_{12} - B_{23})}{\sqrt{\left(\frac{T_1 - T_2}{\overline{M_1M_2}}\right)^2 - 2\left(\frac{T_1 - T_2}{\overline{M_1M_2}}\right)\left(\frac{T_2 - T_3}{\overline{M_2M_3}}\right)\cos(B_{12} - B_{23}) + \left(\frac{T_2 - T_3}{\overline{M_2M_3}}\right)^2}} \tag{20}$$

(d) To obtain the solution for any other three microphones (say No. 2, 3 and 4 instead of 1, 2 and 3) one simply changes each subscript into the corresponding one of the new group. For example, equations (18), (19a), (19b) and (20) become:

$$\tan(A - B_{23}) = \frac{T_3 - T_4}{T_2 - T_3} \frac{\overline{M_2M_3}}{\overline{M_3M_4}} \frac{1}{\sin(B_{34} - B_{23})} - \operatorname{ctn}(B_{34} - B_{23}) \tag{21}$$

$$V = \frac{\overline{M_2M_3}}{(T_2 - T_3)} \cos(A - B_{23}) \tag{22a}$$

$$V = \frac{\overline{M_3M_4}}{(T_3 - T_4)} \cos(A - B_{34}) \tag{22b}$$

$$\frac{\sin(B_{23} - B_{34})}{\sqrt{\left(\frac{T_2 - T_3}{\overline{M_2M_3}}\right)^2 - 2\left(\frac{T_2 - T_3}{\overline{M_2M_3}}\right)\left(\frac{T_3 - T_4}{\overline{M_3M_4}}\right)\cos(B_{23} - B_{34}) + \left(\frac{T_3 - T_4}{\overline{M_3M_4}}\right)^2}} \tag{23}$$

Thus the equations for azimuth and velocity can easily be written for any combination of three microphones in the quadrilateral array, as may be necessary should one microphone become temporarily inoperative.

c. <u>Construction of Station Nomogram</u>

(1) Definitions

In order to simplify computation of azimuth of sound arrival and velocity of propagation over the array, it is desirable that some mathematical device be employed which will yield the desired quantities. It is possible to construct a nomogram for each field station once the positions of the microphones are known by survey and are kept fixed. For an understanding of the principles underlying the construction of the four microphone nomogram, the derivation is presented below:

Let the following definitions apply to Figure IV and the subsequent derivations:

M_1, etc.	microphone positions, numbered in sequence clockwise from true north.
S	source of sound (at infinite distance)
A	azimuth of sound source from true north
R	a radius vector of the quantities $\frac{T_1 - T_3}{M_1M_3}$ and $\frac{T_2 - T_4}{M_2M_4}$, these latter having been defined in subparagraph b above.
Q	azimuth of radius vector R from true north
B_{13}	azimuth of M_3 as seen from M_1
B_{24}	azimuth of M_4 as seen from M_2

Now, adopt the convention that when the index finger of the right hand, with palm upward, is pointed from M_1 in the direction of M_3, the thumb points to positive quantities of $(T_1 - T_3)/\overline{M_1M_3}$; and likewise, that when the index finger of the right hand, with palm upward, is pointed from M_2 in the direction of M_4, the thumb points to positive quantities $(T_2 - T_4)/\overline{M_2M_4}$. In accordance with this convention, for the source of sound S indicated in Figure IV, the quantity $(T_1 - T_3)/\overline{M_1M_3}$ is plotted perpendicularly to the line M_1M_3; likewise the quantity $(T_2 - T_4)/\overline{M_2M_4}$ is plotted perpendicularly to the line M_2M_4. The common end point of these two quantities is, by definition, the end point of the vector R.

(2) <u>Derivation of relations for four-microphone nomogram.</u>

By right triangle trigonometry we see from Figure IV that

$$\sin(B_{13} - Q - 180^\circ) = \frac{1}{R} \cdot \frac{T_1 - T_3}{\overline{M_1M_3}} \tag{24}$$

and $$\sin(360^\circ - B_{24} + Q) = \frac{1}{R} \cdot \frac{T_2 - T_4}{\overline{M_2M_4}} \tag{25}$$

Solving each of the equations for 1/R we have:

$$\frac{1}{R} = \frac{\overline{M_1M_3}}{T_1 - T_3} \sin(B_{13} - Q - 180^\circ) \tag{24a}$$

and $$\frac{1}{R} = \frac{\overline{M_2M_4}}{T_2 - T_4} \sin(360^\circ - B_{24} + Q) \tag{25a}$$

comparing equation (24a) with equation (13a) in subparagraph b above, we find that the nomogram will have to satisfy the following identities:

$$\frac{1}{R} \equiv V; \ \sin(B_{13} - Q - 180^\circ) \equiv \cos(A - B_{13}) \tag{26}$$

Likewise by comparing (25a) with (13b),

$$\frac{1}{R} \equiv V; \ \sin(360^\circ - B_{24} + Q) \equiv \cos(A - B_{24}) \tag{27}$$

Equation (26) establishes the relation between A and Q. This can be ascertained as follows:

By trigonometry we know that $\sin(90^\circ - X) = \cos X$. By comparison of this relation with equation (26) we have the correspondence

$X = A - B_{13}$

$90^\circ - X = B_{13} - Q - 180^\circ$

Hence, $Q = A - 270^\circ$,

or adding 360° to both sides,

$$\underline{Q = A + 90^\circ} \tag{28}$$

Likewise equation (27) should establish the same relationship between A and Q. To check, we proceed as follows:

By trigonometry, $-\sin(-X) = \cos(X - 90^\circ) = \sin X$.

$$X - 90^\circ = A - B_{24}$$

$$X = 360^\circ - B_{24} + Q$$

Hence, $$Q = A - 270^\circ \, , \tag{29}$$

or adding 360° to both sides,

$$\underline{Q = A + 90^\circ} \, .$$

Therefore, the nomogram will provide the means to compute graphically the azimuth A of sound arrival and the velocity V of propagation if the relations $1/R \doteq V$ and $Q \doteq A + 90^\circ$ are incorporated therein according to the convention established above.

(3) General features of the four-microphone nomogram

The nomogram for the four microphone array will have the appearance of Figure V, with salient features as follows:

(a) A scale of time difference $(T_2 - T_4)$ will be plotted normal to line M_2M_4 in units of $(T_2 - T_4)/\overline{M_2M_4} = 1$.

(b) A scale of time difference $(T_1 - T_3)$ will be plotted normal to line M_1M_3 in units of $(T_1 - T_3)/\overline{M_1M_3} = 1$.

(c) Azimuth of sound arrival will be read on the circular scale by entry in the grid of $(T_1 - T_3)$ and $(T_2 - T_4)$, with due regard for the signs of these time differences.

(d) Velocity V will be read on the radius according to a scale calibrated in relation to the reciprocal of the velocity, at the point located by the two time differences.

4. Analysis

a. In performing the analysis of recordings extreme care will need to be exercised in order not to overlook significant signals. Recordings can be classified into three categories as illustrated in Fig. I, according to the extent of background noise:

(1) Class A Recording: Extremely low background noise, the ink trace being essentially a straight line. Obviously, this condition presents the least difficulty for detecting a significant arrival. It will generally occur during conditions of calm or very light winds.

(2) Class B Recording: Possible signal arrival approximately same amplitude as background noise. This type of recording presents the greatest difficulty for analysis. It requires exceptionally detailed inspection of traces of all microphones to discover "wave shapes" which bear similarity on the four microphones. It is to be expected that noise will be random and therefore "wave shapes" corresponding to noise will bear little or no identity; however, a significant signal should appear on all four microphones with strong suggestions of identity; i.e., "wave shapes" should appear similar.

(3) Class C Recording: Extremely high background noise; this type of recording will generally occur during periods of high winds where natural wind screening of microphones is insufficient, or during periods of exceptional atmospheric turbulence and instability. Generally, background noise of this intensity will preclude reading of the recording for a significant arrival, even if such a signal had been detected by the microphones, since the background noise will probably exceed considerably the possible intensity of a significant arrival, and hence so distort any arrival as to cause it to lose its points of identity among the four microphones. A record of this character will, nevertheless, require careful inspection and analysis for possible significant arrivals, as noise never remains continuously high but changes in amplitude periodically.

b. Detailed procedure for testing suspected signals for significance.

In the course of proceeding with analysis of recordings as outlined in paragraph a above, those arrivals (in view of appearance of identity) will be tested for significance by use of the station nomograms as follows:

(1) Record arrival time of suspected signal at each microphone.

(a) Selection of points of identity. Make a detailed one-to-one comparison of the "wave shape" on all microphones for the suspected arrival. If available, use a light table to facilitate this comparison. After cal..ul study of the "wave shape" select the three most obvious points of identity; that is, select a peak (as point A of Class A recording, Figure I, a valley (as point B of Figure I, or a "cross-over point" (point at which pen excursion crosses zero line down through noise trace, as point C of Figure I). Label these points according to a logical convention such as A_1, A_2, A_3, the subscripts corresponding to microphone numbers, then B_1, B_2, B_3, etc.

(b) Calibration of time-scale. Next, calibrate the time-scale along the margin of the recording. Find the manual time signals inserted on both sides of the points of identity chosen. With the use of a template corresponding to the arc with which the recording pen traverses the chart roll, find the intersections of the manual time signals with the 5-second time pulses. Then count seconds between manual time signals and cross-check with time interval between insertion of manual signals for assurance that timing mechanism has performed properly.

(c) Read arrival time of points of identity. With the time-scale so calibrated, read the arrival times of the several points of identity to the nearest half second, taking care that the time is read at the intersection of an arc drawn from the point of identity to the time-scale, this arc being the equivalent of that traversed by the recording pen. (A template made from a portion of the chart roll, one for each particular recorder and so labelled, should be made for this purpose, simply by causing the pen to traverse the entire width of the chart roll, the arc then being used as a guide for cutting the template.) Tabulate these arrival times at the four microphones in terms of hour, minutes, and seconds.

(d) Comparison of points of identity. Compute differences in arrival of the points of identity A and B, and B and C, for each microphone in the array. Compare corresponding differences of arrival times of points of identity among the four microphones. If there is marked agreement in corresponding differences, the suspected arrival is exceptionally similar on all microphones in the array. If there are some discrepancies in corresponding differences, the recording should not be considered valueless, since background noise may have caused some phase distortion random on the microphones in the array.

(e) Compute average arrival time of suspected signal. In either case, average the arrival times of points of identity A, B, and C for each microphone. Use this average arrival time in computations with the station nomogram prescribed below.

c. Multiple arrivals

(1) In the event a significant signal has been detected and evaluated for azimuth of arrival and velocity of propagation, it is highly probable that additional significant signals have been recorded in the general "time vicinity". This circumstance is entirely plausible, on the basis of the following reasoning: The significant signal may be a sound wave that has propagated an exceedingly long distance through the atmosphere. Certain meteorological conditions of the troposphere and the stratosphere therefore presumably exist which are favorable to this long distance sound propagation. Generally, these conditions are such that several paths of propagation will be traversed by the sound wave to the distant position of the array. The individual path lengths are different, as are the meteorological conditions encountered at certain portions of these paths, with the result that arrival times of the same sound wave along the several paths will be different. Multiple paths are illustrated in Figure VI.

(2) The determination of a significant signal should accordingly be immediately followed by an equally intensive search of the recordings for additional significant signals in the same time vicinity. It is difficult to prescribe on theoretical considerations a time interval within which additional arrivals should occur, but an extrapolation of experimental data secured to date suggests that multiple arrivals from the same source may be separated from one minute to as much as three hours. Recordings should therefore be searched over an interval three hours previous to and following the arrival of a significant signal and any additional suspected signals should be evaluated for azimuth of arrival and for velocity of propagation. In general, if the several suspected signals result from multiple paths of propagation from an identical source, the azimuths of arrival will probably agree within 20° but the velocities of propagation may be very widely different. A

signal of this sort should <u>not</u> be discarded; in fact, the wide discrepancy in velocity adds credence to the fact that a distant sound source <u>has</u> been detected by the array.

d. Arrivals by way of antipodes path

It should be borne in mind that Infrasonic System M-2 is capable of detecting low frequency sound waves from a source at any distance on the earth's surface. Therefore, there are always two major paths of propagation to a particular array; one the most direct (and shortest) path, and the other, the indirect (and longest) path by way of the antipodes * of the geographic position of the array. The direct and indirect paths are illustrated in Figure VII. Note that the phenomenon of multiple paths can occur with both direct and indirect paths of propagation. Therefore, it can be generally concluded that whenever a significant signal has been detected and determined to exist, it is possible that a number of additional significant signals exist on the recordings at plus and/or minus a considerable number of hours from the significant signal first discovered. It has already been pointed out in paragraph c above that the recordings should be particularly carefully scanned in time for a three-hour period prior to and following the arrival time of a significant signal, so as to determine the existence of multiple arrivals. The possibility of paths by way of the antipodes adds an additional interval of time that warrants especially detailed consideration. To estimate the magnitude of this interval, one can reason as follows: Sound waves in the earth's atmosphere travel approximately 10° of a great circle per hour. Thus a sound wave would require roughly 36 hours to travel completely around the earth.

It should be further noted that in view of the long interval of time that may elapse between the arrival of direct and antipodes signals, the local meteorological conditions at the array can change materially with consequent change in background noise. This weather factor may operate to deny identification of both direct and antipodes paths at one array. However, it is also likely that fortuitous circumstances can exist, and it is accordingly of paramount importance that the exceptionally detailed inspection of the recordings for the 72-hour period centering on the significant arrival be carried out.

5. Sample Computation

a. Reading of Records

Figures VIII, IX, X, and XI are reproductions of portions of simulteneous recordings obtained at an experimental station.

The evaluations of the azimuth and velocity of the arrival is accomplished as follows: The four recordings are compared against each other by means of a light box and an identical point is selected on each recording. With the aid of a template which places the trace of the pen at the appropriate time mark for each individual recorder,

---

* The antipodes of a point on the earth's surface is the end-point of a diameter passing through the given point.

the exact point on the time scale for each of these chosen points is determined. This time scale, appearing at the left edge of the chart, is mechanically divided into nominal five second intervals. The time scale at the right edge of the chart is manually calibrated at fixed intervals against WWV time. In the illustrated recording, this manual time mark appears at 1547Z. In order to determine the exact time of arrival for each of the selected points, this manual time mark is transferred to the five second scale and the exact time of arrival evaluated by measuring from this point.

b. Computations

The arrival times are recorded on the "Computation Sheet for Nomograms", Fig. XII. The indicated time differences are then computed and recorded. On nomogram B/O, Fig. XIII, a point is found on the oblique coordinate grid which corresponds to -49.5 seconds on the $T_1 - T_3$ axis and + 31 seconds on the $T_2 - T_4$ axis as indicated by an X. The intersection of the circumference with the radius vector drawn through the plotted point indicates the azimuth of arrival as 2.5 degrees, and the length of this radius vector as scaled off along the velocity scale at the bottom of the nomogram indicates the velocity of propagation as 367 yards per second.

SECRET

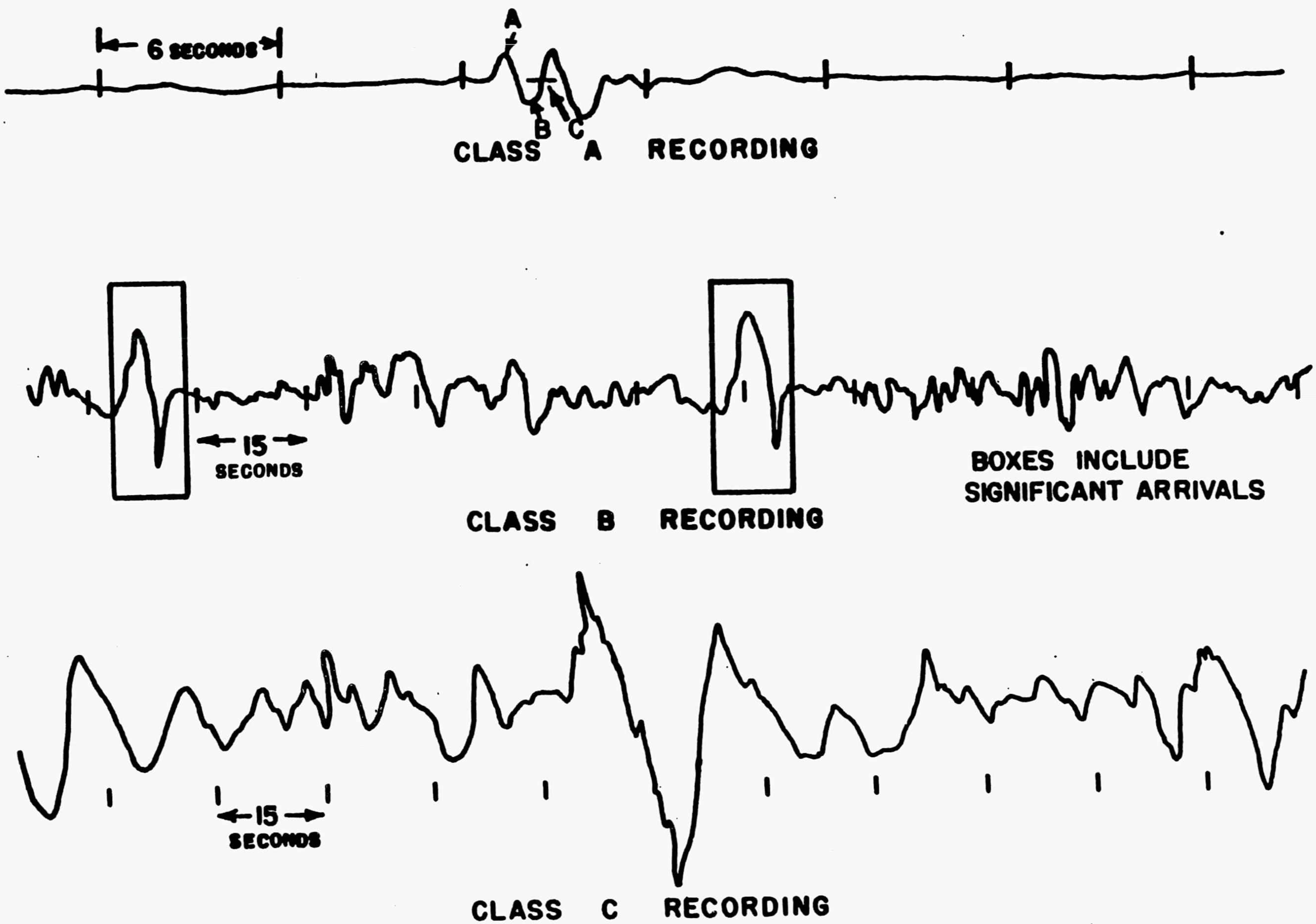

FIGURE I
APPENDIX D

SECRET

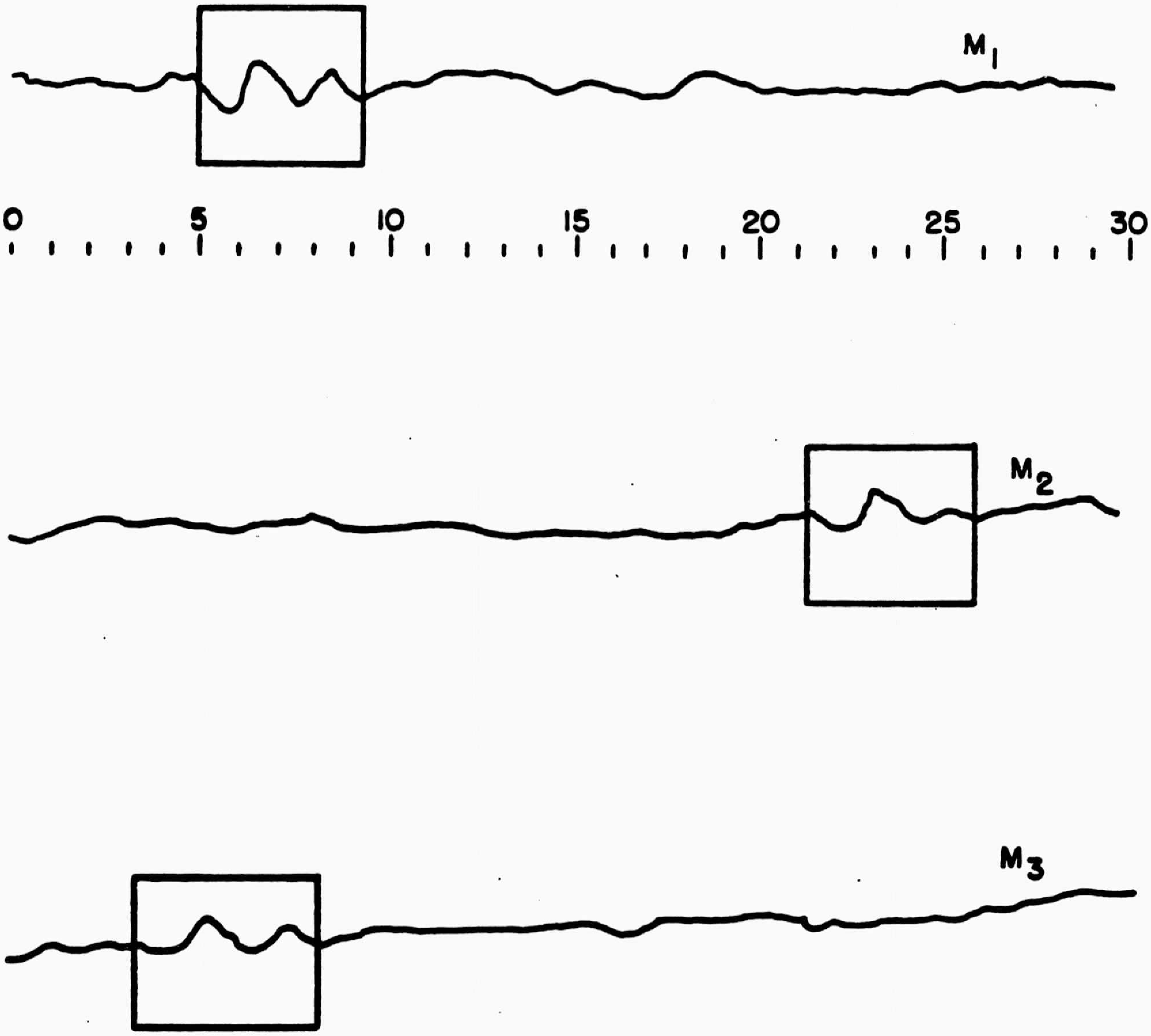

BOX ENCLOSES SIGNIFICANT SIGNAL

NOTE GENERAL SIMILARITY OF "WAVE SHAPE" WITHIN BOXES.

FIGURE II
APPENDIX D

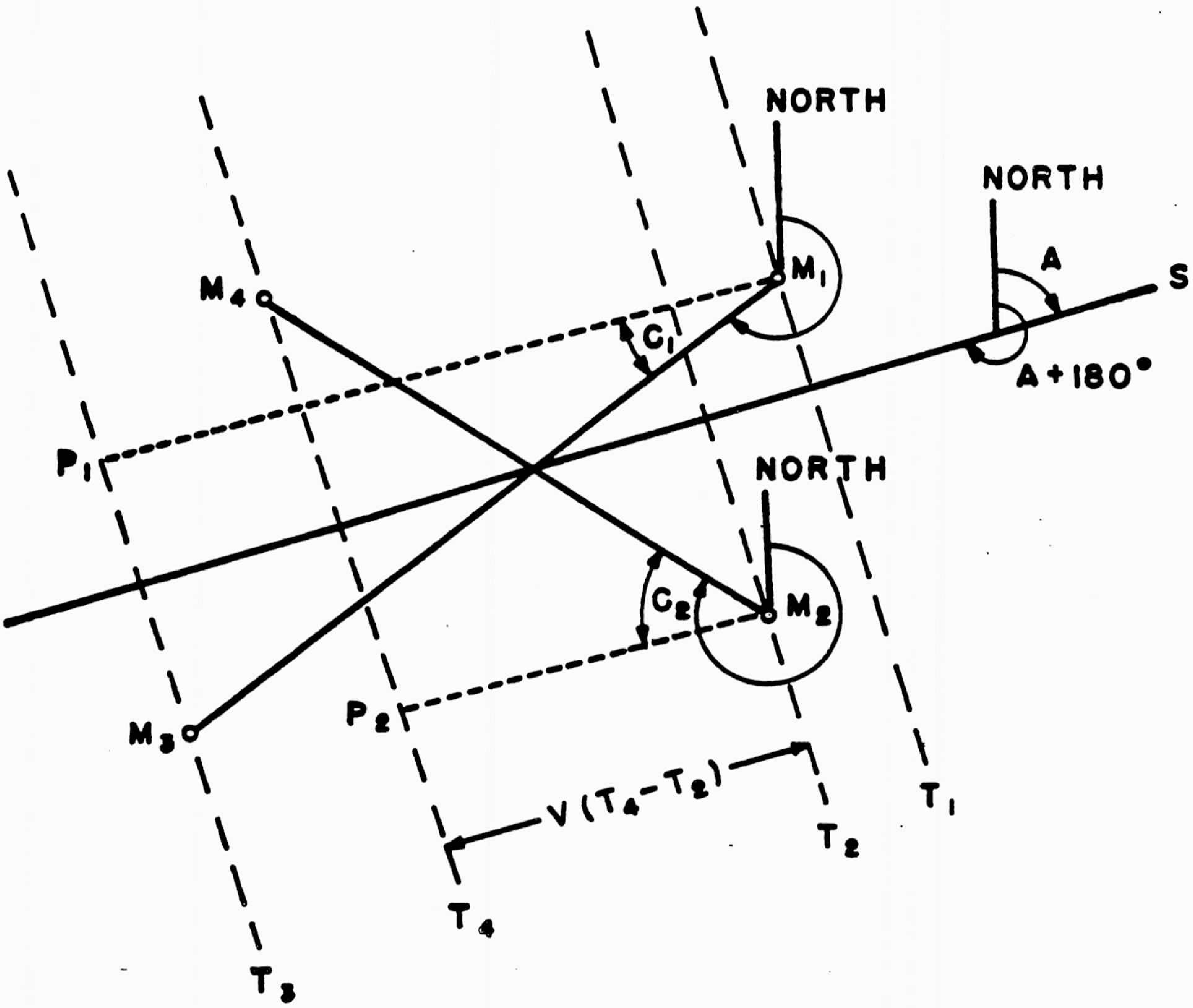

FIGURE III
APPENDIX D

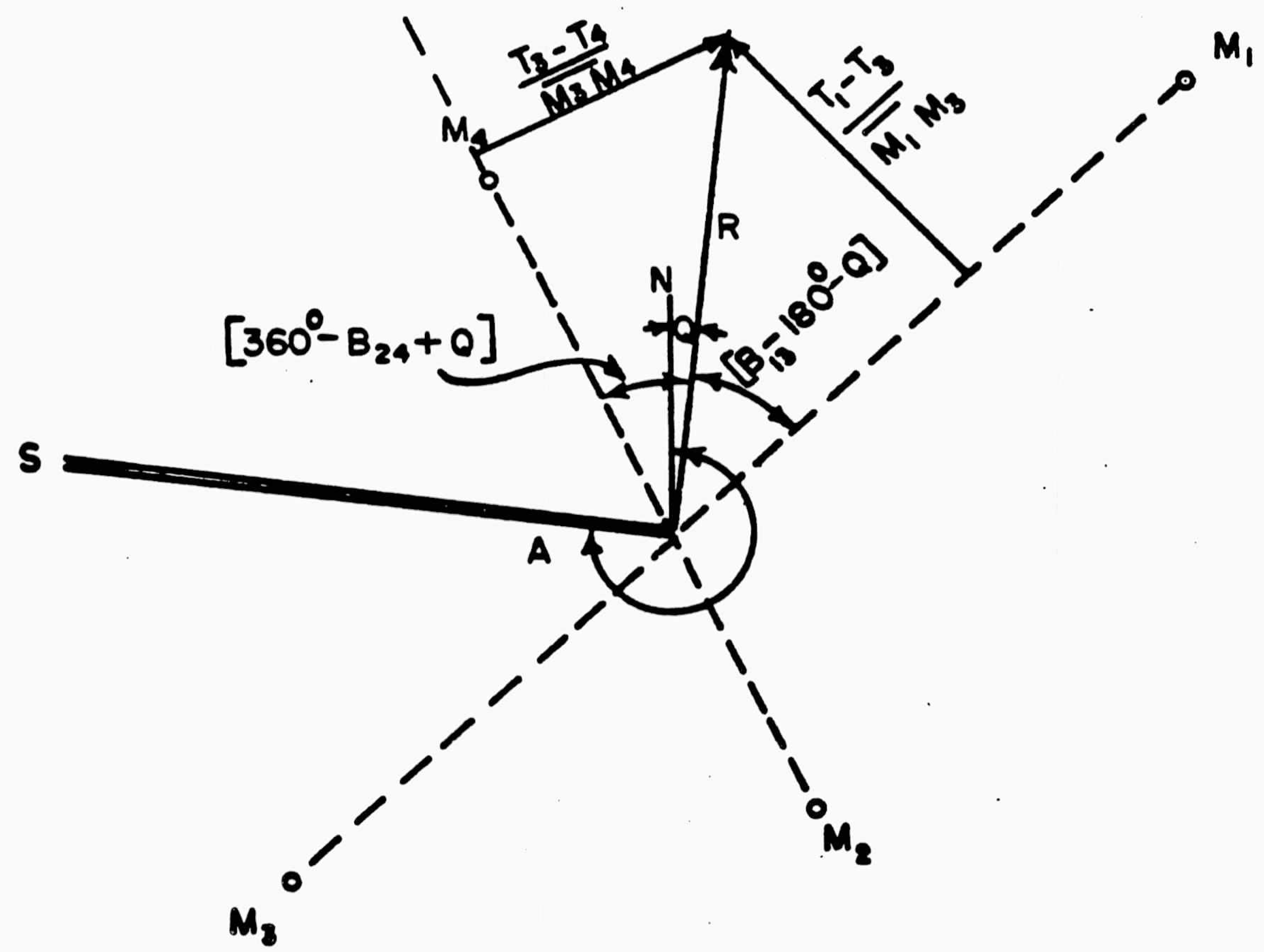

FIGURE IV
APPENDIX D

~~SECRET~~

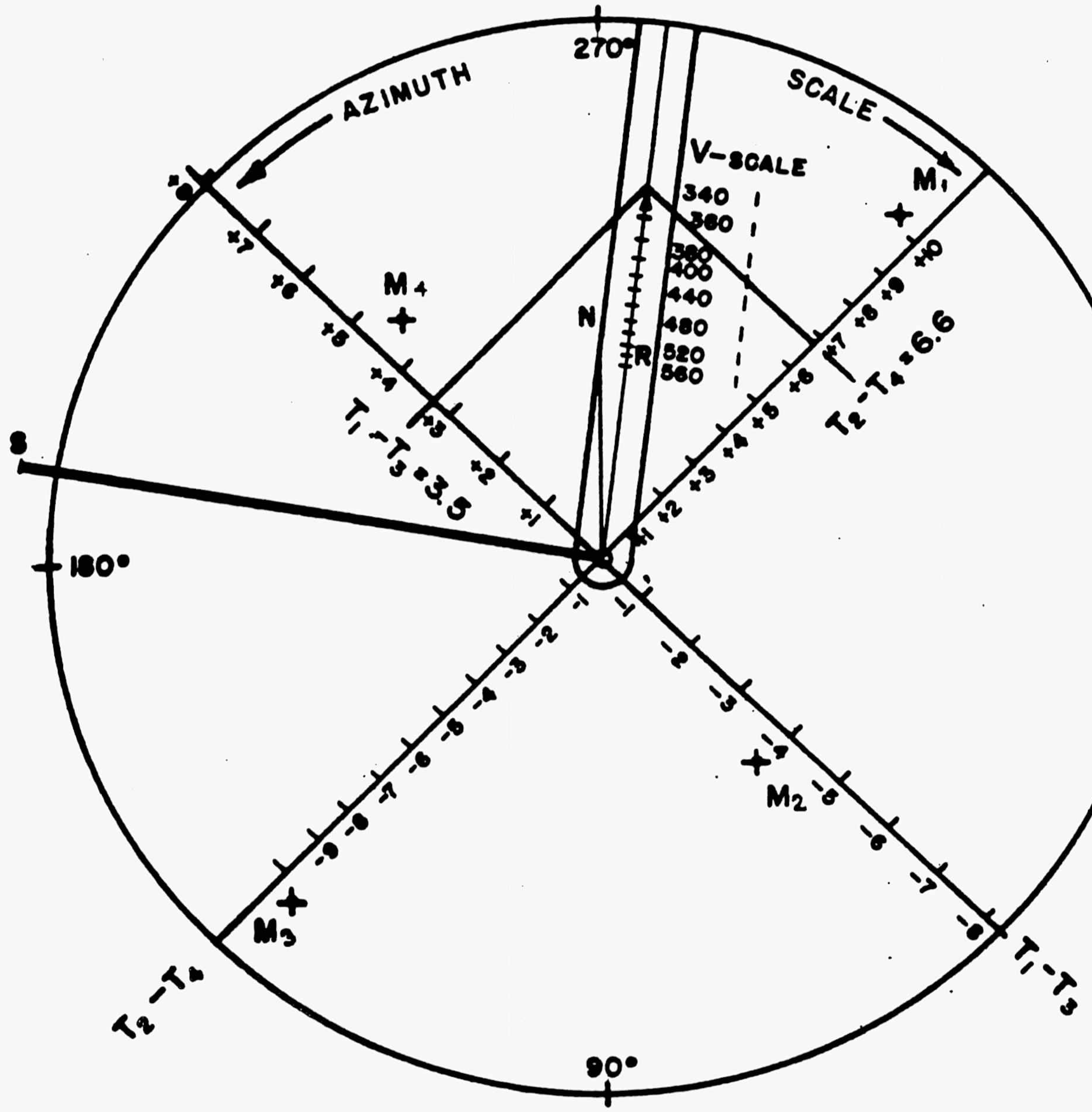

SKETCH OF 4- MICROPHONE NOMOGRAM

~~SECRET~~

FIGURE V
APPENDIX D

~~SECRET~~

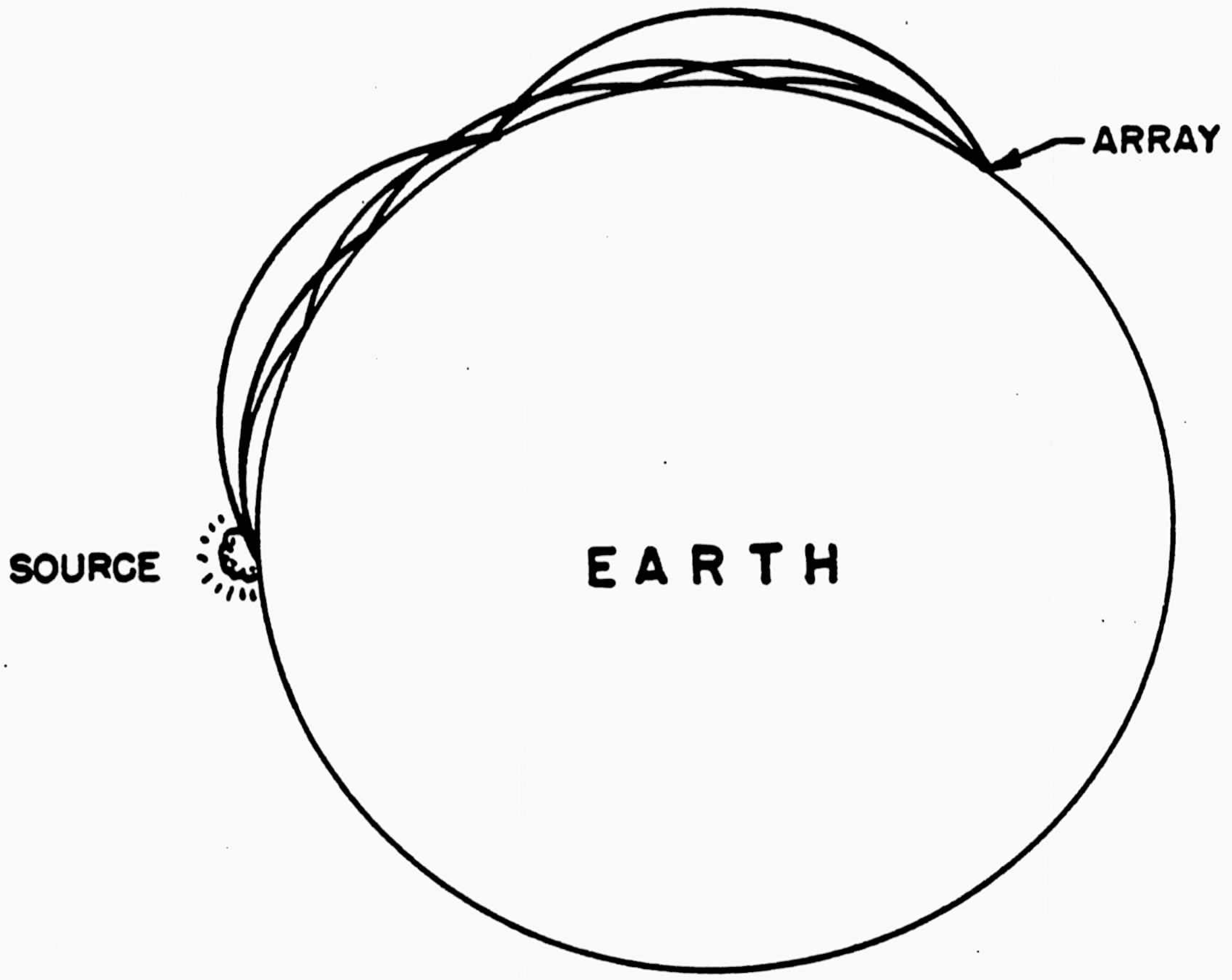

ILLUSTRATION OF
MULTIPLE PATHS

~~SECRET~~

FIGURE VI
APPENDIX D

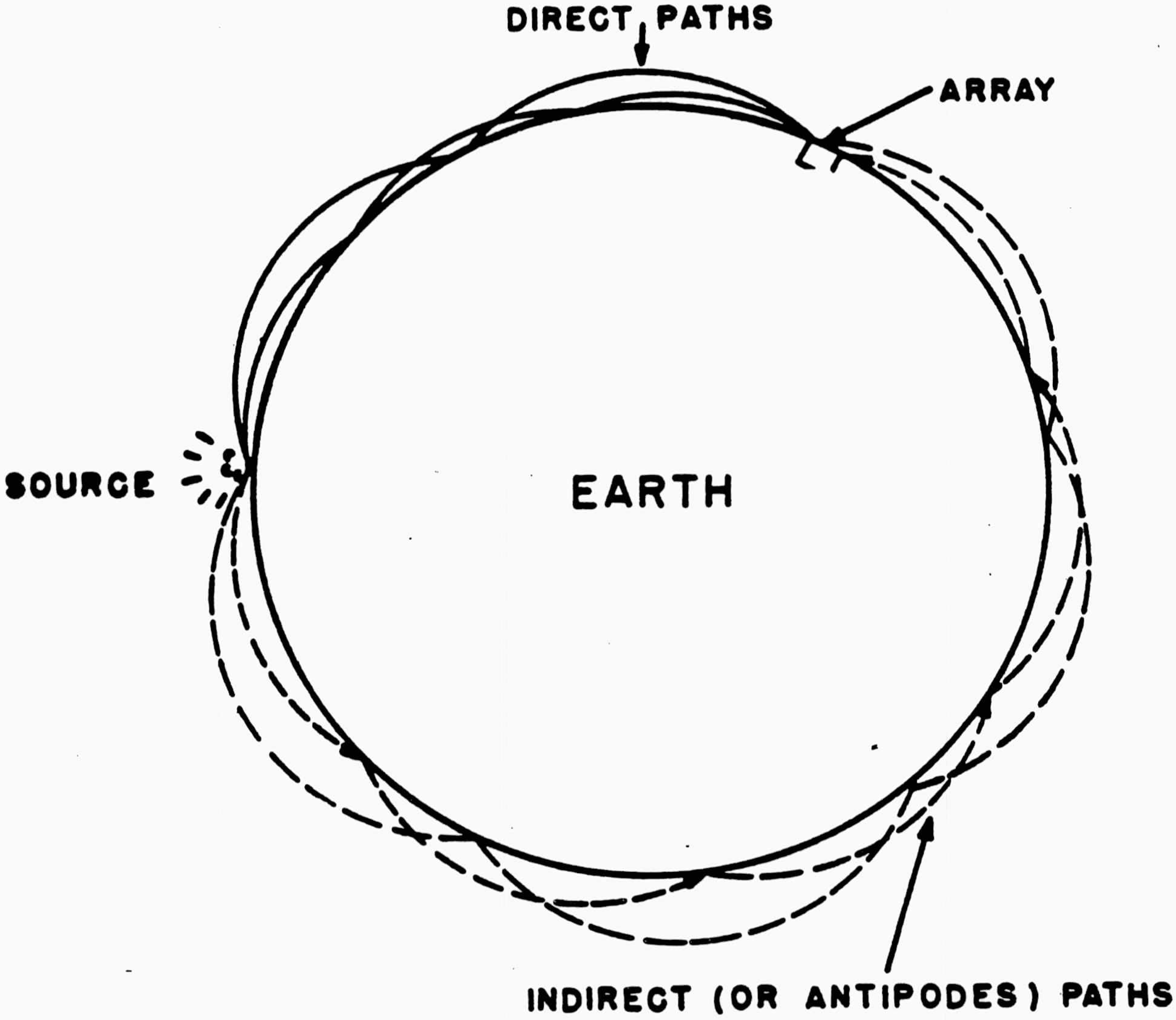

ILLUSTRATION OF
DIRECT AND INDIRECT PATHS

FIGURE VII
APPENDIX D

CHART B/O

14 Feb. 1948 1545 Z
DAY MONTH YEAR
DATE TIME

$T_1 - T_3$ = -40.5

$T_2 - T_4$ = +31

NOTE: INDICATE WHETHER + OR −.

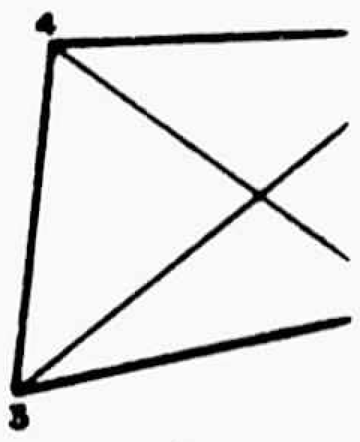

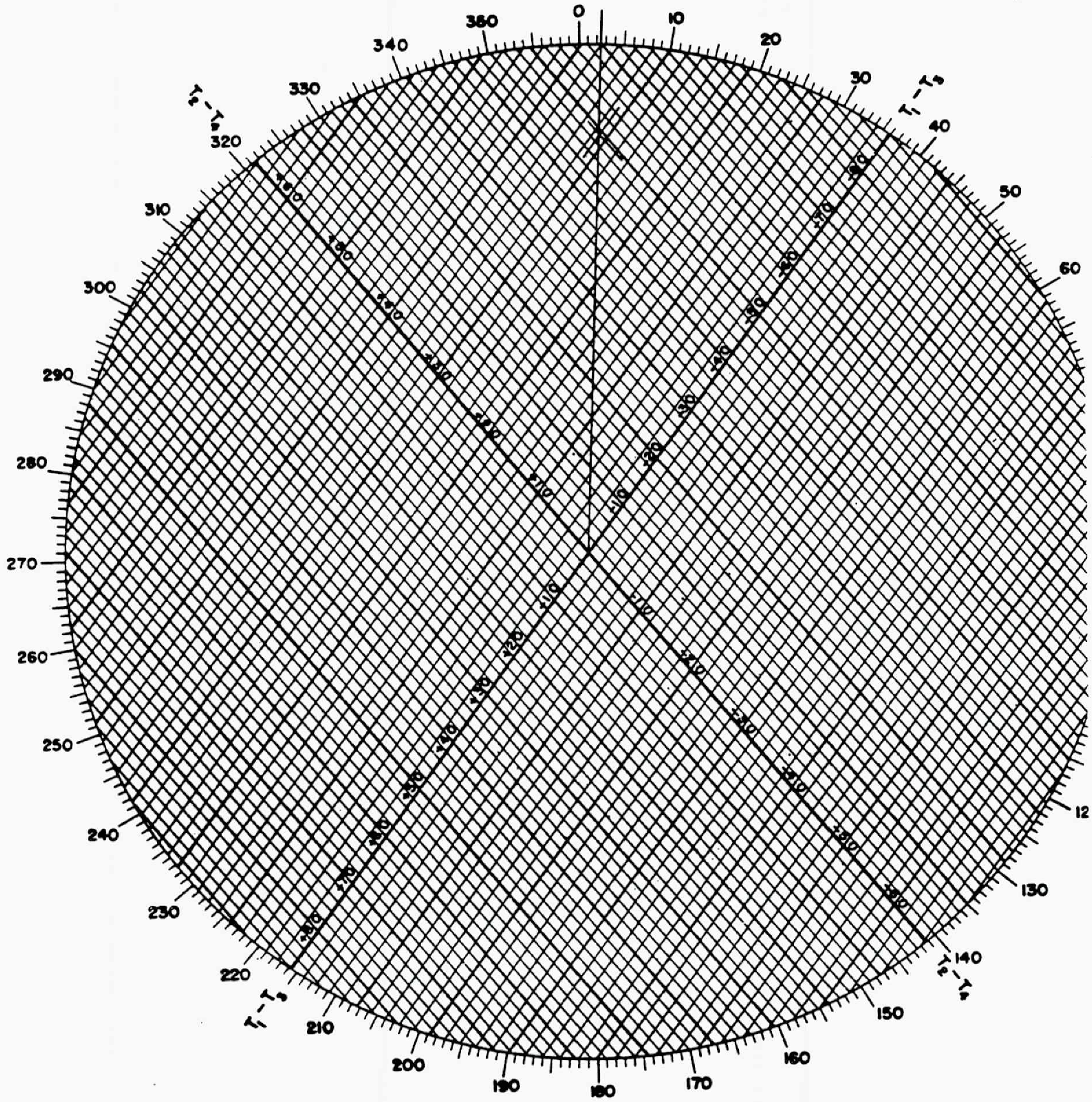

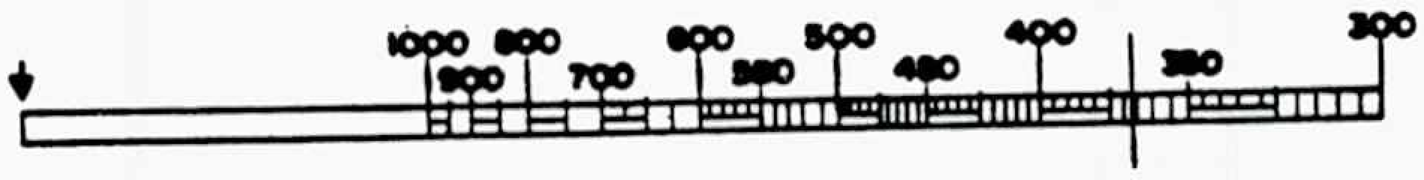

Fig. 13

FIGURE]
APPENDIX

NOMOGRAM COMPUTATION DATA

STATION	ARRIVAL DATE	STARTING TIME	TIME FACTOR	
B	14 FEBRUARY 1948			
READ BY	**DATE**	**VERIFIED BY**	**DATE**	**WORK SHEET NO.**
P. B.	1 MARCH 1948	J. J.	1 MARCH 1948	10

MICRO. NO.	NUMBER OF PIPS (+ OR –)	ARRIVAL TIME HR.	MIN.	SEC.	NOMOGRAM	TIME DIFFERENCE (+ OR –)	AZIMUTH (DEGREES)	VELOCITY (YDS. PER SEC.)	REMARKS
1		15	45	50	0	#1 - #3= – 49.5 #2 - #4= + 31	2.°5	367	
2		15	46	27	1	#2 - #3= – 12.5 #3 - #4= + 43.5	2.°5	371	
3		15	46	39.5	2	#3 - #4= + 43.5 #1 - #4= – 06	3.°0	370	
4		15	45	56	3	#1 - #2= – 37 #1 - #4= – 06	2.°0	364	
					4	#1 - #2= – 37 #2 - #3= – 12.5	2.°0	365	

COMPUTED BY	DATE	VERIFIED BY	DATE	CHECKED BY
M. T.	2 MARCH 1948	R. B	2 MARCH 1948	

SCEL-SC FORM 1191

APPENDIX C
FIGURE XI

~~SECRET~~

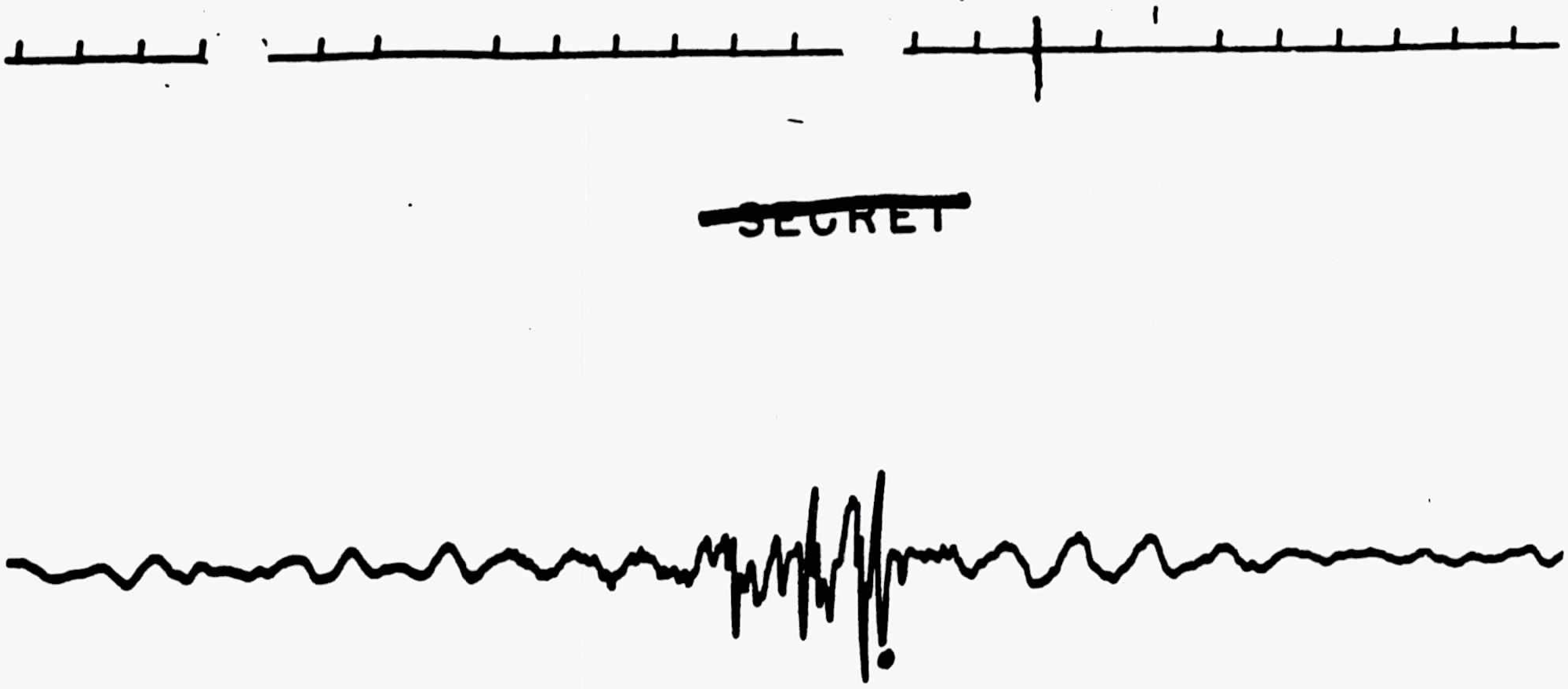

STATION BIRCH
14 Feb. 1948
Microphone #1
15h 45m 47.2s Z

FIGURE VIII
APPENDIX D

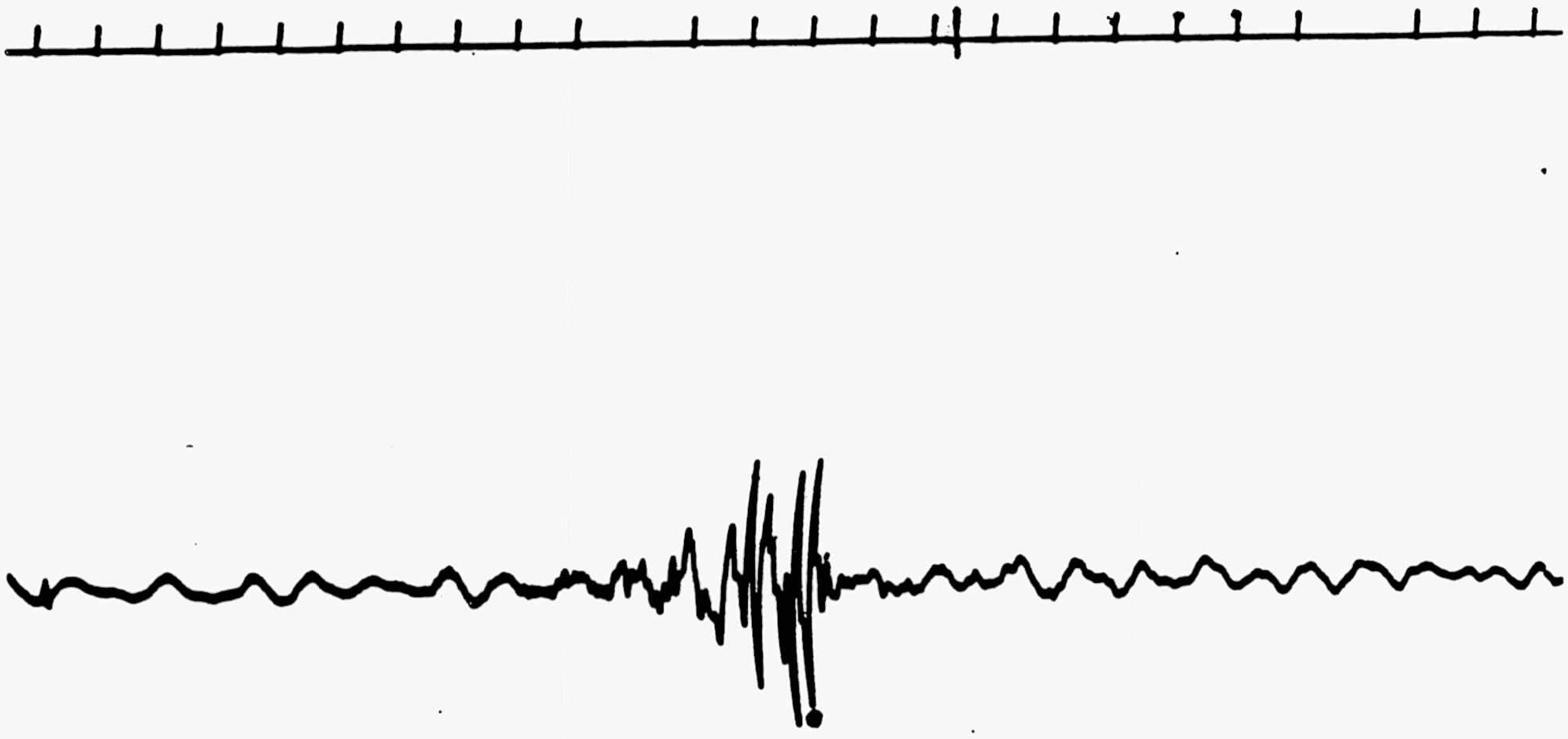

STATION BIRCH
14 Feb. 1948
Microphone #2
15h 46m 25.68s Z

FIGURE IX
APPENDIX D

~~SECRET~~

~~SECRET~~

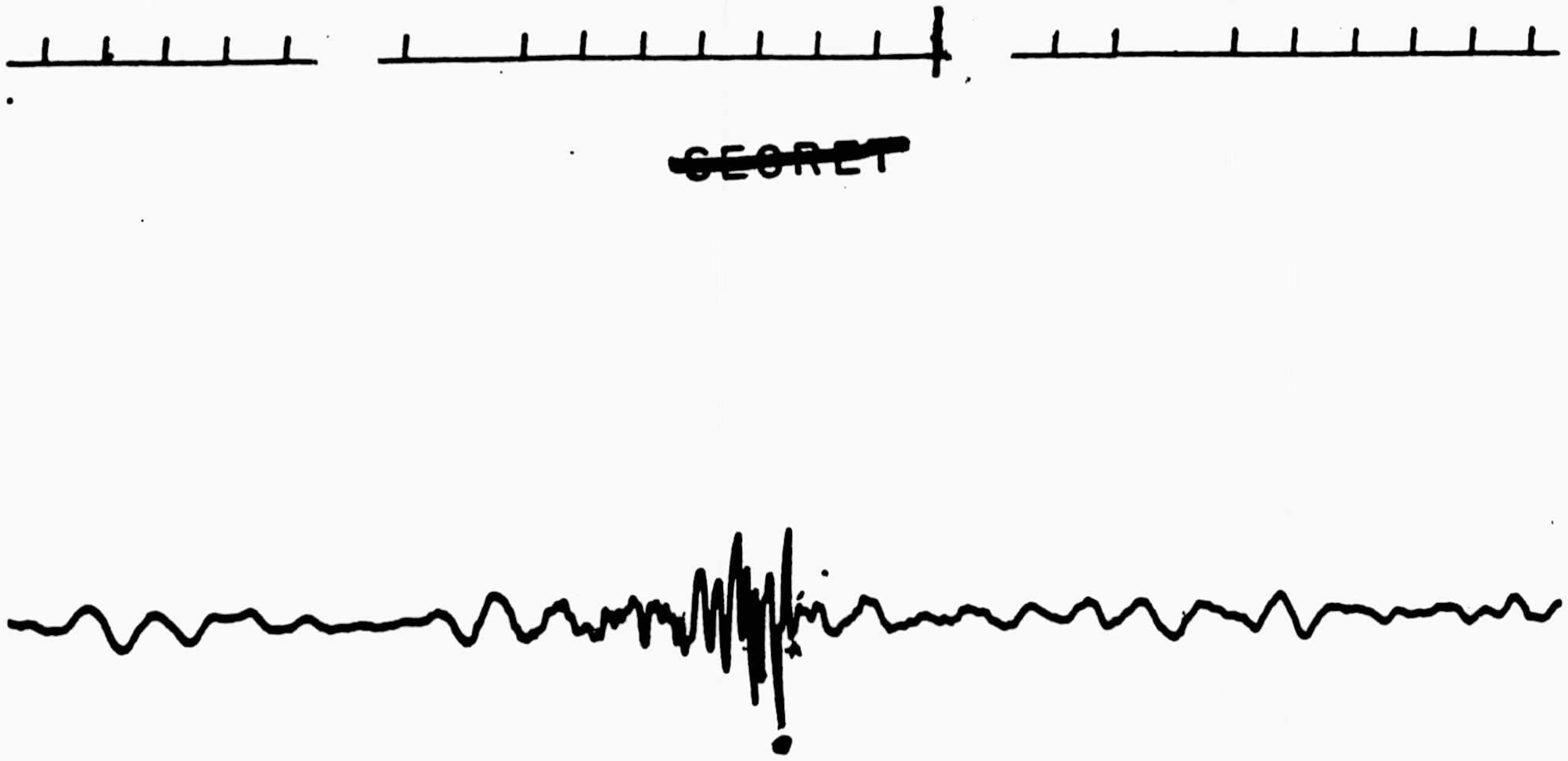

STATION BIRCH
14 Feb. 1948
Microphone #3
15h 46m 39.2s Z

FIGURE X
APPENDIX D

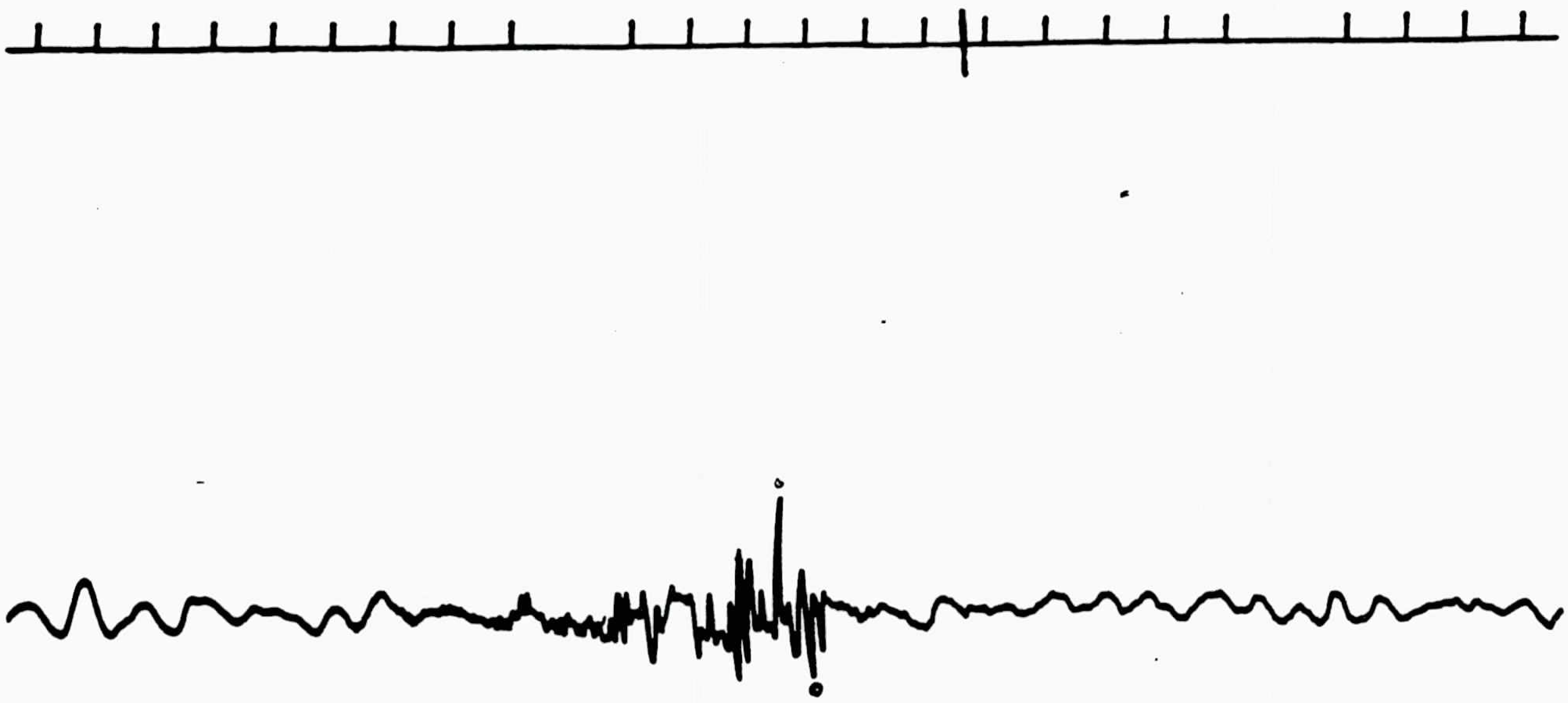

STATION BIRCH
14 Feb. 1948
Microphone #4
15h 45m 52.92s Z

FIGURE XI
APPENDIX D

~~SECRET~~

APPENDIX E

"ANALYSIS OF THE SOUND PROPAGATION FIELD OF AN ATMOSPHERE OF VARIABLE TEMPERATURE AND WIND"

I. INTRODUCTION

The propagation of sound through the atmosphere is a phenomenon which has been exploited for a number of military and scientific purposes. From the military point of view, development of sound ranging techniques during World War I led to the "spotting" of enemy field artillery positions. The accuracies of gun locations and the military value of this intelligence proved to be such that sound ranging continued as an instrument of military observation during the interim period between World Wars I and II. During this period and well into World War II the Signal Corps at the request of the Field Artillery, engaged in intensive investigations of the propagation of sound through the atmosphere, particularly with the end view of evaluating meteorological effects on sound propagation so as to increase the accuracy of sound position finding. The salient results of these investigations have been reported in Signal Corps publications listed in the attached bibliography. Perhaps the most characteristic feature of this Signal Corps work is that the atmosphere was treated in its dynamic state rather than a statistical state; that is to say, the actual variations of temperature, humidity, wind direction and wind speed were considered in evaluating the sound paths through the atmosphere. Since the meteorological state of the atmosphere, as expressed by these parameters, is subject to radical change with time and location, a technique for the analysis of the propagation field of an atmosphere of variable temperature and wind had to be devised. It is essentially this technique, extended to exceptionally long ranges, that is reported in this Appendix.

From the scientific point of view the analysis of sound propagation to long distances can be exploited to determine the meteorological characteristics of the upper atmosphere, provided the source position, detection positions, instant of detonation, and certain other factors are known to sufficient accuracy. Investigations of this type have been conducted by Whipple, Gutenberg, and others. The Signal Corps conducted scientific studies of this type during the Arco, Idaho explosions of October 1946 (explosions conducted by the Army-Navy Munitions Board). These studies have led to conclusions which are considered to be of great import to the problem of long range detection of large explosions. A section of this Appendix is devoted to a discussion of the Arco, Idaho studies conducted by the Signal Corps.

Inasmuch as the technique for analysis of the sound propagation field of an atmosphere where temperature, humidity, wind direction and wind speed are independent functions of a space parameter is not readily available in the literature, the basic equations and techniques for this purpose are derived in this Appendix.

II. EQUATIONS OF MOTION

A. Differential equations for the generalized case

The differential equations of a sound ray in an atmosphere where temperature and humidity may vary over all space, producing a scalar velocity of sound $V = f(x, y, z)$, and where the wind varies over all space so that the components of velocity can be represented as $u = u(x, y, z)$, $v = v(x, y, z)$ and $w = w(x, y, z)$, have been previously set forth (reference 1, page 18) and are as follows:

$$\frac{dx}{dt} = \lambda V + u; \quad \frac{dy}{dt} = \mu V + v; \quad \frac{dz}{dt} = \nu V + w, \qquad \text{(A)}$$

where λ, μ, ν are the direction cosines of the normal to the wave surface at $P(x,y,z)$ and t is time. Equations (A) represent the differential equations of a family of space curves; we define a sound ray or path as one member of this family, having a unique value λ_o, μ_o, and ν_o at some point of the path and a unique variation of λ, μ, ν along the path. Therefore, to identify a particular sound path the differential equations relating the variation of λ, μ, ν with x, y, z along the path must be stated. These equations have likewise been set forth previously (reference 1, pp. 18-21) and are as follows:

$$\frac{1}{\lambda}\left[\frac{d\lambda}{dt} + \frac{\partial V}{\partial x} + \lambda\frac{\partial u}{\partial x} + \mu\frac{\partial v}{\partial x} + \nu\frac{\partial w}{\partial x}\right]$$
$$= \frac{1}{\mu}\left[\frac{d\mu}{dt} + \frac{\partial V}{\partial y} + \lambda\frac{\partial u}{\partial y} + \mu\frac{\partial v}{\partial y} + \nu\frac{\partial w}{\partial y}\right] \qquad \text{(B)}$$
$$= \frac{1}{\nu}\left[\frac{d\nu}{dt} + \frac{\partial V}{\partial z} + \lambda\frac{\partial u}{\partial z} + \mu\frac{\partial v}{\partial z} + \nu\frac{\partial w}{\partial z}\right]$$

The six equations (A) and (B) are sufficient to determine the position in space of all sound paths emanating from a given source of sound.

B. Reduction to case of atmosphere homogeneous along surfaces concentric with the earth

In this case $V = F(r)$. Take the x-direction of the coordinate system (see Figure I) in the azimuth of sound propagation. Let the gradients of temperature and wind normal to the XZ-plane be negligible; i.e., the translational effects normal to XZ are negligibly small compared to the range traversed by the path in the XZ-plane. We thus replacc the spherical earth by a cylinder of equivalent radius and set v = constant; hence

$$\frac{\partial v}{\partial x} = \frac{\partial v}{\partial y} = \frac{\partial v}{\partial z} = 0; \mu = 0; \nu = \sqrt{1 - \lambda^2}$$

If u' is the observed horizontal wind component in the azimuthal direction of sound propagation, then

$$u = u' \cos \theta; \; v = \text{constant}; \; w = u' \sin \theta \qquad (C)$$

Since $u' = f(r)$ only, note that $u = \varphi(r, \theta)$ and $w = \int(r, \theta)$, where θ and r are the polar angle and radius, respectively, from the center of the earth to the general point $P(x, z)$ on the sound path (see Figure I).

Equations (B) reduce to the following equations, on substitution of the relations expressed by (C) above and on introduction of the angle β (i.e., the angle of elevation of the normal to the wave surface, measured with respect to the horizontal plane through Point P):

1. The direction of the normal to the wave surface:

$$d\theta - d\beta = \cos \beta \frac{\partial V}{\partial r} dt + \frac{u'}{r} \cdot \sin^2 \beta \, dt + \frac{\partial u'}{\partial r} \cdot \cos^2 \beta \, dt; \qquad (D)$$

2. Time-rate change of the polar angle θ:

$$r\frac{d\theta}{dt} = V \cos \beta + u'; \qquad (E)$$

3. Time-rate change of the radius vector r:

$$\frac{dr}{dt} = V \sin \beta; \qquad (F)$$

noting that $\lambda = \cos(\beta - \theta)$ and $\nu = \sin(\beta - \theta)$.

C. Snell's law of refraction for a curved earth with temperature, humidity and horizontal wind component in a given azimuth varying radially.

Integrating equations (D), (E), and (F), with relations established by equation (A), we deduce Snell's law of refraction for a curved earth with atmosphere in motion:

$$\frac{V}{r \cos \beta} + \frac{u'}{r} = \frac{V_o}{b \cos \alpha} + \frac{u_o'}{b} = \text{constant} \qquad (G)$$

Note that the second-member arises from the meteorological conditions V_o and u_o' existing at the source (or microphone positions); hence this term for a constant meteorological condition is a function of the angle α only.

D. The criterion curve $\left(\frac{b}{r} V + \frac{b}{r} u'\right)$

By Snell's Law, equation (G), we note that at the maximum height of the sound path, at which $\beta = 0$, we have the condition

$$\frac{b}{r} V + \frac{b}{r} u' = \frac{V_o}{\cos \alpha} + u_o' \qquad \text{(H)}$$

Thus if to the temperature* sounding $\frac{b}{r} V$ as a function of height we add the wind sounding expressed in $\frac{b}{r} u'$, we have the criterion curve $\left(\frac{b}{r} V + \frac{b}{r} u'\right)$. Note that at the maximum height of the sound path, the abscissa value of this criterion curve must be equal to the characteristic parameter for the path $\left(V_o / \cos \alpha + u_o'\right)$, which characteristic parameter can be measured directly by a plane array of microphones (3 or more) on the ground, suitably spaced, in terms of arrival times of sound and survey data, and without recourse to meteorological data. This characteristic parameter has, in Signal Corps usage, been designated as V_h, the apparent velocity of sound in the horizontal plane, and is computed directly from the nomograms discussed in Appendix D of this report.

E. Maximum height of the path

The level of total refraction, i.e., the maximum height of the path, can be determined immediately from the criterion curve. Thus by Figure II we see that the level of total refraction is given by the intersection of the abscissa $V_o/\cos \alpha + u_o' = V_h$ with the meteorological distribution given by the criterion curve $\left(\frac{b}{r} V + \frac{b}{r} u'\right)$.

F. Evaluation of the angle β.

Solving Snell's Law, equation (G) for $\cos \beta$ we have, by algebraic manipulation,

$$\cos \beta = \frac{\frac{b}{r} V}{\frac{b}{r} V + \left[\frac{V_o}{\cos \alpha} + u_o' - \left(\frac{b}{r} V + \frac{b}{r} u'\right)\right]}$$

The term in the brackets is simply the difference between the criterion curve and the value of the path parameter. The other term $\frac{b}{r} V$ in the equation is the temperature sounding. We thus have a graphical means for evaluating the angle β. Solving for the term in the brackets we find

$$\frac{V_o}{\cos \alpha} + u_o' - \left(\frac{b}{r} V + \frac{b}{r} u'\right) = \frac{b}{r} V \left(\frac{1}{\cos \beta} - 1\right)$$

On a graph of $\frac{b}{r} V$ plotted against height, we can provide lines of constant β, as indicated in Figure III.

---

* $V = 20.1\sqrt{T^1}$ meters per second, where T^1 is the meteorologist's virtual temperature (reference 1, pages 14-17)

The angle β can be determined from this graph by proceeding as follows:

1. Measure the distance between the criterion curve and the path parameter with a pair of dividers;

2. Set this distance vertically from the base h = o along the $\frac{b}{r}V$ value read from the temperature plot at that level for which we wish β;

3. The end-point of the divider is the value of β desired. Thus a rectangular linear coordinate grid, with temperature and β-lines superimposed, proves a useful graphical aid in computing maximum path heights and the angle β at significant meteorological levels.

III. INTEGRATION OF THE EQUATIONS OF MOTION

Solving equations (E) and (F) simultaneously we obtain

$$\frac{ds}{b} = \frac{dr}{r \tan\beta} + \frac{u' dr}{Vr \sin\beta}, \qquad \text{(I)}$$

where s is the great circle projection on the earth of the sound path. To integrate this equation we need $\sin\beta$ as a function of r, or we need to replace dr, r, u', and V by functions of β. The latter procedure proves preferable.

A. Representation of the velocity profile by a radial power law

We set

$$\cos\beta = \cos\alpha \cdot \left(\frac{r}{b}\right)^{\gamma} = \frac{\frac{b}{r} V}{\frac{V_0}{\cos\alpha} + u_0' - \frac{b}{r} u'} \qquad \text{(J)}$$

This is almost equivalent to selecting layers over which the velocity of sound and the wind vary linearly. Differentiating (J) and substituting (I) we find

$$ds = -\frac{b\,d\beta}{\gamma} - \frac{bu'd\beta}{\gamma V \cos\beta}. \qquad \text{(K)}$$

This is the differential equation for the range in a layer characterized by the parameter γ for the velocity profile, with the angle β as the variable of integration. Before integration it is helpful to determine the significance of the two terms, for which we need to solve the time equation.

B. The integration

1. The range term.

By combining equations (F) and (I) we have

$$ds = \frac{b}{r} \cdot \frac{dr}{\tan\beta} + \frac{b}{r}u' \cdot dt \qquad \text{(L)}$$

Comparing equations (K) and (L) we see that the first term of (K) is the range increment resulting from refraction due to both temperature and wind, while the second term is merely the translational range term resulting from the motion of the medium. We are then justified in taking the mean values $\overline{\frac{b}{r} u'}$ and $\overline{\frac{b}{r} V}$ for the layer to compute the second and much smaller term, securing thereby

$$s = -\frac{b}{\gamma}(\beta_2 - \beta_1) - \frac{b}{\gamma} \cdot \frac{\overline{\frac{b}{\gamma} u'}}{\frac{b}{r} V} \cdot \left[gd^{-1} \beta_2 - gd^{-1} \beta_1 \right], \tag{M}$$

where gd is the Gudermannian.

By computing γ successively from the values β_2 and β_1 at the top and bottom of each layer, and the values $(b + h_2)$ and $(b + h_1)$, equation (M) can be applied repeatedly to determine the great circle distance traversed along the earth's surface by the sound path.

2. The time of travel.

Equation (F) can be written

$$dt = \frac{-b}{\frac{b}{r} V} \cdot \frac{1}{\gamma} \cdot \sec \beta \, d\beta.$$

If over the layer we take the mean value $\overline{\frac{b}{r} V}$ which we can readily judge from the temperature we obtain

$$t = \frac{-b}{\gamma} \cdot \frac{1}{\overline{\frac{b}{r} V}} \left[gd^{-1} \beta_2 - gd^{-1} \beta_1 \right], \tag{N}$$

where all symbols are as previously defined. This is the equation for the time of travel, expressed simply in terms of the angles β_2 and β_1 at the top and bottom of the layer, the mean temperature distribution giving $\overline{\frac{b}{r} V}$, the radius of the earth b, and the profile parameter γ.

IV. UPPER ATMOSPHERE STRUCTURE DEDUCED FROM ARCO, IDAHO SOUND DATA - OCTOBER 1946

The technique of analysis of the sound propagation field described in Sections II and III above has been applied to data recorded by the Signal Corps during the Army-Navy Munitions Board Tests at Arco, Idaho, October 1946. The details of analysis and the computations are too lengthy to present in this Appendix; however, an outstanding recording was secured at Green River, Wyoming, at a distance of 337 KM from Arco on 16 October 1946, which together with meteorological sounding data to a height of 27 KM, enabled an analysis to be made of the upper atmosphere leading to significant conclusions on long distance propagation of sound. A brief discussion of the salient features of this analysis follows.

A. Green River Recordings

Figure IV is a reproduction of the recordings secured at Green River, Wyoming on 16 October 1946. It will be noted that four discrete sound arrivals have been read from the record, characteristics of which repeat on the individual microphones in the triangular array of dimensions approximately 20,000 feet on a side. A tabulation of arrival time, azimuth, apparent velocity in the horizontal plane, and period of the arrivals follows:

ARRIVAL	ELAPSED TIME FROM DETONATION (sec.)	AZIMUTH	APPARENT VELOCITY* IN HORIZONTAL (mps)	PERIOD (seconds)
A	1119	314°	337	2.5
B	1209	313°	343	3.0
N	1220	313°	348	3.0
C	1230	316°	373	2.0
	TRUE AZIMUTH	310.6°		

* Characteristic path parameter (see Section II)

B. Sound path analysis

Analysis of atmospheric structures which would have had to prevail above the limit of the meteorological sounding (26 KM) on 16 October 1946 to satisfy the observed total times of travel and the computed azimuths and velocities of arrival, has shown that the first arrival (Arrival A) was totally refracted at the "first" inversion, i.e., that inversion characteristic of the stratosphere from 30-60 KM. In particular, Arrival A was computed as totally refracted at 57 KM. The 90-second delay in arrival of Arrival B could not be explained as a multiple bounce, since the atmospheric structure deduced for Arrival A showed that only direct paths for Arrivals B, N, and C were valid. The parametric equations for Arrivals B, N, and C were then set down, for each of which the observed travel times and distances to be accounted for by meteorological structures above 57 KM were expressed. On simultaneous solution of these equations it was determined that above the 57 KM level, the sound velocity profile was characterized by a decrease of velocity with height, reaching a minimum value, and then increasing with height. Particularly a minimum sound velocity of 315 meters per second was computed at 105 KM, and a maximum height of path for Arrival C at 110 KM. The sound velocity profile computed from these arrivals is shown in Figure V, together with representative upper atmosphere temperature distributions proposed by Fred L. Whipple in 1943 and the NACA Tentative Standard Atmosphere.

C. Significance of Arco data analysis for long range sound detection

The conclusions gleaned from the sound propagation analysis of the Arco data have been considered of exceptional import to long range sound transmission by the atmosphere. Previous investigators in the sound field had limited their interpretation of upper atmosphere effects on sound propagation to the so-called "first inversion", i.e., the 30 to 60 KM level. However, in Appendix A of this report, Dr. Fred B. Daniels shows by an extension of Schrödinger's analysis that long range sound propagation is possible by total refraction of sound waves of period one (1) to ten (10) seconds at the 100 KM level. The Arco sound data and the propagation analysis stated briefly above confirm Daniels' extension of Schrödinger's analysis.

The Signal Corps sound data secured at ranges of 7608 KM, 11,428 KM, and 32,423 KM from the source during Operation CROSSROADS in July 1946 is the only known experimental data suggesting the feasibility of sound detection of an atom bomb at globally-distributed locations. Unfortunately, pressure of time and personnel limitations preparatory to the tests denied the opportunity to establish triangular arrays of microphones at the sites manned by Signal Corps personnel (reference Section II of this report). As a result, no data are available on the CROSSRAODS tests relating to the path parameters, i.e., the apparent horizontal velocity at each detection location. Although the Arco data definitely establish the sound transmissibility of the 100 KM region, it cannot, however, be stated conclusively that the CROSSROADS waves were totally refracted in this region.

Granting that the atmospheric structure at the 100 KM level may be the mechanism by means of which exceptionally long range sound propagation can be effected, the physical properties establishing the velocity profile are as yet not clearly understood. Whereas at lower levels the effect of meteorological parameters of temperature, wind, and to a lesser extent, humidity, have been expressed in terms of sound velocity, the 100 KM region marks the beginning of the ionosphere as well as the "second" inversion. Therefore, the extent to which total refraction in the Arco sound data (and possibly also CROSSROADS) has been due to temperature, and the extent to which this refraction has been due to a dissociated medium, have not been evaluated.

BIBLIOGRAPHY

1. Lukes, George D., SCL Engineering Report S-6, dated 20 December 1940, entitled "Sound Ranging for Artillery, Volume 1: A Theory of Sound Propagation through the Atmosphere and an Application to Sound Ranging."

2. Lukes, George D., SCL Engineering Report No. 753, dated 1 January 1942, entitled "Sound Ranging for Artillery, Volume 2: Discussion and Illustration of Methods of Evaluating Meteorological Corrections along the Sound Path."

3. Crenshaw, Craig M., Eatontown Signal Laboratory Engineering Memorandum No. 50, dated 18 May 1944, entitled "Field Testing of Horizontal Homogeneity of the Atmosphere as Applied to Sound Ranging."

4. Crenshaw, Craig M., Eatontown Signal Laboratory Engineering Memorandum No. 53, dated 18 May 1944, entitled "Correlation of Meteorological Conditions with the Accuracy of Corrected Azimuths Obtained in Sound Ranging Operations."

5. Crenshaw, Craig M., Eatontown Signal Laboratory Engineering Memorandum No. C-3, dated 29 December 1944, entitled "Range Determination from the Overall Travel Time of Sound." (Confidential)

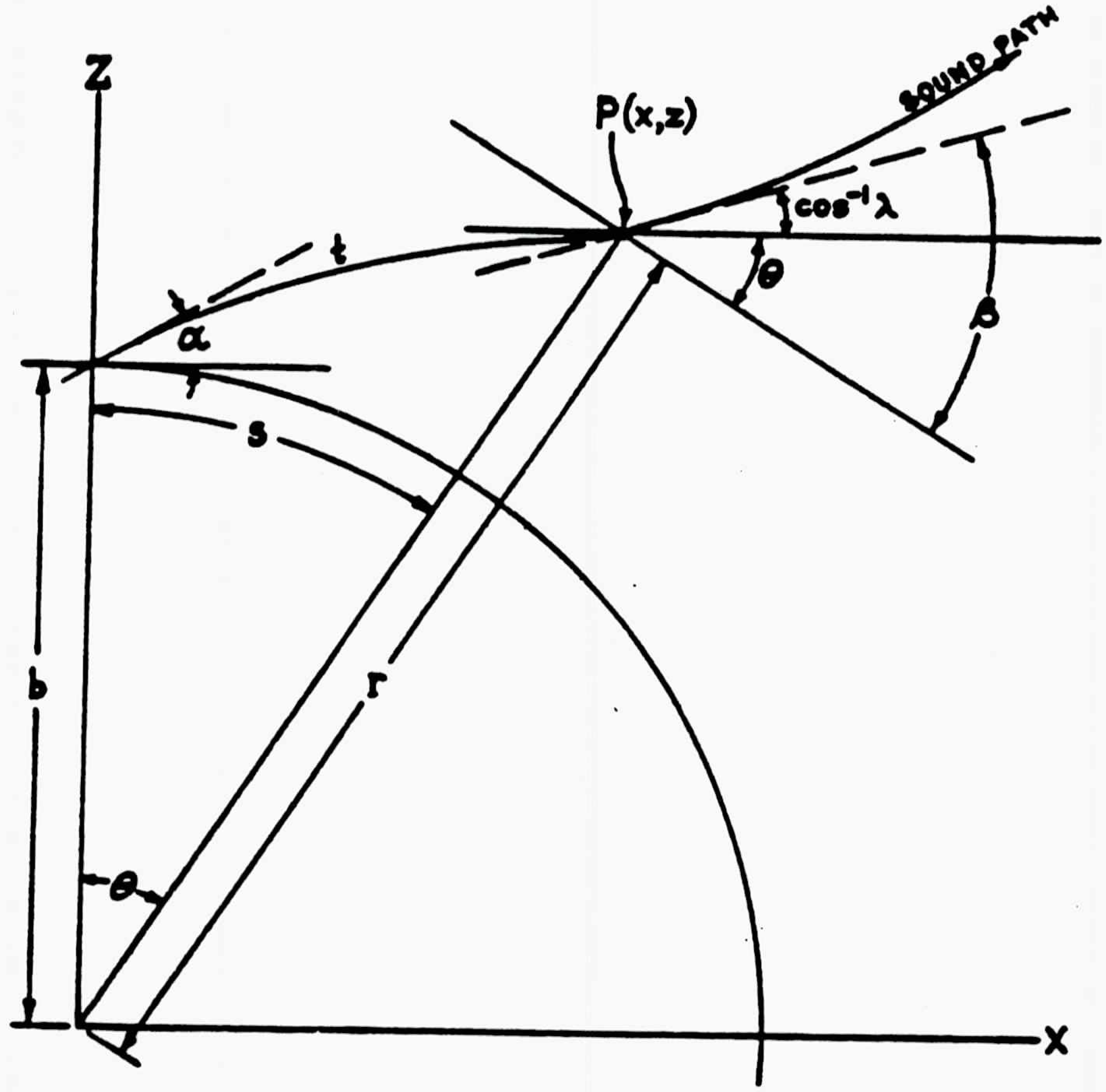

FIGURE I
APPENDIX E

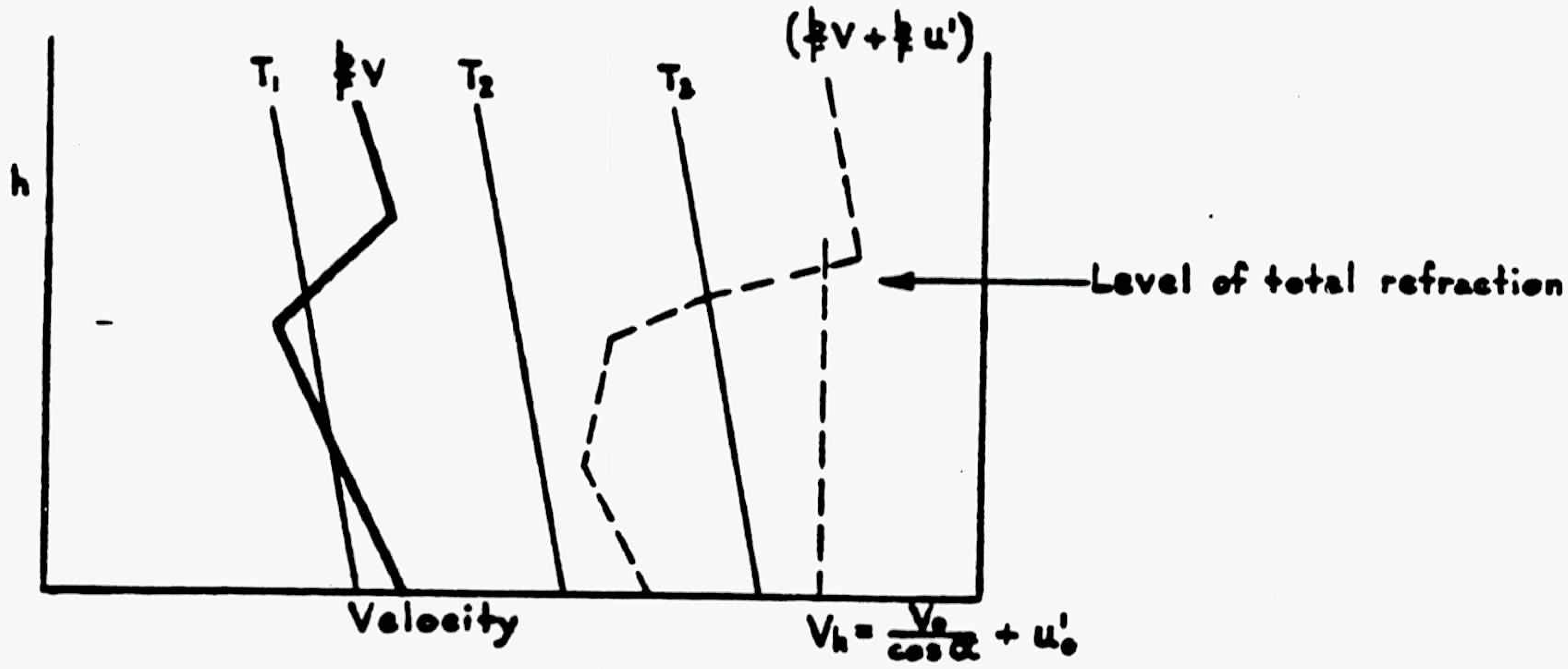

FIGURE II.

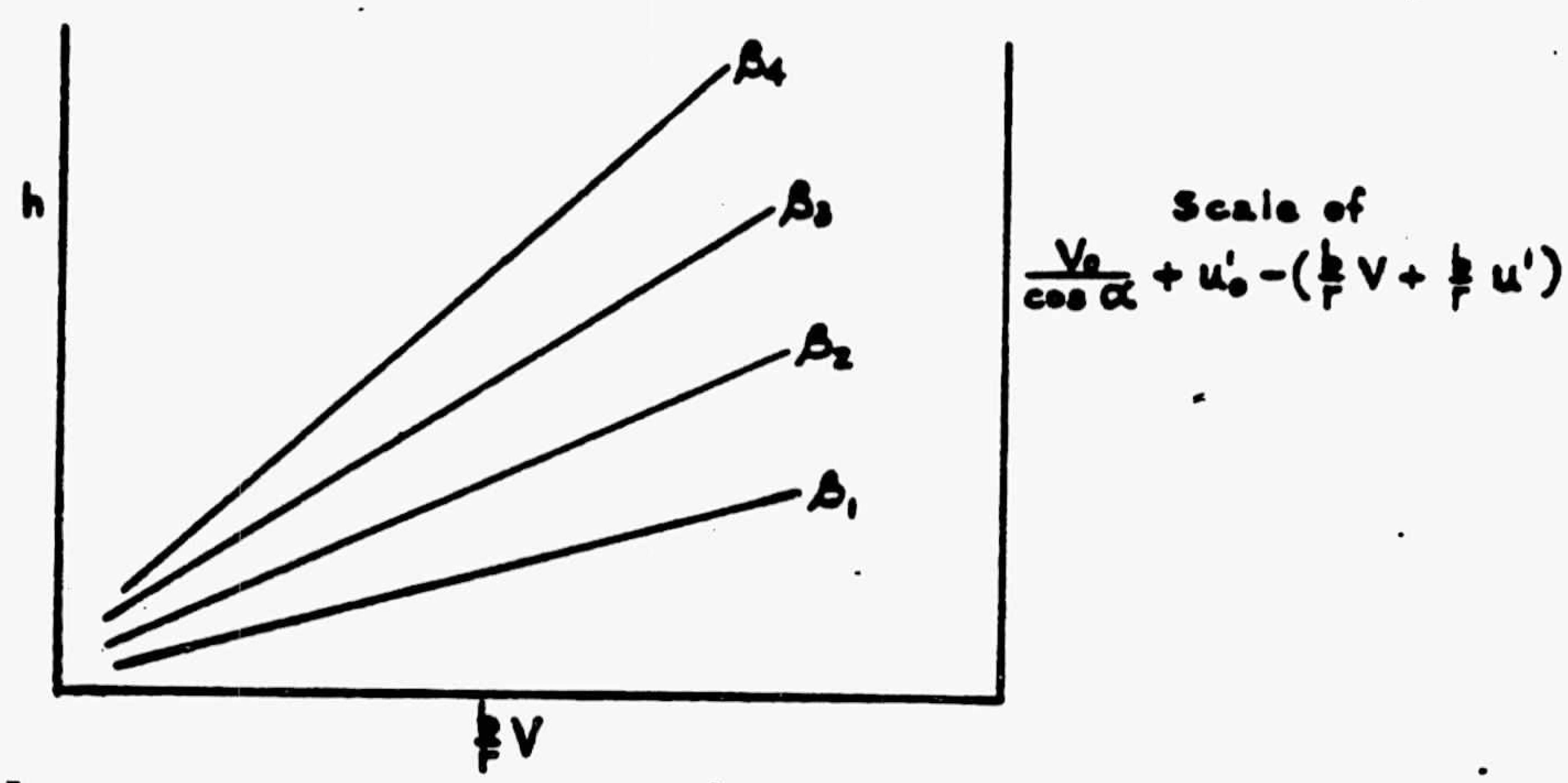

FIGURE III.

FIGURE II, III
APPENDIX E

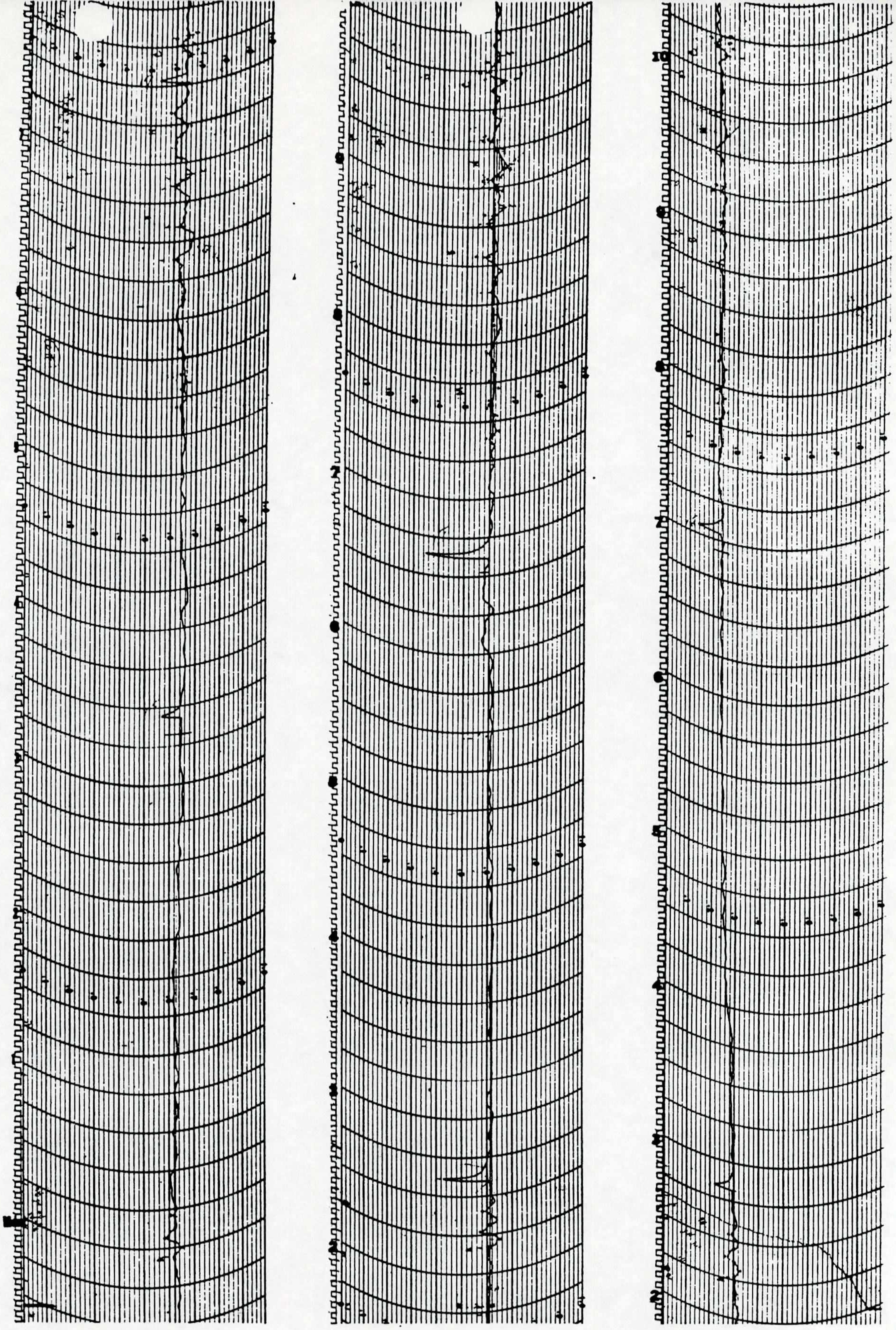

GREEN RIVER, WYOMING
16 OCTOBER 1946
DISTANCE FROM ARCO, IDAHO - 337KM. FIGUF
⊓⊔ = 1 SECOND APPENI

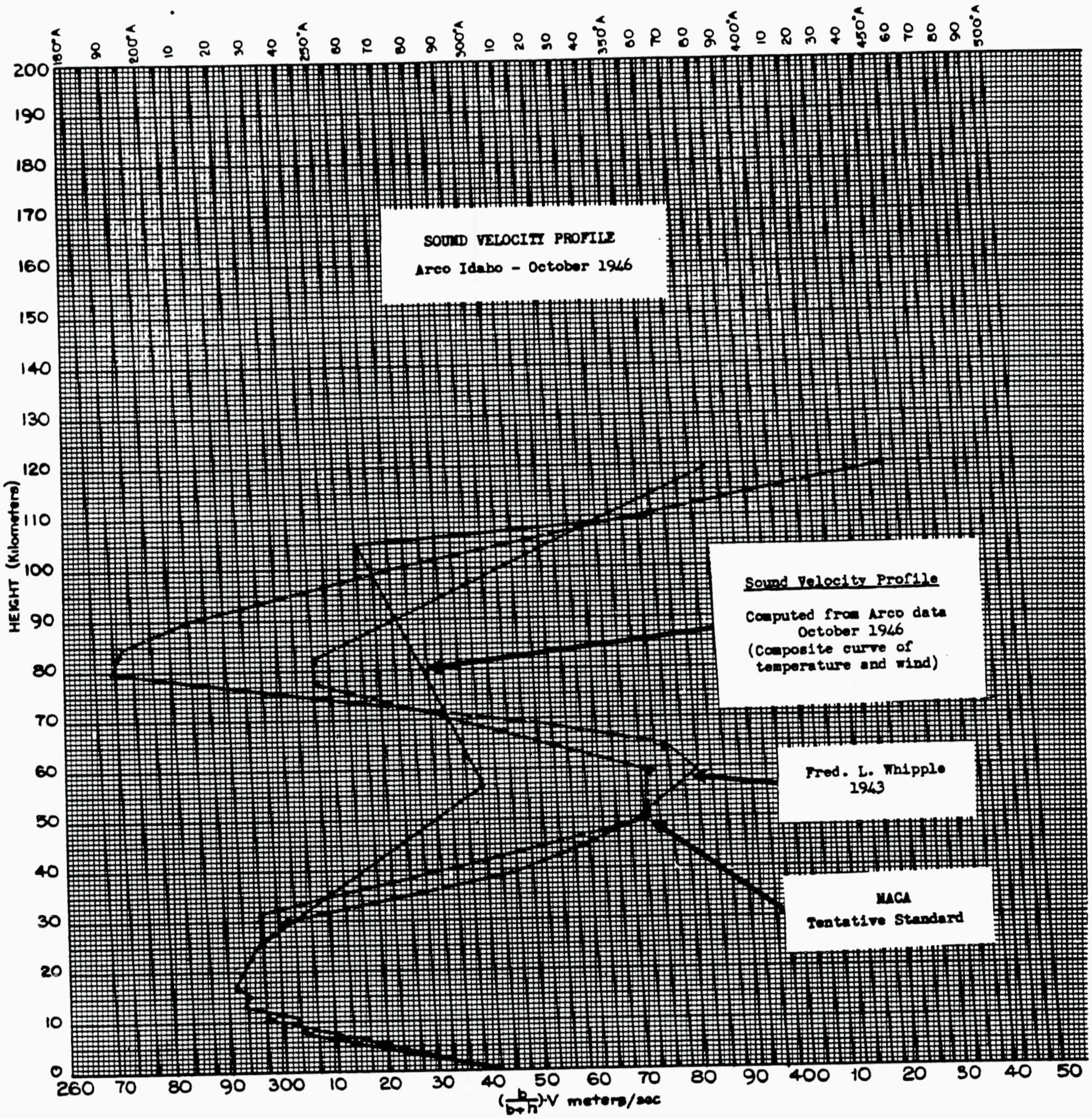

FIGURE V
APPENDIX E

~~CONFIDENTIAL~~

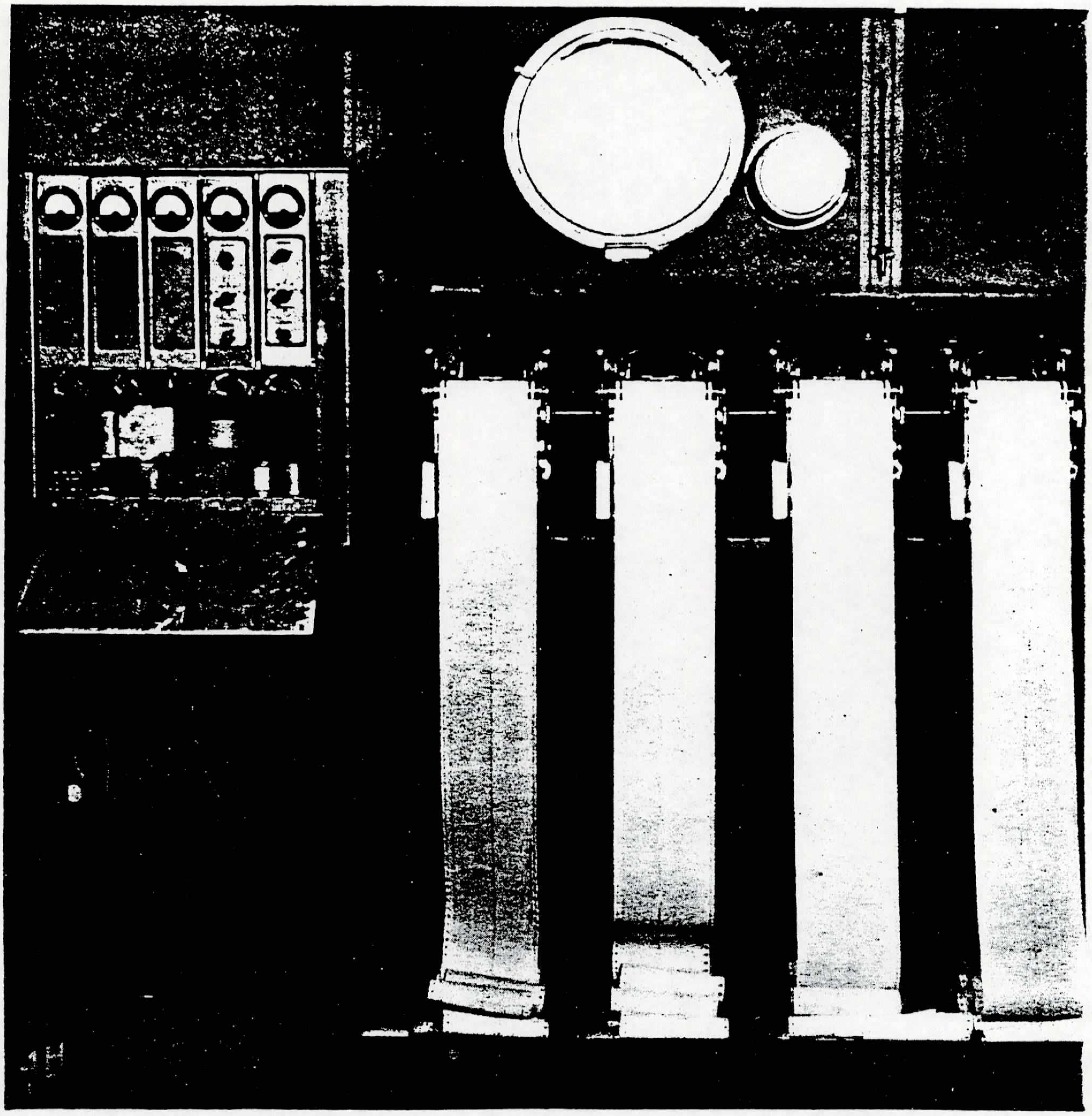

~~CONFIDENTIAL~~

PROJECT "SPECTACLES"
CENTRAL STATION INSTALLATION . (Experimental).
Interior Room Front View . Showing Five-Channel Amplifier Equipment
And Four-Channel Continuous Recording Equipment

DATE 9-13-48 SIGNAL CORPS ENGINEERING LABORATORIES NO. SCEL 23446-S

~~CONFIDENTIAL~~

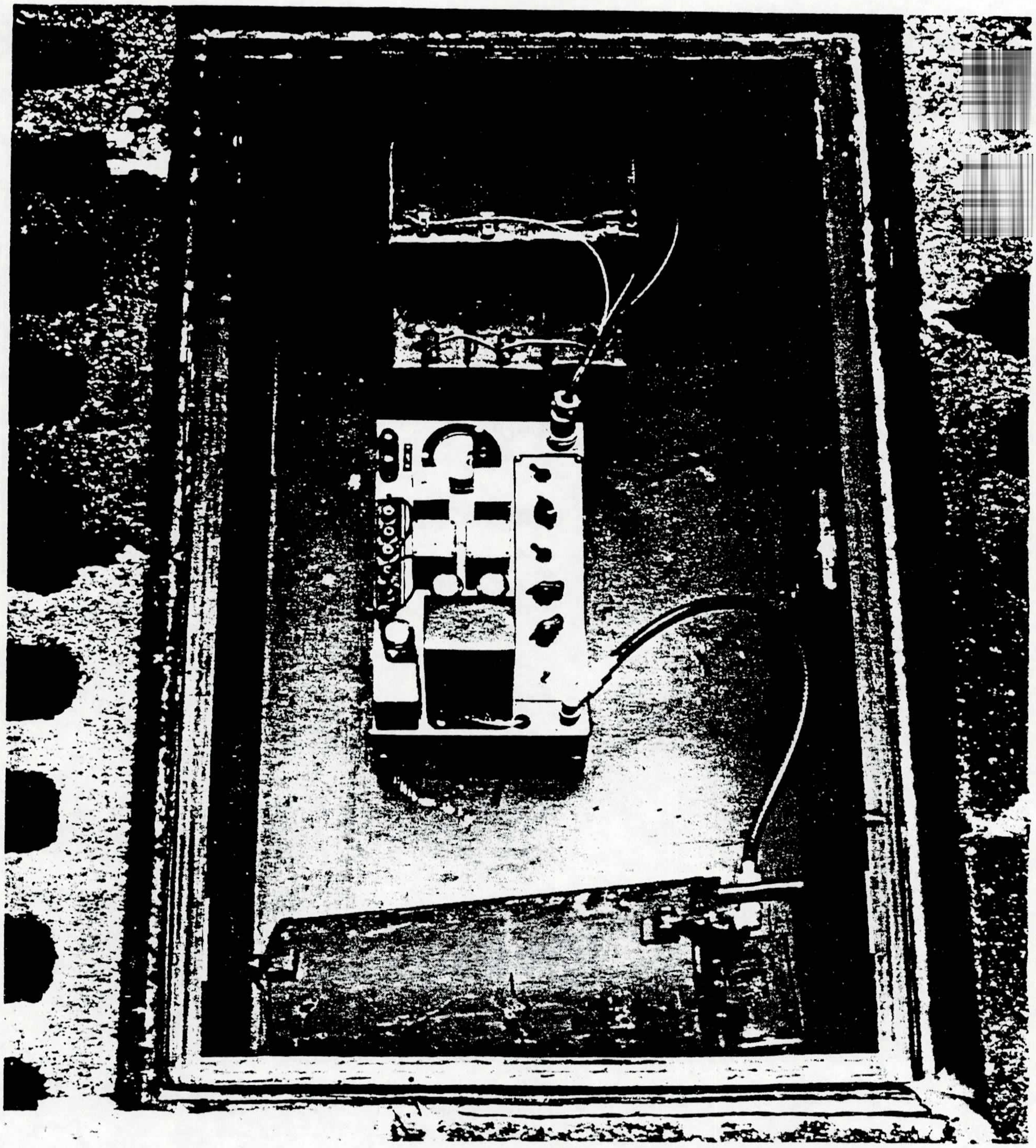

~~CONFIDENTIAL~~

PROJECT "SPECTACLES"

OUTPOST STATION INSTALLATION . (Experimental)

Downward Interior View . Weather Chest, Cover Removed . Showing Microphone Capacitance Bridge, Amplifier Equipment and Battery Power Supply

DATE 9-13-48 SIGNAL CORPS ENGINEERING LABORATORIES NO. SCEL 23445-S

~~CONFIDENTIAL~~

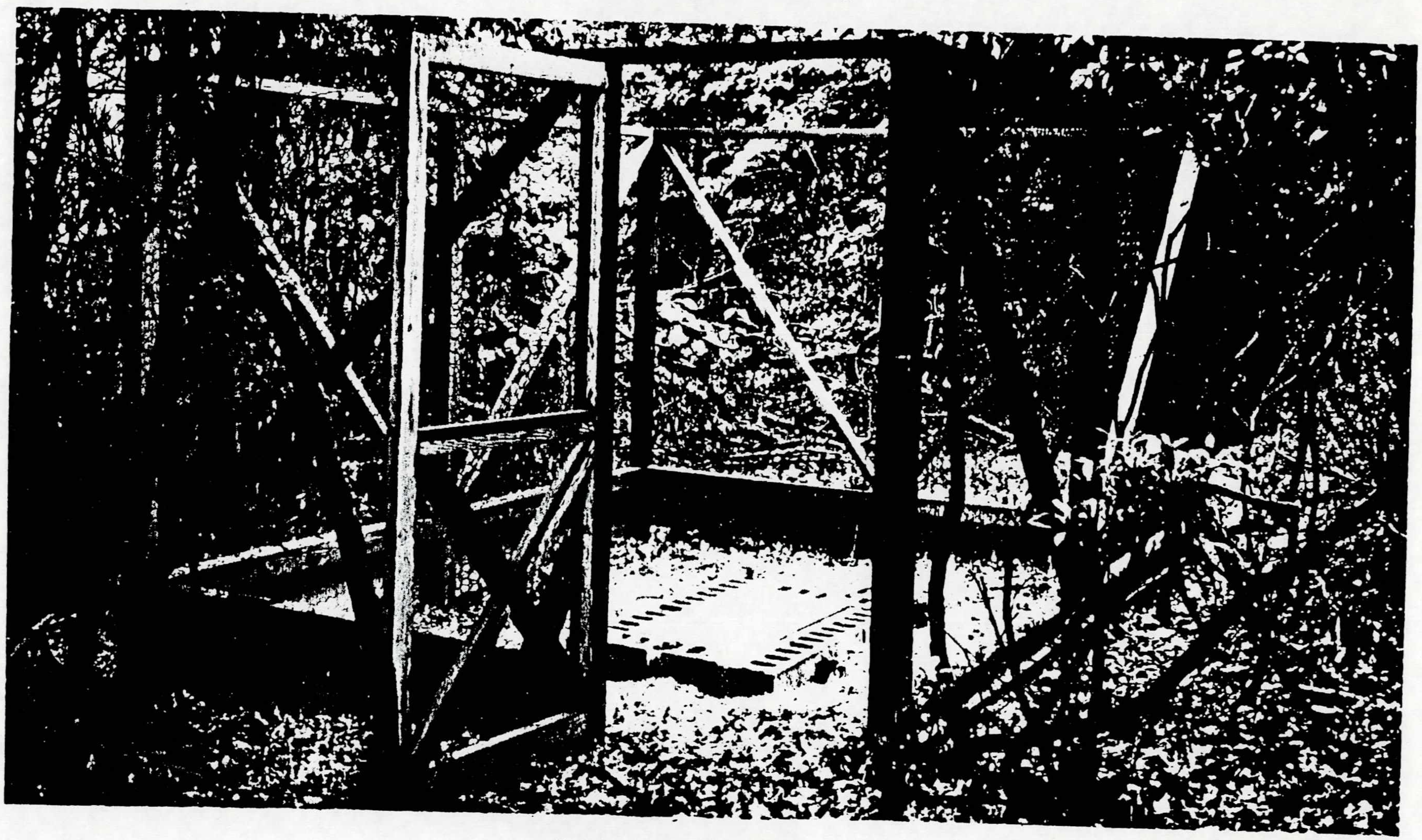

~~CONFIDENTIAL~~

PROJECT "SPECTACLES"
OUTPOST STATION INSTALLATION . (Experimental)
Outdoor Overall View . Showing Security Fence and Equipment in Weatherproof Chest

~~SECRET~~

~~SECRET~~

18

20

21

22

23

24

25

26

27

28

29

31